

I

A PERTURBATION THEORY OF THE APPROACH TOWARD SEDIMENTATION
EQUILIBRIUM IN THE ULTRACENTRIFUGE AND AN ANALYSIS OF A
PROPOSED FAST METHOD FOR REACHING EQUILIBRIUM

II

THE DETAILED INTERPRETATION OF THE ANOMALOUS ELECTRON
DIFFRACTION PHOTOGRAPHS OF SOME SYMMETRICAL GAS MOLECULES
WITH THE AID OF COMPLEX SCATTERING AMPLITUDES

Thesis by

Girair Mihran Nazarian

In Partial Fulfillment of the Requirements

For the Degree of

Doctor of Philosophy

California Institute of Technology

Pasadena, California

1957

ACKNOWLEDGMENTS

It is with great pleasure that I express my sincere thanks and appreciation to Professor Verner Schomaker for the opportunity he has given me to complete my course of graduate study. For his patient instruction and understanding combined with his unusual grasp of science I am equally grateful.

I also treasure the many years of association I have had with Professor John G. Kirkwood with whom I first did theoretical research. His method of approach toward science has always been an inspiration to me and will undoubtedly continue to influence my scientific thinking for a long time to come.

To Dr. Rafael A. Pasternak and to Dr. Jerome R. Vinograd I am grateful for the opportunity they gave me to work on the ultracentrifuge problem and for their continued interest and guidance.

To Professors Linus Pauling, Carl Niemann, and William N. Lacey I also owe thanks for permitting me to return to the Institute after such an unusually long absence.

I also thank Mr. Chi-Hsiang Wong and Mr. Darwin W. Smith for their generous help in connection with the electron diffraction calculations.

As for my wife, Anne, and our parents, both in Asbury Park and in Pasadena, there are no words which I can find to express my indebtedness to them for their understanding, patience, and unquestioning faith in me throughout these many years.

The financial assistance given me by the California Institute of Technology, the Office of Naval Research and the Du Pont Co. is greatly appreciated.

ABSTRACT

I. The transient concentration distribution in the ultracentrifuge is obtained in the form of a power series expansion in a small parameter by a perturbation treatment of the appropriate differential equation. The problem reduces in zero order to that of sedimentation in a constant gravitational field.

The theory is used for determining which initial step distributions lead to the fastest approach to equilibrium. The saving in time as compared to the conventional uniform initial distribution is also calculated.

II. The neglect of a phase shift in the theory of scattering has been shown by Schomaker and Glauber to be the reason why electron diffraction investigations in the past led to distorted structures for certain molecules otherwise expected to be symmetrical. Complex scattering amplitudes for use in calculating theoretical intensity patterns are now available as a result of the work of Hoerni and Ibers. In the present investigation we reinterpret the diffraction photographs of a number of these molecules in terms of symmetrical structures. The bond lengths in these molecules are thus determined accurately. In addition, further confirmation is provided for the theory.

TABLE OF CONTENTS

<u>PART</u>	<u>TITLE</u>	<u>PAGE</u>
I	A PERTURBATION THEORY OF THE APPROACH TOWARD SEDIMENTATION EQUILIBRIUM IN THE ULTRACENTRIFUGE AND AN ANALYSIS OF A PROPOSED FAST METHOD FOR REACHING EQUILIBRIUM	
	GENERAL INTRODUCTION	1
	A. THEORY OF THE APPROACH TOWARD EQUILIBRIUM	
	1. Introduction	2
	2. Mathematical Formulation of the Problem	6
	3. Mathematical Formulation of the Exact Solution	18
	4. Perturbation Method	27
	5. Zero-Order Solution	30
	6. First-Order Solution	34
	7. Comparison with Archibald's Numerical Results	50
	B. FAST METHOD FOR REACHING EQUILIBRIUM	
	1. Introduction	64
	2. Derivation of the Optimum Step Functions	65
	3. Time Required to Reach Equilibrium	83
	4. Experimental Results	90
	Appendix I	92
	Appendix II	95
	References	99
	Publication	101
II	THE DETAILED INTERPRETATION OF THE ANOMALOUS ELECTRON DIFFRACTION PHOTOGRAPHS OF SOME SYMMETRICAL GAS MOLECULES WITH THE AID OF COMPLEX SCATTERING AMPLITUDES	
	A. INTRODUCTION	105
	B. OSMIUM TETROXIDE	112
	C. TUNGSTEN HEXAFLUORIDE	120
	D. TUNGSTEN HEXACARBONYL	126
	E. MOLYBDENUM HEXACARBONYL	138
	F. TUNGSTEN HEXACHLORIDE	147
	G. MOLYBDENUM HEXAFLUORIDE	153
	References	159

A PERTURBATION THEORY OF THE APPROACH TOWARD
SEDIMENTATION EQUILIBRIUM IN THE ULTRACENTRIFUGE AND
AN ANALYSIS OF A PROPOSED FAST METHOD FOR REACHING
EQUILIBRIUM

GENERAL INTRODUCTION (1)

The possibility of obtaining particle mass from a study of the sedimentation equilibrium set up in the presence of an external gravitational field has long been recognized. The initial experiments in this direction by Perrin (2) and Westgren (3) naturally made use of the earth's gravitational field as the external force acting to produce a non-uniform equilibrium distribution of the particles suspended in a suitable medium. However, the use of gravity for such measurements is limited to the case where the particles in suspension are sufficiently massive and dense as to result in an appreciable effect. For the study of colloidal and lighter particles such as large molecules by the sedimentation method an external force thousands of times that of gravity is required. Dumansky (4), as early as 1913, attempted to make use of centrifugal force for this purpose by rotating the solution in an ordinary laboratory centrifuge. However, he was unable to obtain satisfactory results because of failure on his part to recognize the importance of taking precautions to avoid convection currents. It remained for Svedberg (5), some ten years later, to examine the experimental situation more carefully. He found that by using a small sector-shaped sample and taking great care to maintain a constant

temperature he was able to eliminate convection currents and thereby perform "faultless sedimentation in centrifugal fields 5000 times the force of gravity." For this new research tool he proposed the name ultracentrifuge, the connotation being that quantitative sedimentation experiments could be carried out in the instrument. In these first experiments, in which the technical problems were of primary concern, the particles investigated were fine-grained gold sols, it being possible to use these as test objects. Having surmounted the chief practical obstacles, Svedberg (6) now applied the instrument to the determination of the molecular weight of proteins* and it is in this realm that the ultracentrifuge has perhaps attained its greatest importance.

A. THEORY OF THE APPROACH TOWARD EQUILIBRIUM

1. Introduction

In conjunction with his experimental work, Svedberg (7) derived (in analogy with the method of Perrin for the case of gravity) by means of a kinetic as well as a thermodynamic argument, the theoretical equation necessary for calculating the molecular weight from the observed concentration distribution at equilibrium. However, since

* In fact, it was the ultracentrifuge which first showed that proteins actually have definite molecular weights.

a rather long time (of the order of days) is usually required before equilibrium is sensibly attained, it was desirable to have a theoretical understanding of the transient process during which the initially uniform concentration distribution passes over into the final distribution. To obtain the concentration as a function of position for all values of the time, it is necessary to solve the time-dependent differential equation which describes the approach to equilibrium and involves the phenomenological constants D and S , the coefficient of diffusion and the sedimentation constant, respectively. This equation is nothing more than the continuity equation for the case where there are currents of matter due to diffusion and to sedimentation and is simply an expression of the conservation of matter. Ever since it was first derived for the centrifuge by Lamm (8), many attempts have been made to obtain its solution. Faxen (9) obtained an approximate solution using elegant mathematical techniques. However, the evaluation of the result requires such a large amount of tedious calculation that it has not been carried out. It is therefore of interest only from a purely mathematical standpoint. Next to attempt a solution was Oka. Having shown (10) that the equilibrium result can be derived from the time-independent differential equation, he then proceeded to investigate (11) the time-dependent equation by expressing it in the form of the Sturm-Liouville eigenvalue problem. Although he was able to carry out the solution in a formal manner, he saw that he could not obtain numerical results without the necessity of extremely lengthy calculations as had been true in the case of Faxen's solution. He therefore returned to the original eigenvalue equation and carried

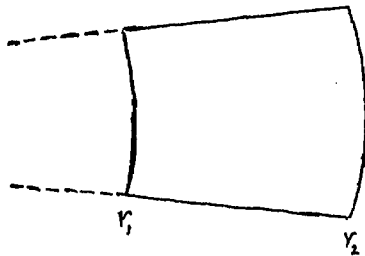
out a perturbation treatment. This was an excellent idea. Unfortunately, however, he made a very poor choice for the perturbation parameter from a physical standpoint in that the application of his results is restricted to the case where the experimental conditions are such that the final concentration distribution differs but slightly from uniformity. His solution is therefore of little use for describing what takes place during centrifugation under the usual conditions employed in such experiments. Finally, Archibald (12) attacked the problem obtaining an exact solution somewhat similar in form to that obtained by Oka but whereas Oka had not attempted to continue on with the necessary computations, Archibald carried them out for a specific representative set of experimental conditions. However, one must repeat these lengthy calculations for any other set of conditions that might be considered. The solution is thus not in a conveniently usable form, an essentially numerical solution being required for each application to a specific case. Under these circumstances the solution of Archibald is not of much greater value than that which would be obtained by a purely numerical integration of the differential equation. Archibald (13), realizing this situation as well as the next person, therefore tried to obtain an approximate solution which would be more amenable to direct computation. He succeeded in this but because he made his approximations within the same mathematical framework as he had used in obtaining the exact solution, his result is not physically appealing, containing as it does quantities which (because of the numerous transformations of variables and non-systematic approximations made throughout the derivation) are only indirectly related to

the clear-cut experimental quantities which enter the problem.

In view of the existing situation as outlined above, a manageable solution of the ultracentrifuge differential equation is still to be sought. Now the corresponding differential equation in the gravity case has been solved exactly by Mason and Weaver (14), the solution having a very convenient form both for computation and for physical interpretation. As has been stated by Beams (15) and Dr. Pasternak (16), this solution should give approximately valid results for sedimentation in the ultracentrifuge since the radius of the latter is large compared to the height of the sedimenting column, i.e., the field is relatively uniform over the length of the column and the effect due to the sector shape is small. This then forms the basis of the analysis to be presented here. In order to carry out the approximation method in a systematic manner, we return to the eigenvalue formulation as used by Oka but put it in such a form that we can choose as the perturbation parameter a quantity the value of which is a measure of the deviation of the centrifuge problem from that of the uniform field case. Under these circumstances the zero-order approximation corresponds to the Mason and Weaver solution and the correction terms can be obtained by the application of standard perturbation theory. We have carried out the explicit solution and calculations through the first-order terms although the zero-order approximation turns out to be amazingly accurate (as shown by calculating results for the same example as considered by Archibald in his exact calculation) and quite sufficient for the dimensions occurring in the usual apparatus.

2. Mathematical Formulation of the Problem

Consider a sector-shaped cell with radial sides and bounded by cylindrical surfaces at the distances r_1 and r_2 from an axis of rotation. A cross-section of the cell is shown here.



We take as our frame of reference that which is most appropriate for the problem, namely, a system of cylindrical coordinates r , θ , and z (with unit vectors \underline{e}_1 , \underline{e}_2 , \underline{e}_3), collectively denoted by the vector \underline{r} having as origin some point on the axis of rotation. If a solution is placed in the cell, the current density $\underline{j}(r, t)$ and concentration $c(r, t)$ of dissolved substance must at all times, t , obey the continuity equation

$$\nabla \cdot \underline{j} = - \frac{\partial c}{\partial t} \quad (1)$$

which expresses the law of conservation of material: the time rate of decrease of material in a volume element is equal to the net amount of material flowing out through its boundaries per unit time. If the solution is rotated with the constant angular velocity ω , the dis-

solved substance will experience a centrifugal force in the radial direction. Therefore if the initial concentration distribution is a function of r alone, i.e., $C(r, 0) = f(r)$, then it will remain a function of r only for all time. Hence

$$C(r, t) = C(r, 0) \quad (2)$$

Now there are two contributions to the current density \underline{j} . The first, \underline{j}_D , is that produced by the gradient of concentration and may be described in the case of an ideal dilute solution with the aid of the diffusion coefficient, D , by means of the relation

$$\underline{j}_D = -D \nabla C = -D \frac{\partial C}{\partial r} \underline{e}_r \quad (3)$$

The second, \underline{j}_S , is that due to the centrifugal force and may be expressed (again for an ideal dilute solution) in terms of the sedimentation constant, S , which is defined as the sedimentation speed acquired per unit centrifugal acceleration. Since the centrifugal force per unit mass is given by

$$\begin{aligned} \underline{F} &= (\text{speed of particle})^2 \underline{e}_r / r = \frac{(\omega r)^2}{r} \underline{e}_r \\ &= \omega^2 r \underline{e}_r \end{aligned} \quad (4)$$

we have for \underline{V} the velocity acquired

$$\underline{V} \equiv S \underline{F} = S \omega^2 r \underline{e}_r \quad (5)$$

so that

$$\underline{j}_s \equiv c \underline{V} = S \omega^2 r c \underline{e}_1 \quad (6)$$

Thus

$$\begin{aligned} \underline{j}(r, t) &= \underline{j}_D + \underline{j}_s = \left(-D \frac{\partial c}{\partial r} + S \omega^2 r c \right) \underline{e}_1 \\ &= \underline{j}(r, t) \end{aligned} \quad (7)$$

Since in cylindrical coordinates, the divergence of a vector

$$\underline{G} = \underline{e}_1 G_1 + \underline{e}_2 G_2 + \underline{e}_3 G_3 \quad \text{is given by}$$

$$\nabla \cdot \underline{G} = \frac{1}{r} \frac{\partial (r G_1)}{\partial r} + \frac{1}{r} \frac{\partial G_2}{\partial \theta} + \frac{\partial G_3}{\partial z} \quad (8)$$

the continuity equation for our problem becomes

$$\frac{1}{r} \frac{\partial}{\partial r} \left[r \left(D \frac{\partial c}{\partial r} - S \omega^2 r c \right) \right] = \frac{\partial c}{\partial t} \quad (9)$$

which is Lamm's equation. The solution of this equation $C(r, t)$ must satisfy the initial condition

$$C(r, 0) = f(r) \quad (10)$$

where $f(r)$ is the given initial distribution. In addition, the solution must satisfy the boundary condition that there can be no flow through the surfaces at $r=r_1$ and $r=r_2$, which means that \underline{j} must

vanish for these values of r . From equation 7 we find this condition to have the following mathematical form

$$D \frac{\partial c}{\partial r} - S \omega^2 r c = 0 \quad ; \quad r = r_1, \quad r = r_2 \quad (11)$$

The problem is now completely defined. One must solve equation 9 for $C(r,t)$ subject to the conditions given by equations 10 and 11.

In order to express the problem in a form which will make clear the difference between the centrifuge case being treated here and the uniform gravitational field case solved by Mason and Weaver (14), we introduce the dimensionless variable \mathcal{R} defined by

$$\mathcal{R} = \frac{r - \bar{r}}{r_2 - \bar{r}} = \frac{r - \bar{r}}{\bar{r} - r_1} \quad (12)$$

where

$$\bar{r} = \frac{1}{2} (r_1 + r_2)$$

so that the possible values of \mathcal{R} lie between +1 and -1, with the value 0 for $r = \bar{r}$. An alternative variable ρ can be defined by

$$\rho = \frac{r - r_1}{r_2 - r_1} = \frac{r - r_1}{H} \quad (13)$$

where

$$H = r_2 - r_1$$

and therefore gives the fraction of the distance from r_1 to r_2 which is associated with the position r . Thus for

$$\begin{aligned} r &= r_1, & \rho &= 0 \\ r &= \bar{r}, & \rho &= 1/2 \\ r &= r_2, & \rho &= 1. \end{aligned}$$

The relation between ρ and λ is

$$\lambda = 2\rho - 1 \tag{14}$$

For the present we use λ as the position variable although we shall replace it by ρ whenever we find it convenient to do so. Introducing the parameter λ defined by

$$\lambda = \frac{r_2 - r_1}{r_2 + r_1} = \frac{H}{2\bar{r}} \tag{15}$$

we can write

$$r = \bar{r} (1 + \lambda \lambda) \tag{16}$$

Defining a mean speed \bar{V} by

$$\bar{V} \equiv S \omega^2 \bar{r} \tag{17}$$

we introduce the dimensionless variable \hat{c} by means of the expression

$$t = \frac{H}{\bar{V}} \tau \quad (18)$$

Since H/\bar{V} is the time required for a particle having a speed \bar{V} to fall through the length of the cell, the significance of τ is clear.

Expressing equations 9 and 11 in terms of these new quantities we find

$$\frac{2}{(1+\lambda r)} \frac{\partial}{\partial r} \left\{ (1+\lambda r) \left[\frac{1}{\alpha} \frac{\partial c}{\partial r} - (1+\lambda r) c \right] \right\} = \frac{\partial c}{\partial \tau} \quad (19)$$

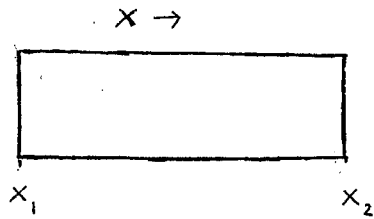
$$\frac{\partial c}{\partial r} = \alpha (1+\lambda r) c \quad ; \quad r = \pm 1 \quad (20)$$

where α is a dimensionless parameter defined by

$$\alpha = \frac{\bar{V} H}{2 D} \quad (21)$$

This is the formulation of the problem with which we shall be concerned.

In order to compare with the uniform gravitational field problem we derive the corresponding equations for that case. Consider a rectangular-shaped cell with parallel sides of length L being bounded by planes at x_1 and x_2 .



Suppose a solution is placed in this cell and exposed to a uniform gravitational force acting in the positive x direction. If the initial concentration distribution of solute is a function of x alone, then we shall have

$$C = C(x, t)$$

and in analogy with equations 3 and 6, we have

$$J_x(x, t) = -D \frac{\partial c}{\partial x} + Vc$$

where V is constant. Therefore since the continuity equation for the present case is given by

$$\frac{\partial J_x}{\partial x} = - \frac{\partial c}{\partial t}$$

we find

$$\frac{\partial}{\partial x} \left[D \frac{\partial c}{\partial x} - Vc \right] = \frac{\partial c}{\partial t} \quad (22)$$

with the boundary condition

$$D \frac{\partial c}{\partial x} - Vc = 0 \quad ; \quad x = x_1, x = x_2 . \quad (23)$$

In terms of the dimensionless variables

$$\rho' = \frac{x-x_1}{x_2-x_1} = \frac{x-x_1}{L}$$

$$\tau' = \frac{V}{L} t$$

and

$$\alpha' = \frac{VL}{2D}$$

equations 22 and 23 become

$$\frac{\partial}{\partial \rho'} \left[\frac{1}{2\alpha'} \frac{\partial c}{\partial \rho'} - c \right] = \frac{\partial c}{\partial \tau'} \quad (24)$$

and

$$\frac{\partial c}{\partial \rho'} = 2\alpha' c \quad ; \quad \rho' = 0, \rho' = 1. \quad (25)$$

These are the equations for the uniform gravitational field case and are analogous to those for the centrifuge case, equations 19 and 20. Now if in equations 19 and 20 we use

$$r = 2\rho - 1$$

$$dr = 2d\rho$$

and set $\lambda = 0$ (keeping α constant), we find that they become identical in form with equations 24 and 25, differing only in that $\rho' = (x-x_1)/L$ is replaced by $\rho = (r-r_1)/H$ and $V = \text{constant}$ is replaced by

$V = S\omega^2 \bar{r}$. Therefore λ is a parameter which is suitable for the perturbation procedure we have in mind. Since

$$\lambda = \frac{r_2 - r_1}{r_2 + r_1} = \frac{H}{2\bar{r}}$$

we see that $0 < \lambda \leq 1$, the value 1 being attained only for the case $r_1 = 0$. The usual values of r_1 and r_2 dealt with in the ultracentrifuge are of the order of 5 cm. with their difference being approximately 0.5 cm., so that

$$\lambda \approx \frac{0.5}{10} = 0.05$$

We may therefore expect to get rapid convergence of a series expansion in powers of λ . We postpone the perturbation treatment of equation 19 for the present and first obtain some familiar results for the sake of completeness. At equilibrium,

$$C(r, \tau) = C(r)$$

$$\frac{\partial C}{\partial \tau} = 0$$

so that equation 19 becomes

$$\frac{d}{dr} \left\{ (1 + \lambda r) \left[\frac{dc}{dr} - \alpha (1 + \lambda r) c \right] \right\} = 0$$

which means

$$(1 + \lambda r) \left[\frac{dc}{dr} - \alpha (1 + \lambda r) c \right] = \text{constant}$$

The boundary condition, equation 20, requires the constant to be zero, giving

$$\frac{dc}{dr} - \alpha(1 + \lambda r) c = 0$$

or

$$c(r) = A e^{\alpha(r + \frac{1}{2}\lambda r^2)} \quad (26)$$

For the ratio of the equilibrium concentrations at the bottom ($r = 1$) and top ($r = -1$) of the cell we therefore find

$$c_2/c_1 = e^{2\alpha} \quad (27)$$

which provides a very simple interpretation of the parameter α . In terms of the variable γ equation 26 has the form

$$\begin{aligned} c(r) &= B \exp\left(\frac{2\alpha}{r_2^2 - r_1^2} r^2\right) \\ &= B \exp\left(\frac{\omega^2 S}{2D} r^2\right) \end{aligned} \quad (28)$$

We now derive an alternative expression for the equilibrium distribution by means of a statistical mechanical argument (it may also be derived from thermodynamics). By the method of Boltzmann we have for an ideal solution

$$c(r_{II})/c(r_I) = e^{-[\epsilon(r_{II}) - \epsilon(r_I)]/kT}$$

where $\epsilon(r)$ is the potential energy of a molecule at r due to the external force. Since in the centrifuge for a molecule of mass m and partial specific volume \bar{v} suspended in a solution of density d we have as the net external force

$$F = m(1 - \bar{v}d) \omega^2 r = - \frac{d\epsilon}{dr} ,$$

we obtain by integrating over a sufficiently small range of r (so that $\bar{v}d$ may be treated as a constant)

$$\epsilon(r_{II}) - \epsilon(r_I) = -m(1 - \bar{v}d) \frac{1}{2} \omega^2 (r_{II}^2 - r_I^2)$$

Since

$$m/k = M/R$$

where M is the molecular weight, we have finally

$$c(r_{II})/c(r_I) = e^{M(1 - \bar{v}d) \omega^2 (r_{II}^2 - r_I^2) / 2RT} \quad (29)$$

Solving for M we obtain the familiar expression by means of which the molecular weight can be calculated from the concentration distribution at equilibrium

$$M = \frac{2RT \ln [c(r_{II})/c(r_I)]}{(1-\bar{v}d) \omega^2 (r_{II}^2 - r_I^2)} \quad (30)$$

Since we have from equation 28 that

$$c_{II}/c_I = e^{\frac{\omega^2 S}{2D} (r_{II}^2 - r_I^2)}$$

we find on comparing with equation 29

$$\frac{\omega^2 S}{2D} (r_{II}^2 - r_I^2) = \frac{M(1-\bar{v}d) \omega^2 (r_{II}^2 - r_I^2)}{2RT}$$

or

$$S/D = M(1-\bar{v}d)/RT \quad (31)$$

which has the form of the usual expression arising in problems involving diffusion in the presence of an external field and was first obtained by Einstein in the course of his investigations on the Brownian motion. It was first applied to the ultracentrifuge by Svedberg. Equations 30 and 31 are the two fundamental formulae used in sedimentation equilibrium calculations.

3. Mathematical Formulation of the Exact Solution

The problem as formulated in the preceding section is the following. We must find a function $C(n, \tau)$ which is a solution of the differential equation

$$\frac{2}{(1+\lambda n)} \frac{\partial}{\partial n} \left\{ (1+\lambda n) \left[\frac{1}{\alpha} \frac{\partial C}{\partial n} - (1+\lambda n) C \right] \right\} = \frac{\partial C}{\partial \tau} \quad (32)$$

and satisfies the boundary condition

$$\frac{\partial C}{\partial n} = \alpha (1+\lambda n) C \quad ; \quad n = \pm 1 \quad (33)$$

as well as the initial condition

$$C(n, 0) = f(n) \quad (34)$$

where $f(n)$ is the given initial distribution.

Consider now the function $g(n, \tau)$ defined as follows

$$C(n, \tau) = e^{\lambda \frac{\alpha}{2} n^2} e^{\frac{\alpha}{2} (n+1) \tau} g(n, \tau) \quad (35)$$

In terms of this function the differential equation can be shown to

take the form

$$\frac{2}{\alpha} \frac{\partial^2 g}{\partial r^2} + \lambda \cdot \frac{2}{\alpha} w(r) \frac{\partial g}{\partial r} - [\alpha/2 + \lambda w(r)] g = \frac{\partial g}{\partial \tau}$$

where

$$w(r) = \alpha r + (1 + \lambda r)^{-1}$$

The boundary condition becomes

$$\frac{\partial g}{\partial r} = \frac{\alpha}{2} g \quad ; \quad r = \pm 1$$

and the initial condition is

$$g(r, 0) = e^{-\lambda \frac{\alpha}{2} r^2} e^{-\frac{\alpha}{2}(r+1)} f(r)$$

(Note that in this way we have eliminated λ from the boundary condition.) We now separate the variables in the usual manner, setting

$$g(r, \tau) = u(r) \varphi(\tau)$$

which gives

$$\frac{2}{\alpha} \varphi u'' + \lambda \cdot \frac{2}{\alpha} w \varphi u' - [\alpha/2 + \lambda w] \varphi u = \varphi' u ,$$

and dividing through by $u\varphi$, the left side becomes a function of r only and the right side a function of τ only. Since r and τ can be varied independently, the equality of the two sides of the equation

means that each side must be a constant, say $-\varepsilon$. Thus

$$\frac{2}{\alpha} \frac{u''}{u} + \lambda \frac{2}{\alpha} \omega \frac{u'}{u} - [\alpha/2 + \lambda\omega] = \frac{\varphi'}{\varphi} = -\varepsilon$$

$$\varphi \sim e^{-\varepsilon\tau}$$

and therefore

$$g \sim u e^{-\varepsilon\tau} \tag{36}$$

The equation for u is

$$u'' + \lambda\omega u' - \frac{\alpha}{2} (\alpha/2 + \lambda\omega) u + \varepsilon \frac{\alpha}{2} u = 0 \tag{37}$$

with the boundary condition

$$u'(\pm 1) = \frac{\alpha}{2} u(\pm 1) \tag{38}$$

We wish to find a function $\rho(r)$ such that by multiplying equation 37 by $\rho(r)$ the terms containing u'' and u' can be written as $(\rho u')'$, i.e., self-adjoint form. This means that we require ρ to be such that

$$\rho(u'' + \lambda\omega u') = (\rho u')' = \rho u'' + \rho' u'$$

and therefore

$$\rho \lambda \omega = \rho' \quad (39)$$

or

$$\rho'/\rho = \lambda \omega = \lambda \alpha r + \lambda (1 + \lambda r)^{-1}$$

Integrating, we obtain

$$\ln \rho = \lambda \frac{\alpha}{2} r^2 + \ln(1 + \lambda r)$$

so that ρ is found to be

$$\rho = (1 + \lambda r) e^{\lambda \frac{\alpha}{2} r^2} \quad (40)$$

Multiplying equation 37 by this function ρ , we therefore obtain

$$(\rho u')' - \frac{\alpha}{2} (\frac{\alpha}{2} + \lambda \omega) \rho u + \varepsilon \frac{\alpha}{2} \rho u = 0$$

and setting

$$\begin{aligned} q(r) &= \frac{\alpha}{2} (\frac{\alpha}{2} + \lambda \omega) \rho = \frac{\alpha}{2} (\frac{\alpha}{2} \rho + \rho') \\ \sigma(r) &= \frac{\alpha}{2} \rho \end{aligned} \quad (41)$$

we have

$$(\rho u')' - q u + \varepsilon \sigma u = 0 \quad (42)$$

which has the form of the generalized Sturm-Liouville eigenvalue problem (17). From the general properties of this equation we know that its solutions satisfying the boundary condition, equation 38, consist of a complete set of real orthogonal eigenfunctions U_0, U_1, U_2, \dots with corresponding real eigenvalues $\epsilon_0, \epsilon_1, \epsilon_2, \dots$. For non-periodic boundary conditions, such as we have here, the ϵ_n are simple, i.e., no two linearly independent eigenfunctions can belong to the same eigenvalue. The condition of orthogonality satisfied by the eigenfunctions can be shown to be the following

$$\int_{-1}^1 dr \sigma U_n U_m = 0 \quad ; \quad n \neq m$$

If we normalize the U_n such that

$$\int_{-1}^1 dr \rho U_n^2 = 1$$

we can evidently write (remembering that $\sigma = \frac{\alpha}{2} \rho$)

$$\int_{-1}^1 dr \rho U_n U_m = \delta_{nm} = \begin{cases} 1 & ; \quad n = m \\ 0 & ; \quad n \neq m \end{cases} \quad (43)$$

It is easily shown that $\epsilon_n \geq 0$ by means of the following argument.

$$\epsilon_n = \epsilon_n \int_{-1}^1 dr \rho U_n^2 = \frac{2}{\alpha} \int_{-1}^1 dr (\epsilon_n \sigma U_n) U_n$$

But we have from the differential equation that

$$\varepsilon_m \sigma u_m = -(\rho u_m')' + g u_m$$

Introducing this into the preceding equation, we get

$$\begin{aligned} \varepsilon_m &= \frac{2}{\alpha} \int_{-1}^1 dr \left[-(\rho u_m')' + g u_m \right] u_m \\ &= -\frac{2}{\alpha} \int_{-1}^1 dr (\rho u_m')' u_m + \frac{2}{\alpha} \int_{-1}^1 dr g u_m^2 \end{aligned}$$

But from equation 41 we have

$$g = \frac{\alpha}{2} \left(\frac{\alpha}{2} \rho + \rho' \right)$$

Introduction of this expression for g and integration by parts of the terms containing $(\rho u_m')'$ and ρ' yields

$$\begin{aligned} \varepsilon_m &= -\frac{2}{\alpha} \left[\rho u_m' u_m \right]_{-1}^1 + \frac{2}{\alpha} \int_{-1}^1 dr \rho (u_m')^2 + \frac{\alpha}{2} \int_{-1}^1 dr \rho u_m^2 \\ &\quad + \left[\rho u_m^2 \right]_{-1}^1 - 2 \int_{-1}^1 dr \rho u_m u_m' \end{aligned}$$

Now because of the boundary condition, equation 38, the integrated portions combine to vanish and we are left with

$$\varepsilon_m = \frac{2}{\alpha} \int_{-1}^1 dr \rho \left[u_m' - \frac{\alpha}{2} u_m \right]^2 \quad (44)$$

Since

$$p = (1 + \lambda r) e^{\lambda \frac{\alpha}{2} r^2}$$

and

$$0 < \lambda \leq 1$$

$$-1 \leq r \leq 1$$

we see that

$$p \geq 0$$

and therefore it follows that

$$\varepsilon_m > 0$$

The eigenvalue zero occurs for $n=0$, say, if

$$u_0'(r) = \frac{\alpha}{2} u_0(r) \tag{45}$$
$$\varepsilon_0 = 0$$

which obviously satisfies the boundary condition as well as the differential equation. Since we have from equations 35 and 36 that

$$c(r, \tau) \sim e^{\lambda \frac{\alpha}{2} r^2} e^{\frac{\alpha}{2} (r+1)} u_m(r) e^{-\varepsilon_m \tau} \tag{46}$$

we see that the term $n=0$ is the only one remaining as $\tau \rightarrow \infty$ because

$$\epsilon_0 = 0$$

$$\epsilon_n > 0 \quad ; \quad n=1, 2, \dots$$

The solution of equation 45 is

$$u_n \sim e^{\frac{\alpha}{2} r^2}$$

so that

$$c(r, \infty) \sim e^{-\lambda \frac{\alpha}{2} r^2} e^{-\alpha r}$$

which is in agreement with our previous result, equation 26. In order to complete the formal solution of the problem, we must satisfy the initial condition

$$c(r, 0) = f(r)$$

Since the u_n form a complete set we can make the following expansion

$$e^{-\lambda \frac{\alpha}{2} r^2} e^{-\frac{\alpha}{2}(r+1)} f(r) = \sum_{n=0}^{\infty} A_n u_n(r)$$

where the A_n are easily determined by making use of the orthonormality condition satisfied by the u_n and are found to be given by

$$A_n = \int_{-1}^1 dr \rho u_n e^{-\lambda \frac{\alpha}{2} r^2} e^{-\frac{\alpha}{2}(r+1)} f(r) \quad (47)$$

We can now write as our complete formal solution

$$c(r, \tau) = e^{\lambda \frac{\alpha}{2} r^2} e^{\frac{\alpha}{2}(r+1)} \sum_{n=0}^{\infty} A_n u_n(r) e^{-\epsilon_n \tau} \quad (48)$$

where u_n and ϵ_n satisfy the following differential equation (re-arranging equation 37)

$$\frac{2}{\alpha} u_n'' - \frac{\alpha}{2} u_n + \frac{2}{\alpha} \lambda w(r) \left[u_n' - \frac{\alpha}{2} u_n \right] = -\epsilon_n u_n \quad (49)$$

$$w(r) = \alpha r + (1 + \lambda r)^{-1}$$

under the boundary condition

$$u_n'(\pm 1) = \frac{\alpha}{2} u_n(\pm 1) \quad (50)$$

The solutions will satisfy the orthogonality condition

$$\int_{-1}^1 dr (1 + \lambda r) e^{\lambda \frac{\alpha}{2} r^2} u_n u_m = 0 ; n \neq m \quad (51)$$

and are to be normalized such that

$$\int_{-1}^1 dr (1 + \lambda r) e^{\lambda \frac{\alpha}{2} r^2} u_n^2 = 1 \quad (52)$$

Finally, the constants A_n are given by

$$A_n = \int_{-1}^1 (1 + \lambda r) u_n e^{-\frac{\alpha}{2}(r+1)} f(r) \quad (53)$$

where $f(r)$ is the given initial concentration distribution.

This then completes the derivation of the exact formal solution. The problem remaining, of course, is that of solving equation 49 and as we know from the work of Archibald and his predecessors, its exact treatment must lead to a solution which is not convenient for practical purposes. From our discussion in section 2 concerning the parameter λ , it is clear that the most profitable procedure will be to represent the solution in a power series expansion in λ i.e., treat the actual problem as a perturbation of the problem for which $\lambda = 0$, and this is the procedure we shall adopt in the next section.

4. Perturbation Method

The differential equation to be solved is the following (equation 49)

$$\frac{2}{\alpha} u_n'' - \frac{\alpha}{2} u_n + \frac{2}{\alpha} \lambda w (u_n' - \frac{\alpha}{2} u_n) = -\epsilon_n u_n$$

where

$$w = \alpha r + (1 + \lambda r)^{-1}$$

so that we have in a more explicit form

$$\frac{2}{\alpha} u_m'' - \frac{\alpha}{2} u_m + \frac{2}{\alpha} \lambda \left[\alpha r + (1 + \lambda r)^{-1} \right] \left[u_m' - \frac{\alpha}{2} u_m \right] = -\epsilon_m u_m \quad (54)$$

If we define a set of operators $H^{(s)}$ by

$$H^{(0)} = \frac{2}{\alpha} \frac{d^2}{dr^2} - \frac{\alpha}{2} \quad (55)$$

$$H^{(1)} = \frac{2}{\alpha} (\alpha r + 1) \left(\frac{d}{dr} - \frac{\alpha}{2} \right) \quad (56)$$

$$H^{(s)} = \frac{2}{\alpha} (-r)^{s-1} \left(\frac{d}{dr} - \frac{\alpha}{2} \right) \quad (57)$$

$$s = 2, 3, \dots$$

we can write equation 54 in the form

$$\left\{ H^{(0)} + \lambda H^{(1)} + \lambda^2 H^{(2)} + \dots \right\} u_m = -\epsilon_m u_m \quad (58)$$

If we now take u_m and ϵ_m to have the following form

$$u_m = u_m^{(0)} + \lambda u_m^{(1)} + \lambda^2 u_m^{(2)} + \dots \quad (59)$$

$$\varepsilon_m = \varepsilon_m^{(0)} + \lambda \varepsilon_m^{(1)} + \lambda^2 \varepsilon_m^{(2)} + \dots \quad (60)$$

and introduce these expansions into equation 58, we get

$$\left\{ H^{(0)} + \lambda H^{(1)} + \dots \right\} \left\{ u_m^{(0)} + \lambda u_m^{(1)} + \dots \right\} = - \left\{ \varepsilon_m^{(0)} + \lambda \varepsilon_m^{(1)} + \dots \right\} \left\{ u_m^{(0)} + \lambda u_m^{(1)} + \dots \right\}$$

Equating coefficients of like powers of λ results in the following set of equations

$$\begin{aligned} H^{(0)} u_m^{(0)} &= -\varepsilon_m^{(0)} u_m^{(0)} \\ H^{(1)} u_m^{(0)} + H^{(0)} u_m^{(1)} &= -\varepsilon_m^{(0)} u_m^{(1)} - \varepsilon_m^{(1)} u_m^{(0)} \end{aligned} \quad (61)$$

⋮

Using equation 59 in the boundary condition

$$u_m'(\pm 1) = \frac{\alpha}{2} u_m(\pm 1)$$

and again collecting like powers of λ , we get

$$\begin{aligned} u_m^{(0)'}(\pm 1) &= \frac{\alpha}{2} u_m^{(0)}(\pm 1) \\ u_m^{(1)'}(\pm 1) &= \frac{\alpha}{2} u_m^{(1)}(\pm 1) \end{aligned} \quad (62)$$

⋮

so that $u_m^{(0)}, u_m^{(1)}, \dots$ all satisfy the same boundary condition. Equations 61 together with equations 62 determine $u_m^{(0)}, u_m^{(1)}, \dots$ and the cor-

responding $\epsilon_n^{(0)}, \epsilon_n^{(1)}, \dots$. Also introducing the expansion for u_n given by equation 59 into the formula for A_n , equation 53, we find

$$A_n = A_n^{(0)} + \lambda A_n^{(1)} + \dots$$

where

$$A_n^{(0)} = \int_{-1}^1 dr u_n^{(0)} e^{-\frac{\alpha}{2}(r+1)} f(r)$$

$$A_n^{(1)} = \int_{-1}^1 dr [u_n^{(1)} + r u_n^{(0)}] e^{-\frac{\alpha}{2}(r+1)} f(r) \quad (63)$$

⋮

Thus the solution $C(r, \tau)$ given by equation 48 is

$$C(r, \tau) = e^{\lambda \frac{\alpha}{2} r^2} e^{\frac{\alpha}{2}(r+1)} \sum_{n=0}^{\infty} \{A_n^{(0)} + \lambda A_n^{(1)} + \dots\} \{u_n^{(0)} + \lambda u_n^{(1)} + \dots\} e^{-[\epsilon_n^{(0)} + \lambda \epsilon_n^{(1)} + \dots] \tau} \quad (64)$$

5. Zero-Order Solution

If we set $\lambda = 0$, keeping α fixed, we obtain the zero-order approximation which corresponds exactly to the rigorous solution of Mason and Weaver (14) for the uniform gravitational field problem. Thus equation 64 becomes

$$C^{(0)}(r, \tau) = e^{\frac{\alpha}{2}(r+1)} \cdot \sum_{n=0}^{\infty} A_n^{(0)} u_n^{(0)}(r) e^{-\epsilon_n^{(0)} \tau} \quad (65)$$

where from the first of equations 61 and 62 we know that $u_n^{(0)}$ must satisfy

$$H u_n^{(0)} = -\epsilon_n^{(0)} u_n^{(0)}$$

or

$$\frac{2}{\alpha} u_n^{(0)''} - \frac{\alpha}{2} u_n^{(0)} = -\epsilon_n^{(0)} u_n^{(0)}$$

with the boundary condition

$$u_n^{(0)'}(\pm 1) = \frac{\alpha}{2} u_n^{(0)}(\pm 1)$$

From the work of Mason and Weaver we can write down the solution at once.

$$u_0^{(0)}(r) = B_0 e^{\frac{\alpha}{2}(r+1)} \quad (66)$$

$$u_m^{(0)}(r) = B_m X_m(r) \quad (67)$$

$$X_n(r) = \cos \frac{n\pi}{2}(r+1) + \frac{\alpha}{n\pi} \sin \frac{n\pi}{2}(r+1) \quad (68)$$

$$E_0^{(0)} = 0 \quad (69)$$

$$E_n^{(0)} = \frac{n^2 \pi^2}{2 \alpha} \left(1 + \frac{\alpha^2}{n^2 \pi^2} \right) \quad (70)$$

$$n = 1, 2, \dots$$

where the B_n are to be determined by the application of the normalization condition (zero-order in λ), equation 52

$$\int_{-1}^1 dr [u_n^{(0)}]^2 = 1$$

This yields

$$B_0^2 = \frac{\alpha}{e^{2\alpha} - 1} \quad (71)$$

$$B_n^2 = \left(1 + \frac{\alpha^2}{n^2 \pi^2} \right)^{-1} \quad (72)$$

$$n = 1, 2, \dots$$

The only remaining quantity in equation 65 to be determined is $A_n^{(0)}$.

If we consider the case for which the initial concentration distribution is uniform, i.e.,

$$f(r) = C_0$$

the first of equations 63 yields

$$\frac{A_n^{(0)}}{C_0} = \int_{-1}^1 dr u_n^{(0)} e^{-\frac{\alpha}{2}(r+1)} \quad (63a)$$

and introducing the expressions for $u_0^{(0)}$ and $u_n^{(0)}$ from equations 66 and 67 we find on carrying out the necessary integrations

$$\frac{A_0^{(0)}}{C_0} = 2 B_0 \quad (73)$$

$$\frac{A_n^{(0)}}{C_0} = \frac{4 B_n \alpha [1 - (-1)^n e^{-\alpha}]}{n^2 \pi^2 (1 + \frac{\alpha^2}{n^2 \pi^2})} \quad (74)$$

$$n = 1, 2, \dots$$

Introducing these expressions for $A_0^{(0)}$ and $A_n^{(0)}$ along with the expressions given for $u_0^{(0)}$, $u_n^{(0)}$, $\epsilon_0^{(0)}$, $\epsilon_n^{(0)}$, B_0^2 and B_n^2 into equation 65 we have in terms of the variable ρ

$$\rho = (r - r_1)/H = \frac{1}{2}(r+1) \quad ; \quad 0 \leq \rho \leq 1$$

$$\frac{C^{(0)}(\rho, \tau)}{C_0} = \frac{2\alpha}{e^{2\alpha} - 1} e^{2\alpha\rho} + \quad (75)$$

$$+ 4\alpha e^{\alpha\rho} e^{-\frac{\alpha}{2}\tau} \sum_{n=1}^{\infty} \frac{[1 - (-1)^n e^{-\alpha}]}{n^2 \pi^2 (1 + \frac{\alpha^2}{n^2 \pi^2})^2} [\cos n\pi\rho + \frac{\alpha}{n\pi} \sin n\pi\rho] e^{-\frac{n^2 \pi^2}{2\alpha} \tau}$$

our final expression for the zero-order approximation. For completeness we repeat the definitions of the quantities α and τ ,

$$\alpha = \frac{\bar{V} H}{2 D} = \frac{1}{2} \ln(c_2/c_1)_{\text{equil}}$$

$$\tau = \frac{\bar{V}}{H} t$$

where

$$\bar{V} = S \omega^2 \bar{r} = S \omega^2 (r_1 + r_2)/2$$

6. First-Order Solution

Having obtained $u_m^{(0)}$ and $\epsilon_m^{(0)}$ we may now consider the determination of $u_m^{(1)}$ and $\epsilon_m^{(1)}$ from the second of equations 61 and 62,

$$H^{(1)} u_m^{(0)} + H^{(0)} u_m^{(1)} = -\epsilon_m^{(0)} u_m^{(1)} - \epsilon_m^{(1)} u_m^{(0)}$$

$$u_m^{(1)}(\pm 1) = \frac{\alpha}{2} u_m^{(1)}(\pm 1)$$

We will first carry this out by the method commonly used in the perturbation theory of quantum mechanics. Thus we will expand $u_m^{(1)}$ in terms of the complete set of unperturbed eigenfunctions $u_m^{(0)}$. Although we shall show how this expansion can be summed to yield a closed expression, we will prefer to obtain the solution in closed form by another method, namely, by finding a particular integral of the differential equation.

Since we know from equations 62 that $U_n^{(1)}$ satisfies the same boundary conditions as $U_n^{(0)}$ we can write the following expansion of $U_n^{(1)}$ in the complete set of orthonormal functions $U_m^{(0)}$

$$U_n^{(1)} = \sum_{m=0}^{\infty} C_{nm} U_m^{(0)} \quad (76)$$

where the C_{nm} are as yet to be determined. Introducing this expansion into the above equation for $U_n^{(1)}$, we get

$$H^{(1)} U_n^{(0)} - \sum_{m=0}^{\infty} C_{nm} [\epsilon_m^{(0)} - \epsilon_n^{(0)}] U_m^{(0)} = -\epsilon_n^{(1)} U_n^{(0)} \quad (77)$$

where we have used the fact that

$$H^{(0)} U_m^{(0)} = -\epsilon_m^{(0)} U_m^{(0)}$$

If we now multiply equation 77 by $U_k^{(0)}$ and integrate over the range of the variable ρ making use of the orthonormality property

$$\int_{-1}^1 d\rho U_m^{(0)} U_k^{(0)} = \delta_{mk}$$

we obtain

$$\int_{-1}^1 d\rho U_k^{(0)} H^{(1)} U_n^{(0)} - C_{nk} [\epsilon_k^{(0)} - \epsilon_n^{(0)}] = -\epsilon_n^{(1)} \delta_{nk}$$

so that by taking $k \neq n$ we determine the expansion coefficients to be

$$C_{nk} = \frac{\int_{-1}^1 dr u_k^{(0)} H^{(1)} u_n^{(0)}}{[\epsilon_k^{(0)} - \epsilon_n^{(0)}]} ; k \neq n \quad (78)$$

and by taking $k=n$ we find

$$\epsilon_n^{(1)} = - \int_{-1}^1 dr u_n^{(0)} H^{(1)} u_n^{(0)} \quad (79)$$

We have still to determine C_{nn} . The freedom in its choice is used in such a way that the normalization condition on the functions u_n , equation 52, is satisfied through terms of first order. Thus equation 52

$$\int_{-1}^1 dr (1 + \lambda r) e^{\lambda \frac{\alpha}{2} r^2} u_n^2 = 1$$

yields

$$\int_{-1}^1 dr (1 + \lambda r) (1 + \lambda \frac{\alpha}{2} r^2 + \dots) (u_n^{(0)} + \lambda u_n^{(1)} + \dots)^2 = 1$$

and collecting terms, we have

$$\int_{-1}^1 dr [u_n^{(0)}]^2 + \lambda \int_{-1}^1 dr [(r + \frac{\alpha}{2} r^2) (u_n^{(0)})^2 + 2 u_n^{(0)} u_n^{(1)}] + O(\lambda^2) = 1$$

so that the condition on $u_m^{(1)}$ is the following

$$\int_{-1}^1 dr u_m^{(0)} u_m^{(1)} = -\frac{1}{2} \int_{-1}^1 dr \left[r + \frac{\alpha}{2} r^2 \right] [u_m^{(0)}]^2 \quad (80)$$

Introducing the expansion for $u_m^{(1)}$, we have

$$\begin{aligned} \int_{-1}^1 dr u_m^{(0)} \sum_{m=0}^{\infty} C_{nm} u_m^{(0)} &= C_{nn} \\ &= -\frac{1}{2} \int_{-1}^1 dr \left[r + \frac{\alpha}{2} r^2 \right] [u_m^{(0)}]^2 \end{aligned}$$

as the expression determining C_{nn} . The result obtained on carrying out this integration is

$$C_{00} = -\frac{\alpha}{4} \quad (81a)$$

$$C_{nn} = -\frac{\alpha}{12} \left[1 - \frac{6}{n^2 \pi^2} \right] ; n = 1, 2, \dots \quad (81b)$$

From equation 78 we have the explicit result

$$C_{n0} = -\frac{4 B_0 B_n \alpha}{n^2 \pi^2 \left(1 + \frac{\alpha^2}{n^2 \pi^2} \right)} \left\{ \left[e^{\alpha (-1)^n} + 1 \right] + \frac{1}{\alpha} \left[e^{\alpha (-1)^n} - 1 \right] \left[1 - \frac{4 \alpha^2 / n^2 \pi^2}{\left(1 + \frac{\alpha^2}{n^2 \pi^2} \right)} \right] \right\} \quad (82)$$

$n \neq 0$

and

$$C_{0n} = 0 ; n \neq 0 \quad (83)$$

since

$$H^{(1)} u_0^{(0)} \equiv 0 \quad (84)$$

The remainder of the coefficients are found from equation 78 to be

$$C_{nm} = \frac{8 \left(1 + \frac{\alpha^2}{n^2 \pi^2}\right)}{n^2 \pi^2 \left(1 - \frac{m^2}{n^2}\right)^2} \left[1 - \frac{4 \frac{\alpha^2}{n^2 \pi^2}}{\left(1 - \frac{m^2}{n^2}\right)} \right] B_m B_n \quad (85)$$

$$m+n \text{ odd ; } m, n = 1, 2, \dots$$

and

$$C_{nm} = - \frac{8 \alpha \left(1 + \frac{\alpha^2}{n^2 \pi^2}\right)}{n^2 \pi^2 \left(1 - \frac{m^2}{n^2}\right)^2} B_m B_n \quad (86)$$

$$m+n \text{ even ; } m \neq n ; m, n = 1, 2, \dots$$

Turning now to equation 79, the formula for $\xi_n^{(1)}$, we note that because of equation 84 we have

$$\xi_0^{(1)} = 0 \quad (87)$$

which is not surprising since we know that

$$\xi_0 = 0 = \xi_0^{(0)} + \lambda \xi_0^{(1)} + \dots$$

the term $n=0$ already having been shown to yield the equilibrium contribution, all other terms decaying to zero with increasing τ .

However, on considering $\xi_n^{(1)}$ for $n=1, 2, \dots$ we find from equation 79 after introducing the appropriate functions and integrating, that we also have

$$\xi_n^{(1)} = 0 \quad ; \quad \text{all } n \quad (88)$$

Thus

$$\xi_n = \xi_n^{(0)} + o(\lambda^2)$$

and the zero-order eigenvalue should be an excellent approximation to the exact eigenvalue, especially for our case where $\lambda \approx 0.05$.

Returning now to equation 64 and retaining terms of the first order in λ we can apparently write

$$\begin{aligned} C(r, \tau) &= (1 + \lambda \frac{\alpha}{2} r^2 + \dots) e^{\frac{\alpha}{2}(\lambda+1)\tau} \sum_{n=0}^{\infty} [A_n^{(0)} + \lambda A_n^{(1)} + \dots] [u_n^{(0)} + \lambda u_n^{(1)} + \dots] e^{-[\xi_n^{(0)} + \lambda \xi_n^{(1)} + \dots]\tau} \\ &= e^{\frac{\alpha}{2}(\lambda+1)\tau} \sum_{n=0}^{\infty} e^{-\xi_n^{(0)}\tau} \left\{ A_n^{(0)} u_n^{(0)} + \lambda \left[\frac{\alpha}{2} r^2 A_n^{(0)} u_n^{(0)} + A_n^{(1)} u_n^{(0)} + A_n^{(0)} u_n^{(1)} \right] \right\} \\ &\quad + o(\lambda^2) \end{aligned} \quad (89)$$

We recall that $A_n^{(1)}$ is determined by the initial distribution, $f(r)$, through the second of equations 63, namely

$$A_n^{(1)} = \int_{-1}^1 dr [u_n^{(1)} + r u_n^{(0)}] e^{-\frac{\alpha}{2}(\lambda+1)\tau} f(r)$$

and again considering the case where

$$f(r) = c_0$$

we have

$$\frac{A_n^{(1)}}{c_0} = \int_{-1}^1 dr [u_n^{(1)} + r u_n^{(0)}] e^{-\frac{\alpha}{2}(r+1)} \quad (90)$$

or introducing the expansion for $u_n^{(1)}$

$$\frac{A_n^{(1)}}{c_0} = \int_{-1}^1 dr \sum_{m=0}^{\infty} C_{nm} u_m^{(0)} e^{-\frac{\alpha}{2}(r+1)} + \int_{-1}^1 dr r u_n^{(0)} e^{-\frac{\alpha}{2}(r+1)}$$

and comparing the first term on the right side of this equation with the formula for $A_m^{(0)}$ given by equation 63a, we find that

$$\frac{A_n^{(1)}}{c_0} = \sum_{m=0}^{\infty} C_{nm} \frac{A_m^{(0)}}{c_0} + \int_{-1}^1 dr r u_n^{(0)} e^{-\frac{\alpha}{2}(r+1)} \quad (91)$$

Since

$$u_0^{(0)} \sim e^{\frac{\alpha}{2}(r+1)}$$

the integral in this equation vanishes for the case $n=0$ and since for this case we also have

$$C_{0m} = 0 \quad ; \quad m \neq 0$$

we obtain

$$\frac{A_o^{(i)}}{c_o} = C_{o0} \frac{A_o^{(o)}}{c_o} = -\frac{\alpha}{4} \frac{A_o^{(o)}}{c_o} \quad (92)$$

Also for $n=0$ we have from equation 76

$$u_o^{(ii)} = \sum_{m=0}^{\infty} C_{om} u_m^{(o)}$$

and again using the fact that

$$C_{om} = 0 \quad ; \quad m \neq 0$$

we get the result

$$u_o^{(ii)} = C_{o0} u_o^{(o)} = -\frac{\alpha}{4} u_o^{(o)} \quad (93)$$

Thus for the case $n=0$ the term which multiplies λ in equation 89, namely

$$\left[\frac{\alpha}{2} r^2 \frac{A_o^{(o)}}{c_o} u_o^{(o)} + \frac{A_o^{(i)}}{c_o} u_o^{(o)} + \frac{A_o^{(o)}}{c_o} u_o^{(ii)} \right]$$

can be written in the following simplified form

$$\frac{\alpha}{2} \frac{A_o^{(o)}}{c_o} u_o^{(o)} (r^2 - 1)$$

Hence we have for the equilibrium result

$$\frac{c(r, \infty)}{c_o} = e^{\frac{\alpha}{2}(r+1)} \frac{A_o^{(o)}}{c_o} u_o^{(o)} \left[1 - \lambda \frac{\alpha}{2} (1-r^2) \right] + o(\lambda^2)$$

or introducing the variable ρ and the expressions for $\frac{A_0^{(0)}}{c_0}$ and $u_0^{(0)}$, we have

$$\frac{C(\rho, \infty)}{c_0} = \frac{2\alpha}{(e^{2\alpha} - 1)} e^{2\alpha\rho} [1 - \lambda 2\alpha\rho(1-\rho)] + O(\lambda^2) \quad (94)$$

That this is indeed the correct result can be easily verified. The exact equilibrium distribution is derived in Appendix I and is given by

$$\frac{C(\rho, \infty)}{c_0} = \frac{2\alpha}{(e^{2\alpha} - 1)} e^{2\alpha\rho [1 - \lambda(1-\rho)]} \quad (95)$$

Clearly the result obtained by expanding this expression and retaining terms of first order in λ is identical with equation 94.

Returning now to equation 91, we write it as follows

$$\frac{A_n^{(1)}}{c_0} = \sum_{m=0}^{\infty} C_{nm} \frac{A_m^{(0)}}{c_0} + I_n \quad (96)$$

where

$$I_n = \int_{-1}^1 dx \, x u_n^{(0)} e^{-\frac{\alpha}{2}(n+1)} \quad (97)$$

The explicit result obtained by carrying out this integration is the

following

$$I_n = \frac{4 B_n}{n^2 \pi^2 \left(1 + \frac{\alpha^2}{n^2 \pi^2}\right)^2} \left\{ \left[1 - \frac{3\alpha^2}{n^2 \pi^2}\right] \left[e^{-\alpha} (-1)^n - 1 \right] - \alpha \left[1 + \frac{\alpha^2}{n^2 \pi^2}\right] \left[e^{-\alpha} (-1)^n + 1 \right] \right\} \quad (98)$$

Since C_{nm} and $A_m^{(0)}$ have already been given, equation 96 can be used for calculating $A_n^{(1)}$. $U_n^{(1)}$ can be determined by using the expressions given for C_{nm} in the expansion, equation 76. This then completes the determination of all the quantities necessary for making calculations from equation 89.

However, this is not a very satisfactory form in which to express the solution as it requires the term by term computation of the expansions appearing in the expressions for $U_n^{(1)}$ and $A_n^{(1)}$, as just mentioned. We therefore proceed to derive expressions for these quantities in closed form. This can be done in either of two ways.

The first method is to deal directly with the sums themselves, obtaining their representations in closed form by the device of contour integration in the complex plane. By the choice of appropriate functions which are integrated over suitable contours, the summations can be evaluated. This method is outlined in Appendix II. It requires such a large amount of tedious manipulation, however, that it is very difficult to avoid errors. It is presented here only for its academic interest.

The second and much more satisfactory method is to return to the differential equation for $U_n^{(1)}$, solve it by obtaining a particular solution which is added to the complementary function

satisfying the homogeneous equation and finally determine the two constants of integration by applying the boundary condition and the normalization condition. Having obtained $u_m^{(1)}$ in closed form in this manner, $A_m^{(1)}$ is determined from it by direct integration using equation 90. We proceed now with the details of this method.

The differential equation for $u_m^{(1)}$ is (second of equations 61)

$$\left[H^{(0)} + \varepsilon_m^{(0)} \right] u_m^{(1)} = - \left[H^{(1)} + \varepsilon_m^{(1)} \right] u_m^{(0)} .$$

We have already shown that

$$\varepsilon_m^{(1)} = 0$$

so that we have to solve

$$\left[H^{(0)} + \varepsilon_m^{(0)} \right] u_m^{(1)} = - H^{(1)} u_m^{(0)} .$$

The explicit expressions for the operators $H^{(0)}$ and $H^{(1)}$ and for $u_m^{(0)}$ and $\varepsilon_m^{(0)}$ are

$$H^{(0)} = \frac{1}{2\alpha} \frac{d^2}{d\rho^2} - \frac{\alpha}{2}$$

$$H^{(1)} = \frac{1}{\alpha} \left[2\alpha\rho + (1-\alpha) \right] \left[\frac{d}{d\rho} - \alpha \right]$$

$$u_m^{(0)} = B_m \left[\cos n\pi\rho + \frac{\alpha}{n\pi} \sin n\pi\rho \right]$$

$$\varepsilon_m^{(0)} = \frac{\alpha}{2} + \frac{n^2\pi^2}{2\alpha}$$

$$n = 1, 2, \dots$$

so that

$$H^{(0)} + E_n^{(0)} = \frac{1}{2\alpha} \left[\frac{d^2}{d\rho^2} + n^2\pi^2 \right]$$

Since

$$\left[\frac{d}{d\rho} - \alpha \right] \left[\cos n\pi\rho + \frac{\alpha}{n\pi} \sin n\pi\rho \right] = -n\pi \left(1 + \frac{\alpha^2}{n^2\pi^2} \right) \sin n\pi\rho$$

the differential equation takes on the explicit form

$$\frac{d^2}{d\rho^2} U_n^{(1)} + n^2\pi^2 U_n^{(1)} = D_n [2\alpha\rho + (1-\alpha)] \sin n\pi\rho$$

$$D_n = 2n\pi \left(1 + \frac{\alpha^2}{n^2\pi^2} \right) B_n$$

Thus the homogeneous equation is

$$\frac{d^2}{d\rho^2} U_n^{(1)} + n^2\pi^2 U_n^{(1)} = 0$$

so that

$$\text{complementary function} = k_n \cos n\pi\rho + K_n \sin n\pi\rho$$

The terms of the inhomogeneous part are of the form

$$\begin{aligned} &\rho \sin n\pi\rho \\ &\sin n\pi\rho \end{aligned}$$

which on repeated differentiation yield

$$\rho \sin \rightarrow \rho \cos, \rho \sin, \cos, \sin$$

$$\sin \rightarrow \cos, \sin$$

Since each of these groups contains $\cos n\pi\rho$ and $\sin n\pi\rho$ which are present in the complementary function we must multiply the terms of each group by ρ so that the terms obtained will be different from those in the complementary function. Hence the particular solution is taken in the form

$$U_p = a_1 \rho^2 \cos n\pi\rho + a_2 \rho \cos n\pi\rho + a_3 \rho^2 \sin n\pi\rho + a_4 \rho \sin n\pi\rho$$

Substituting into the differential equation, we find that we must take

$$a_1 = -\alpha \left(1 + \frac{\alpha^2}{n^2\pi^2}\right) B_n$$

$$a_2 = -(1-\alpha) \left(1 + \frac{\alpha^2}{n^2\pi^2}\right) B_n$$

$$a_3 = 0$$

$$a_4 = \frac{\alpha}{n\pi} \left(1 + \frac{\alpha^2}{n^2\pi^2}\right) B_n$$

in order that the left-hand side agrees with the right. Thus we have for our complete solution

$$\frac{U_m^{(1)}}{B_m} = K_n \cos n\pi\rho + K_n \sin n\pi\rho - \left(1 + \frac{\alpha^2}{n^2\pi^2}\right) \left\{ \alpha \rho^2 \cos n\pi\rho + (1-\alpha) \rho \cos n\pi\rho - \frac{\alpha}{n\pi} \rho \sin n\pi\rho \right\}$$

The constants k_n and K_n must be chosen in such a way that this solution satisfies the boundary condition equation 62

$$\frac{dU_n^{(1)}}{d\rho} = \alpha U_n^{(1)} \quad ; \quad \rho = 0$$

(the same must hold at $\rho = 1$; however, this gives nothing new since $E_n^{(1)}$ has already been evaluated) and the normalization condition equation 80

$$\int_{-1}^1 dr U_n^{(0)} U_n^{(1)} = -\frac{1}{2} \int_{-1}^1 dr \left(r + \frac{\alpha}{2} r^2 \right) [U_n^{(0)}]^2$$

which when written more explicitly is

$$\int_0^1 d\rho X_n \frac{U_n^{(1)}}{B_n} = -\frac{\alpha}{24} \left[1 - \frac{6}{n^2 \pi^2} \right] \left[1 + \frac{\alpha^2}{n^2 \pi^2} \right]$$

The boundary condition and this normalization condition provide us with two simultaneous equations for the determination of k_n and K_n . Omitting the further details we state the result one obtains on solving these equations

$$k_n = \frac{1}{2} \left(1 + \frac{\alpha^2}{n^2 \pi^2} \right) - \frac{\alpha}{4}$$

$$K_n = \frac{\alpha}{n\pi} \left(1 + \frac{\alpha^2}{n^2 \pi^2} \right) \left(\frac{1}{\alpha} - \frac{1}{2} \right) - \frac{\alpha^2}{4 n \pi}$$

Our solution can now be written in the form

$$\frac{U_n^{(1)}}{B_n} = h_n^{(1)} - \frac{\alpha}{4} X_n \tag{99}$$

where

$$h_n^{(1)} = \left(1 + \frac{\alpha^2}{n^2\pi^2}\right) \left\{ \left[\left(\rho - \frac{1}{2}\right) + \frac{1}{\alpha} \right] \frac{\alpha}{n\pi} \sin n\pi\rho \right. \\ \left. - \left[\left(\rho - \frac{1}{2}\right) - \alpha\rho(1-\rho) \right] \cos 2n\pi\rho \right\}$$

and as usual

$$X_n = \cos n\pi\rho + \frac{\alpha}{n\pi} \sin n\pi\rho$$

This concludes the derivation for $U_n^{(1)}$.

We now determine $A_n^{(1)}$ (for the initially uniform distribution case). From equation 90 we have

$$\frac{A_n^{(1)}}{c_0} = 2 \int_0^1 d\rho U_n^{(1)} e^{-\alpha\rho} + I_n$$

where I_n , which does not involve $U_n^{(1)}$, is defined by equation 97 and is given explicitly by equation 98. Introducing the expression just found for $U_n^{(1)}$ and carrying out the integration, we find

$$\frac{A_n^{(1)}}{c_0} = \frac{\alpha B_n}{n^2\pi^2 \left(1 + \frac{\alpha^2}{n^2\pi^2}\right)^2} \left\{ \left[\left(\frac{32}{n^2\pi^2} - 1\right) - \frac{\alpha^2}{n^2\pi^2} \right] \left[1 \pm e^{-\alpha} \right] \alpha \right. \\ \left. - \left[6 + \frac{4\alpha^2}{n^2\pi^2} - \frac{2\alpha^4}{n^4\pi^4} \right] \left[1 \mp e^{-\alpha} \right] \right\} \quad (100)$$

where the upper sign is to be taken when n is odd and the lower sign when n is even. From equation 74 we have

$$\frac{A_n^{(0)}}{c_0} = \frac{4\alpha B_n \left[1 \pm e^{-\alpha} \right]}{n^2\pi^2 \left(1 + \frac{\alpha^2}{n^2\pi^2}\right)} \quad (101)$$

so that taking the ratio with equation 100, we get

$$\frac{A_n^{(1)}}{A_n^{(0)}} = \frac{1}{4 \left(1 + \frac{\alpha^2}{n^2 \pi^2}\right)} \left\{ \left[\left(\frac{32}{n^2 \pi^2} - 1 \right) - \frac{\alpha^2}{n^2 \pi^2} \right] \alpha - \left[6 + \frac{4\alpha^2}{n^2 \pi^2} - \frac{2\alpha^4}{n^4 \pi^4} \right] \left[\frac{1 - e^{-\alpha}}{1 + e^{-\alpha}} \right]^{\pm 1} \right\} \quad (102)$$

Multiplying equation 101 by B_n we also find

$$\begin{aligned} B_n \frac{A_n^{(0)}}{C_0} &= \frac{4 B_n^2 \alpha [1 \pm e^{-\alpha}]}{n^2 \pi^2 \left(1 + \frac{\alpha^2}{n^2 \pi^2}\right)} \\ &= \frac{4 \alpha [1 \pm e^{-\alpha}]}{n^2 \pi^2 \left(1 + \frac{\alpha^2}{n^2 \pi^2}\right)^2} \end{aligned} \quad (103)$$

We are now in a position to write down the final result of our perturbation theory of the approach toward equilibrium.

$$\begin{aligned} \frac{C(\rho, \tau)}{C_0} &= \frac{2\alpha}{(e^{2\alpha} - 1)} e^{2\alpha\rho} \left[1 - \lambda 2\alpha\rho(1-\rho) \right] + \\ &+ e^{\alpha\rho} e^{-\frac{\alpha}{2}\tau} \sum_{n=1}^{\infty} e^{-\frac{n^2 \pi^2}{2\alpha}\tau} \frac{B_n A_n^{(0)}}{C_0} \left\{ \left[1 - 2\alpha\lambda\rho(1-\rho) + \lambda \left(\frac{A_n^{(1)}}{A_n^{(0)}} + \frac{\alpha}{4} \right) \right] \chi_n(\rho) + \lambda h_n^{(1)}(\rho) \right\} + \\ &+ o(\lambda^2) \end{aligned} \quad (104)$$

For convenience we repeat the expressions for the quantities appearing in this result.

$$B_n \frac{A_n^{(0)}}{c_0} = \frac{4\alpha [1 \pm e^{-\alpha}]}{n^2 \pi^2 (1 + \frac{\alpha^2}{n^2 \pi^2})^2}$$

$$\left(\frac{A_n^{(1)}}{A_n^{(0)}} + \frac{\alpha}{4} \right) = \frac{1}{4(1 + \frac{\alpha^2}{n^2 \pi^2})} \left\{ \frac{32\alpha}{n^2 \pi^2} - \left[6 + \frac{4\alpha^2}{n^2 \pi^2} - \frac{2\alpha^4}{n^4 \pi^4} \right] \left[\frac{1 - e^{-\alpha}}{1 + e^{-\alpha}} \right]^{\pm 1} \right\}$$

$$X_n(\rho) = \cos n\pi\rho + \frac{\alpha}{n\pi} \sin n\pi\rho$$

$$h_n^{(1)}(\rho) = \left(1 + \frac{\alpha^2}{n^2 \pi^2} \right) \left\{ \left[\left(\rho - \frac{1}{2} \right) + \frac{1}{\alpha} \right] \frac{\alpha}{n\pi} \sin n\pi\rho - \left[\left(\rho - \frac{1}{2} \right) - \alpha\rho(1-\rho) \right] \cos n\pi\rho \right\}$$

Where there are two signs appearing, the upper sign is to be taken when n is odd and the lower sign when n is even.

7. Comparison With Archibald's Numerical Results

As stated in the introduction, section 1, Archibald has made calculations for a specific experiment both from his exact (12) and approximate (13) solutions. The position variable used by Archibald is Z where

$$Z = \frac{\delta}{2} r^2 \quad (105)$$

$$\delta = S \omega^2 / D$$

and he introduces the parameters a and b which are the values of Z at the extremities of the cell. Thus

$$a = z_1 = \frac{\delta}{2} r_1^2 = \frac{S \omega^2}{2 D} r_1^2 \quad (106)$$

$$b = z_2 = \frac{\delta}{2} r_2^2 = \frac{S \omega^2}{2 D} r_2^2$$

These he relates to the experimental quantities by introducing the fundamental formula for S/D , equation 31,

$$S/D = \frac{M(1-\bar{v}d)}{RT}$$

getting

$$a = \frac{M(1-\bar{v}d)\omega^2}{2RT} r_1^2 \quad (107)$$

$$b = \frac{M(1-\bar{v}d)\omega^2}{2RT} r_2^2$$

The data for the specific example he considers in which the dissolved substance was carbon-monoxide hemoglobin are the following

$$M = 68,000 \text{ gms./mole}$$

$$\bar{v} = 0.749 \text{ cm}^3/\text{gm.}$$

$$\omega = 290 \pi \text{ rdns./sec.}$$

$$T = 293^\circ\text{K}$$

with the cell dimensions*

$$r_1 = 4.160 \text{ cm.}$$

$$r_2 = 4.632 \text{ cm.}$$

The values of a and b corresponding to these data are

$$a = 5.0$$

$$b = 6.2$$

In calculating c/c_0 Archibald used only the equilibrium term ($n = 0$) plus the term for $n = 1$, omitting the terms for $n > 2$. Although he found this necessary (in the exact case) because of the extreme labor required to calculate the higher terms, the omission is partly justified due to the rapid decay of these terms as compared to the decay of the term for $n = 1$.

* The value of 4.61 given for r_2 in references 12 and 13 is apparently in error because the value given for b does not agree with that which would be calculated using $r_2 = 4.61$. In J. Phys. and Colloid Chem. 51, 1204 (1947), where Archibald presents this same example, the value given for r_2 is 4.632 which does in fact yield the value for b which is used in all of these publications, namely, 6.2. Because of this last fact and because it is b and not r_2 which enters into Archibald's calculations, we take 4.632 as the value for r_2 .

Dropping the terms beyond $n = 1$, he makes his calculations from a formula of the form

$$\frac{c}{c_0}(z, \tau_A) = K_1 e^z + K_2 N(z) e^{-K_3 \tau_A} \quad (108)$$

where the specific values for K_2 and K_3 and the tabulation of the function $N(z)$ are arrived at after a very lengthy computation based on the data for the given experiment. Of particular interest to us is the value which he gets for K_3 , namely,

$$K_3 = 39.70$$

The time variable τ_A is defined as

$$\tau_A = 2 S \omega^2 t \quad (109)$$

We recall that our time variable τ is defined differently

$$\begin{aligned} \tau &= \frac{\bar{V}}{H} t \\ &= \frac{S \omega^2 \bar{r}}{H} t \end{aligned}$$

so that

$$\tau / \tau_A = \frac{\bar{r}}{2H}$$

or

$$\tau = \frac{\bar{r}}{2H} \tau_A \quad (110)$$

Since

$$\begin{aligned} b - a &= \frac{S \omega^2}{2 D} (r_2^2 - r_1^2) \\ &= \frac{S \omega^2}{D} \bar{r} H \\ &= \frac{\bar{V}}{D} H \end{aligned}$$

and since by definition we have

$$\alpha = \frac{\bar{V} H}{2 D}$$

we find

$$\alpha = \frac{1}{2} (b - a) \quad (111)$$

Thus for the experiment being considered

$$\alpha = 0.6$$

From the time exponential in the term for $n=1$ in equation 104 and from the relation between τ and τ_a given by equation 110, we find that the value of K_3 from our theory is to be calculated from

$$\left[\frac{\alpha}{2} + \frac{\pi^2}{2\alpha} \right] \frac{\bar{r}}{2H} \quad (112)$$

Introducing the appropriate values for the parameters we easily obtain the result 39.70 which is in exact agreement with the rigorous result of Archibald. He states that it required several weeks of computing to obtain K_3 and the labor involved in getting the corresponding quantity

in the term for $n = 2$ seemed prohibitive. We have for any value of n the general result

$$\frac{\bar{r}}{2H} \left\{ \left[\frac{\alpha}{2} + \frac{n^2 \pi^2}{2\alpha} \right] + O(\lambda^2) \right\} \quad (113)$$

for the coefficient of $-\tau_A$ in the time exponential, the first-order correction having been shown to vanish. Since the value of λ for the given experiment is

$$\begin{aligned} \lambda &= \frac{r_2 - r_1}{r_2 + r_1} \\ &= 0.0537 \end{aligned} \quad (114)$$

we are not particularly surprised at the accuracy we have obtained. By means of his approximate formula Archibald calculates a value of 39.77 for K_3 . Aside from being considerably more complex in form than our expression, equation 113, it has the more serious disadvantage in that a number of unsystematic approximations are made in its derivation so that there is no formalism present for its modification in cases where these approximations are not completely satisfactory.

To complete the correspondence between the quantities used by Archibald and those used here, we consider the position variables ρ and z . Now

$$\rho = \frac{r - r_1}{r_2 - r_1}$$

$$= \frac{r_1}{H} \left[\frac{r}{r_1} - 1 \right]$$

But

$$z/a = (r/r_1)^2$$

and therefore we have for the relation between ρ and z

$$\rho = \frac{r_1}{H} \left[(z/a)^{1/2} - 1 \right] \quad (115)$$

For the $n = 1$ term we have from equation 104

$$e^{\alpha \rho} e^{-\left[\frac{\alpha}{2} + \frac{\pi^2}{2\alpha}\right] \frac{\bar{r}}{2H} \tau_A} \cdot \left[\frac{B_1 A_1^{(0)}}{c_0} \right] \left\{ \left[1 - 2\alpha \lambda \rho (1 - \rho) + \lambda \left(\frac{A_1^{(0)}}{A_1^{(0)}} + \frac{\alpha}{4} \right) \right] X_1(\rho) \right. \quad (116)$$

$$\left. + \lambda h_1^{(1)}(\rho) \right\}$$

where, as we have already mentioned,

$$\left[\frac{\alpha}{2} + \frac{\pi^2}{2\alpha} \right] \frac{\bar{r}}{2H} = 39.70$$

for the values of α , \bar{r} , and H being dealt with. From equation

103 we calculate using $\alpha = 0.6$

$$\frac{B_1 A_1^{(0)}}{c_0} = \frac{4\alpha [1 + e^{-\alpha}]}{\pi^2 (1 + \alpha^2/\pi^2)^2}$$

$$= 0.3506$$

and from equation 102

$$\left[\frac{A_1^{(1)}}{A_1^{(0)}} + \frac{\alpha}{4} \right] = \frac{1}{4(1 + \alpha^2/\pi^2)} \left\{ \frac{32\alpha}{\pi^2} - \left[6 + \frac{4\alpha^2}{\pi^2} - \frac{2\alpha^4}{\pi^4} \right] \left[\frac{1 - e^{-\alpha}}{1 + e^{-\alpha}} \right] \right\}$$

$$= 0.0376$$

Introducing these computed results along with the values $\alpha = 0.6$ and $\lambda = 0.0537$ into the expression 116, the $n = 1$ term takes on the following form which is suitable for making calculations

$$0.3506 e^{0.6\rho} \left\{ [1 - 0.0644\rho(1-\rho) + 0.0020] X_1(\rho) + 0.0537 h_1^{(1)}(\rho) \right\} e^{-39.70\tau_A} \quad (117)$$

In Table I we tabulate the functions $X_1(\rho)$ and $h_1^{(1)}(\rho)$

$$X_1(\rho) = \cos \pi \rho + \frac{\alpha}{\pi} \sin \pi \rho$$

$$h_1^{(1)}(\rho) = \left(1 + \frac{\alpha^2}{\pi^2}\right) \left\{ \left[\left(\rho - \frac{1}{2}\right) + \frac{1}{\alpha} \right] \frac{\alpha}{\pi} \sin \pi \rho - \left[\left(\rho - \frac{1}{2}\right) - \alpha \rho(1-\rho) \right] \cos \pi \rho \right\}$$

for the case $\alpha = 0.6$.

We remark here that to a very good approximation the term for $n = 1$, expression 116, vanishes for all times for $\rho = \rho_0$ where ρ_0 is such that

$$X_1(\rho_0) = 0 = \cos \pi \rho_0 + \frac{\alpha}{\pi} \sin \pi \rho_0$$

or

$$\tan \pi \rho_0 = - \frac{\pi}{\alpha} \quad (118)$$

This means that for times such that the terms for $n > 1$ have become negligible, the concentration curves at different times will all pass through a common point ("hinge point") located at $\rho = \rho_0$, having a fixed concentration equal to the equilibrium value for that point. It might appear that this could be made the basis for a method of determining molecular weight since α could be measured by determining the "hinge point", ρ_0 . However, because of the small values of α involved, the value of ρ_0 varies only slightly even for large relative variations in α as can be deduced from equation 118, so that the sensitivity of the method is not sufficient for obtaining quantitative results. One can avoid the difficulty by working at large α values but then the terms for $n > 1$ do not decay as rapidly relative to the $n = 1$ term which means a greater delay in the fixing of the hinge point.

At equilibrium we have from equation 104

$$\frac{c(\rho, \infty)}{c_0} = \frac{2\alpha}{(e^{2\alpha} - 1)} e^{2\alpha\rho} [1 - \lambda 2\alpha\rho(1-\rho)]$$

to within terms of order λ^2 . In Table II we tabulate this function ($\alpha = 0.6$) both in zero order and in first order ($\lambda = 0.0537$) and compare with the exact results given by Archibald. It is seen that the

inclusion of the λ term results in values which are in almost perfect agreement with the true values.

We tabulate the $n = 1$ term, 117, in zero order and in first order for τ_A equal to zero in Table III and for τ_A equal to 0.015 in Table IV comparing with Archibald's exact and approximate results. We find that although our zero-order approximation has a form which is considerably more simple than the formula of Archibald's approximation, it nevertheless leads to slightly more satisfactory results at least for the specific example being considered here.

Since the zero-order and first-order $n = 1$ terms decay at exactly the same rate as the correct $n = 1$ term, we have for the error $\Delta(\tau_A)$ at "time" τ_A

$$\Delta_0(\tau_A) = \Delta_0(0) e^{-39.70 \tau_A}$$

$$\Delta_1(\tau_A) = \Delta_1(0) e^{-39.70 \tau_A}$$

(119)

TABLE I

Tabulation of $X_1(\rho)$ and $h_1^{(1)}(\rho)$ for the Case $\alpha = 0.6$

z	ρ	$X_1(\rho)$	$h_1^{(1)}(\rho)$
5.0	0.000	1.000	0.518
5.1	0.087	1.015	0.527
5.2	0.174	0.953	0.503
5.3	0.261	0.822	0.458
5.4	0.345	0.637	0.405
5.5	0.430	0.404	0.358
5.6	0.513	0.150	0.326
5.7	0.595	-0.111	0.318
5.8	0.678	-0.368	0.335
5.9	0.761	-0.601	0.375
6.0	0.841	-0.787	0.428
6.1	0.922	-0.924	0.482
6.2	1.000	-1.000	0.518

TABLE II

Equilibrium Concentration Distribution ($\alpha = 0.6$)

z	ρ	c/c _o		
		Zero Order	First Order*	Exact
5.0	0.000	0.517	0.517	0.517
5.1	0.087	0.574	0.571	0.572
5.2	0.174	0.637	0.631	0.632
5.3	0.261	0.708	0.699	0.698
5.4	0.345	0.783	0.772	0.772
5.5	0.430	0.866	0.852	0.853
5.6	0.513	0.958	0.943	0.942
5.7	0.595	1.056	1.040	1.042
5.8	0.678	1.167	1.151	1.151
5.9	0.761	1.289	1.274	1.272
6.0	0.841	1.419	1.407	1.406
6.1	0.922	1.563	1.556	1.554
6.2	1.000	1.717	1.717	1.717

$$\overline{|\Delta_o|} = 0.010 \quad , \quad \overline{|\Delta_1|} = 0.001$$

$$|\Delta_o|_{\max} = 0.017 \quad , \quad |\Delta_1|_{\max} = 0.002$$

Δ_o denotes the difference between the zero order and the exact.

Δ_1 denotes the difference between the first order and the exact.

* Using $\lambda = 0.0537$.

TABLE III

Contribution to c/c_0 from the $n=1$ Term for $\tau_A = 0$.

Z	ρ	Arch. Approx.	Zero Order	First Order	Arch. Exact
5.0	0.000	0.380	0.351	0.361	0.363
5.1	0.087	0.405	0.375	0.384	0.387
5.2	0.174	0.401	0.371	0.379	0.380
5.3	0.261	0.367	0.337	0.344	0.348
5.4	0.345	0.301	0.275	0.281	0.281
5.5	0.430	0.209	0.183	0.189	0.188
5.6	0.513	0.094	0.072	0.079	0.074
5.7	0.595	-0.038	-0.056	-0.047	-0.051
5.8	0.678	-0.182	-0.194	-0.182	-0.184
5.9	0.761	-0.323	-0.333	-0.318	-0.315
6.0	0.841	-0.452	-0.457	-0.441	-0.439
6.1	0.922	-0.568	-0.563	-0.546	-0.544
6.2	1.000	-0.652	-0.639	-0.622	-0.625

$$\overline{|\Delta_A|} = 0.017, \quad \overline{|\Delta_0|} = 0.011, \quad \overline{|\Delta_1|} = 0.002$$

$$|\Delta_A|_{\max} = 0.027, \quad |\Delta_0|_{\max} = 0.019, \quad |\Delta_1|_{\max} = 0.005$$

TABLE IV

Contribution to c/c_0 from the $n=1$ Term for $\tau_A = 0.015$.

Z	ρ	Arch. Approx.	Zero Order	First Order	Arch. Exact
5.0	0.000	0.209	0.194	0.199	0.200
5.1	0.087	0.223	0.207	0.212	0.213
5.2	0.174	0.221	0.205	0.209	0.209
5.3	0.261	0.202	0.186	0.190	0.192
5.4	0.345	0.166	0.152	0.155	0.155
5.5	0.430	0.115	0.101	0.104	0.104
5.6	0.513	0.052	0.040	0.044	0.041
5.7	0.595	-0.021	-0.031	-0.026	-0.028
5.8	0.678	-0.100	-0.107	-0.100	-0.101
5.9	0.761	-0.178	-0.184	-0.175	-0.174
6.0	0.841	-0.249	-0.252	-0.243	-0.242
6.1	0.922	-0.313	-0.310	-0.301	-0.300
6.2	1.000	-0.359	-0.352	-0.343	-0.345

$$\overline{|\Delta_A|} = 0.009, \quad \overline{|\Delta_0|} = 0.006, \quad \overline{|\Delta_1|} = 0.001.$$

$$|\Delta_A|_{\max} = 0.014, \quad |\Delta_0|_{\max} = 0.010, \quad |\Delta_1|_{\max} = 0.003.$$

B. FAST METHOD FOR REACHING EQUILIBRIUM

1. Introduction

Although the equilibrium method (1) in the ultracentrifuge is inherently a very powerful one for the study of molecular weight and polydispersity, it suffers from the fact that a long time is often required (of the order of several days) in order to arrive effectively at the equilibrium state. The disadvantage of this lies not only in the resulting delay in the procurement of experimental results. One must also consider the difficulty involved in maintaining a constant speed of rotation and constant temperature in the apparatus over such long periods of time. A further serious disadvantage lies in the fact that many of the substances to which it is desirable to apply the method are not sufficiently stable to endure such lengthy experiments.

Because of these disadvantages, the equilibrium method has not been extensively used. The sedimentation velocity method (1), although not resting on as sound a theoretical basis, has nevertheless been more popular due to the much shorter times required for obtaining results.

In view of this situation, it seemed of importance to investigate the possibility of eliminating the disadvantage of slowness from the equilibrium method. Now in the conventional equilibrium method, one starts with an initially uniform distribution of the substance under investigation in a suitable solvent and allows the processes of sedimentation and opposing diffusion to transport the

material, resulting finally in the appropriate non-uniform equilibrium distribution in the presence of the centrifugal field. A saving of time might be effected if one starts initially with a non-uniform solution in the form of a step function having pure solvent in the top (nearer the axis of rotation) portion of the cell and the solution in the bottom portion,* the reasoning being that by starting in this manner, less material has to be transported in order to arrive at the equilibrium distribution and this might result in a decrease in the time required. The availability of the synthetic boundary cell (18) means that it should be possible to set up the experiment with the step function distribution. The questions are how to make the best choice for the initial distribution for a given experiment and what saving in time can be expected. In order to obtain the answers to these questions we return to the theory of the approach to equilibrium which has been presented in section A.

2. Derivation of the Optimum Step Functions

The approach toward equilibrium is described by the formal solution, equation 48

$$c(\rho, \tau) - c(\rho, \infty) = c^{\lambda \frac{\alpha}{2} (2\rho - 1)^2} e^{\alpha \rho} \sum_{n=1}^{\infty} A_n u_n(\rho) e^{-\epsilon_n \tau} \quad (120)$$

* Professor Schomaker pointed out that there is no need to restrict the step function to this special form and that one should consider a more general form, using a solution of one concentration in the top of the cell and a second solution of a higher concentration in the bottom portion.

We have obtained explicit expressions for u_n and ε_n , which are valid to within terms of order λ^2 , by means of a perturbation treatment

$$u_n(\rho) = u_n^{(0)}(\rho) + \lambda u_n^{(1)}(\rho) + o(\lambda^2)$$

$$\varepsilon_n = \varepsilon_n^{(0)} + o(\lambda^2)$$

where

$$\varepsilon_n^{(0)} = \frac{n^2 \pi^2}{2\alpha} + \frac{\alpha}{2}$$

and

$$\lambda = \frac{r_2 - r_1}{r_2 + r_1}$$

The A_n are constants for a given value of α and are determined by the initial distribution of concentration, $f(\rho)$, through the relation given by equation 53,

$$A_n = 2 \int_0^1 d\rho [1 + \lambda(2\rho - 1)] u_n(\rho) e^{-\alpha\rho} f(\rho) . \quad (121)$$

Because of the rapid increase of $\varepsilon_n^{(0)}$ with n , for the α -values of interest, the deviation from equilibrium is eventually

determined by the leading term ($n = 1$) of the sum in equation 120. We therefore assume that the optimum starting conditions will be such that the necessary condition

$$A_1 = 0$$

is satisfied. Since the initial step distribution which will accomplish this will depend on the value of λ involved, we also express $f(\rho)$ in the perturbation scheme taking

$$f(\rho) = f^{(0)} + \lambda f^{(1)} + \dots$$

$$= C_I ; 0 < \rho < \beta$$

$$C_{II} = C_{II}^{(0)} + \lambda C_{II}^{(1)} + \dots ; \beta < \rho < 1$$

Defining

$$R^{(0)} = C_{II}^{(0)} / C_I$$

$$R^{(1)} = C_{II}^{(1)} / C_I$$

we can write

$$f(\rho) = C_I ; 0 < \rho < \beta$$

$$C_I R^{(0)} [1 + \lambda R^{(1)} / R^{(0)} + \dots] ; \beta < \rho < 1$$

and for the ratio of the concentrations in the two portions of the cell we have

$$\frac{C_{II}}{C_I} = R^{(0)} \left[1 + \lambda R^{(1)}/R^{(0)} + \dots \right] \quad (122)$$

$R^{(0)}$, $R^{(1)}$, \dots and β are to be determined in such a way as to make A_1 vanish.

Introducing this initial distribution into equation 121 and collecting like powers of λ we get

$$A_n = A_n^{(0)} + \lambda A_n^{(1)} + \dots$$

where

$$\begin{aligned} A_n^{(0)} &= 2 \int_0^1 d\rho e^{-\alpha\rho} u_m^{(0)} f^{(0)} \\ A_n^{(1)} &= 2 \int_0^1 d\rho e^{-\alpha\rho} \left\{ [(2\rho-1)u_m^{(0)} + u_m^{(1)}] f^{(0)} + u_m^{(0)} f^{(1)} \right\} \\ &\vdots \end{aligned} \quad (123)$$

with

$$\begin{aligned} f^{(0)} &= C_I \left\{ [1 - A(\rho - \beta)] + R^{(0)} A(\rho - \beta) \right\} \\ f^{(1)} &= C_I R^{(1)} A(\rho - \beta) \\ &\vdots \end{aligned}$$

where we have introduced the unit step function

$$A(x) = \begin{cases} 0 & x < 0 \\ 1 & x > 0 \end{cases}$$

Now setting $A_1^{(0)}$ equal to zero we get from the first of equations 123

$$0 = \int_0^1 d\rho e^{-\alpha\rho} X_1(\rho) \left\{ [1 - A(\rho - \beta)] + R^{(0)} A(\rho - \beta) \right\} \quad (124)$$

$$X_1(\rho) = \cos \pi\rho + \frac{\alpha}{\pi} \sin \pi\rho$$

which on carrying out the integrations leads to the following equation determining $R^{(0)}$ and β

$$R^{(0)} = \frac{\gamma_1 - e^{\beta\alpha}}{\gamma_1 + e^{-(1-\beta)\alpha}} \quad (125)$$

where

$$\gamma_1 = \cos \pi\beta - \left[(\pi^2 - \alpha^2) / 2\pi\alpha \right] \sin \pi\beta$$

Now the equilibrium distributions most favorable for experimental study in the ultracentrifuge are those for which

$$(c_2/c_1)_{\text{equil}} = 2 - 4$$

(1 and 2 denote the extremities of the cell) so that using an assumed value for the molecular weight, M , in the expression

$$\ln(c_2/c_1)_{\text{equil}} = \frac{M(1-\bar{v}d)\omega^2}{2RT} (r_2^2 - r_1^2) \quad (126)$$

one chooses a speed ω such that the concentration ratio will lie in the desired range. The corresponding range for the parameter α is easily calculated from the relation

$$\begin{aligned} \alpha &= \frac{1}{2} \ln(c_2/c_1)_{\text{equil}} \\ &= 0.35 - 0.70 \end{aligned}$$

(We recall that in Archibald's example for which we made calculations in the preceding section, α had the value 0.6.)

To illustrate the nature of the result expressed in equation 125, we calculated $R^{(0)}$ as a function of β for the case $\alpha = 0.6$.

The results are presented in Table V and plotted in Figure 1 (solid curve). The curve shows that there exists a wide range of choices for the location of the synthetic boundary all of which are consistent with the vanishing of $A_1^{(0)}$. It is interesting to note that included in this range there is the choice of pure solvent as the top layer ($R^{(0)} = \infty$) with the boundary placed at $\beta = 0.194$. The degree of freedom in the choice of the initial step function resulting from the presence of the two parameters $R^{(0)}$ and β can also be used to make

$$A_2^{(0)} = 0$$

so that in analogy with equation 124 we take

$$0 = \int_0^1 d\rho e^{-\alpha\rho} \chi_2(\rho) \left\{ [1 - A(\rho - \beta)] + R^{(0)} A(\rho - \beta) \right\}$$

$$\chi_2(\rho) = \cos 2\pi\rho + \frac{\alpha}{2\pi} \sin 2\pi\rho$$

which leads to

$$R^{(0)} = \frac{\chi_2 - e^{\beta\alpha}}{\chi_2 - e^{-(1-\beta)\alpha}} \quad (127)$$

where

$$\gamma_2 = \cos 2\pi\beta - \left[(4\pi^2 - \alpha^2) / 4\pi\alpha \right] \sin 2\pi\beta .$$

The results calculated from this equation, again for the case $\alpha = 0.6$, are presented in Table VI and plotted in Figure 1 (dashed curves). The simultaneous solution of equations 125 and 127 yields the particular choice for $R^{(0)}$ and β such that both $A_1^{(0)}$ and $A_2^{(0)}$ vanish. This is easily obtained as the point of intersection of the solid and dashed curves in Figure 1 with the result

$$\beta = 0.535$$

$$R^{(0)} = 2.15$$

Since $A_2^{(0)}$ is usually quite small regardless of the nature of the initial distribution, this result is not particularly important from a practical standpoint. In applying the fast method the chief emphasis should be placed on the attempt to have conditions as ideal as possible for the vanishing of $A_1^{(0)}$.

We illustrate the appearance of the optimum initial distributions in Figure 2 which is a plot of three of the possible choices for the initial step function all of which cause $A_1^{(0)}$ to vanish, with the central one ($\beta = 0.535$) also causing $A_2^{(0)}$ to vanish. For comparison we include the equilibrium distribution which is given by the continuous curve. It is clear that the optimum step functions do

not have to be good approximations to the final distribution. Apparently sedimentation and diffusion play a vital role in determining the suitability of a given step function. The criterion of the vanishing of A_1 appears to be the only logical one to apply, giving the barest requirements which must be met by an optimum initial distribution. Of course we expect, however, that if we cause an increasing number of the A_n to vanish by introducing more and more parameters into the initial distribution (more steps) we will be approximating the final distribution more and more closely since we know that all the A_n will vanish only if we start with the actual equilibrium distribution.

Thus far, in deriving the optimum step functions, we have been concerned only with the zero-order approximation. We wish now to examine the effect of including the first order term in equation 122

$$\frac{C_{II}}{C_I} = R^{(0)} \left[1 + \lambda \frac{R^{(1)}}{R^{(0)}} \right] + O(\lambda^2)$$

We therefore return to the second of equations 123 which is the formula for $A_n^{(1)}$. Specializing to the case $n = 1$ and equating to zero we have

$$0 = \int_0^1 d\rho e^{-\alpha\rho} \left\{ [(2\rho-1)u_1^{(0)} + u_1^{(1)}] f^{(0)} + u_1^{(0)} f^{(1)} \right\}$$

TABLE V

Position of the Step and the Corresponding Ratio of Concentrations in the Layers such that $A_1^{(0)}$ Vanishes.

Calculated from Equation 125 for the Case $\alpha = 0.6$, i.e.,

$$(c_2/c_1)_{\text{equil}} = 3.32 .$$

β	$R^{(0)}$
0.000-0.194	neg.
0.194	$+\infty$
0.20	30
0.25	5.2
0.30	3.4
0.35	2.72
0.40	2.42
0.45	2.26
0.50	2.17
0.55	2.14
0.60	2.16
0.65	2.22
0.70	2.32
0.75	2.49
0.80	2.78
0.85	3.30
0.90	4.37
0.95	7.69
1.00	∞

TABLE VI

Position of the Step and the Corresponding Ratio of Concentrations in the Layers such that $A_2^{(0)}$ Vanishes.

Calculated from Equation 127 for the Case $\alpha = 0.6$, i.e.,

$$(c_2/c_1)_{\text{equil}} = 3.32 .$$

β	$R^{(0)}$
0.000-0.01	neg.
0.02	3.11
0.05	1.38
0.10	1.17
0.20	1.10
0.30	1.09
0.40	1.13
0.50	1.35
0.51	1.43
0.52	1.56
0.53	1.81
0.54	2.43
0.55	6.66
0.56	-1.92
0.57	-0.21
0.58	0.25
0.59	0.44
0.60	0.56
0.70	0.82
0.80	0.83
0.90	0.74
1.00	$-\infty$

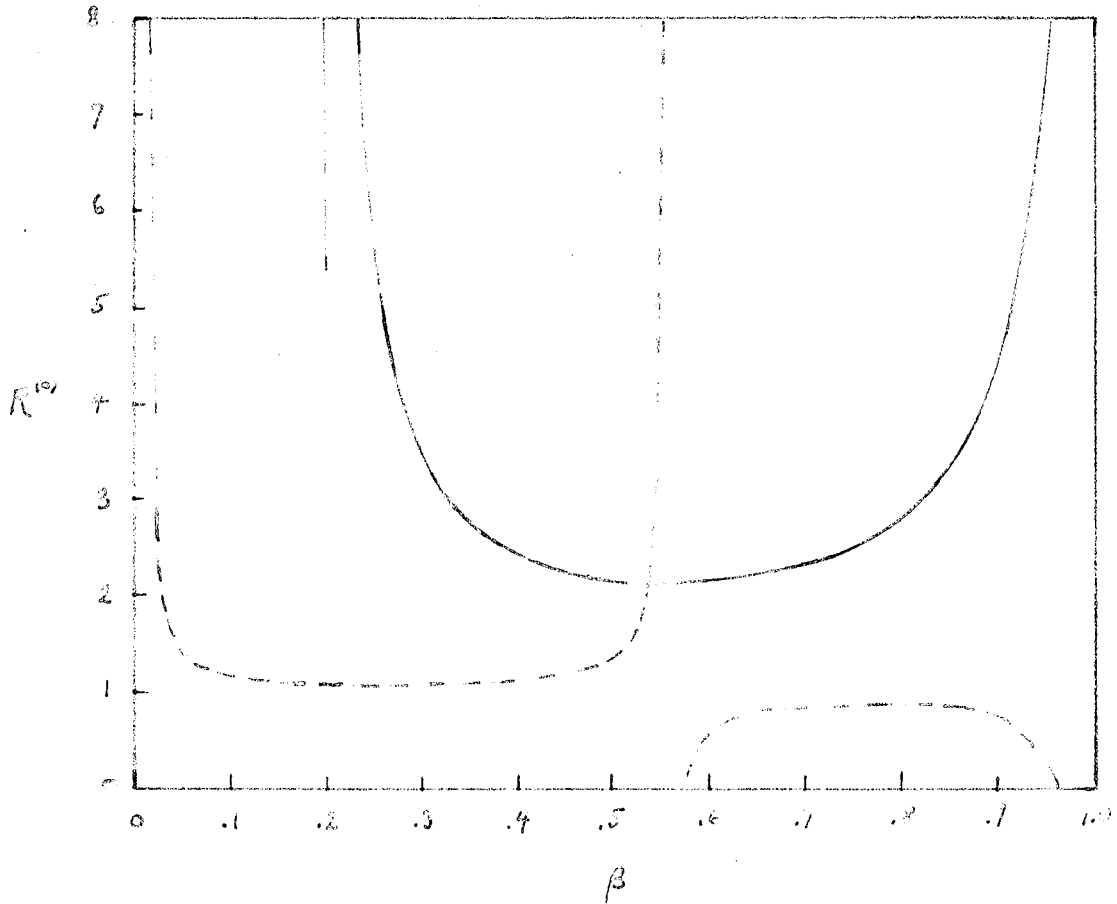


Figure 1. Position of the step, β , and the corresponding relative concentrations in the layers, $R^{(0)}$, such that:

$$A_1^{(0)} = 0 \quad (\text{solid curve})$$

$$A_2^{(0)} = 0 \quad (\text{dashed curve})$$

Calculated for the case $\alpha = 0.6$, i.e., $(c_2/c_1)_{\text{equil}} = 3.52$.

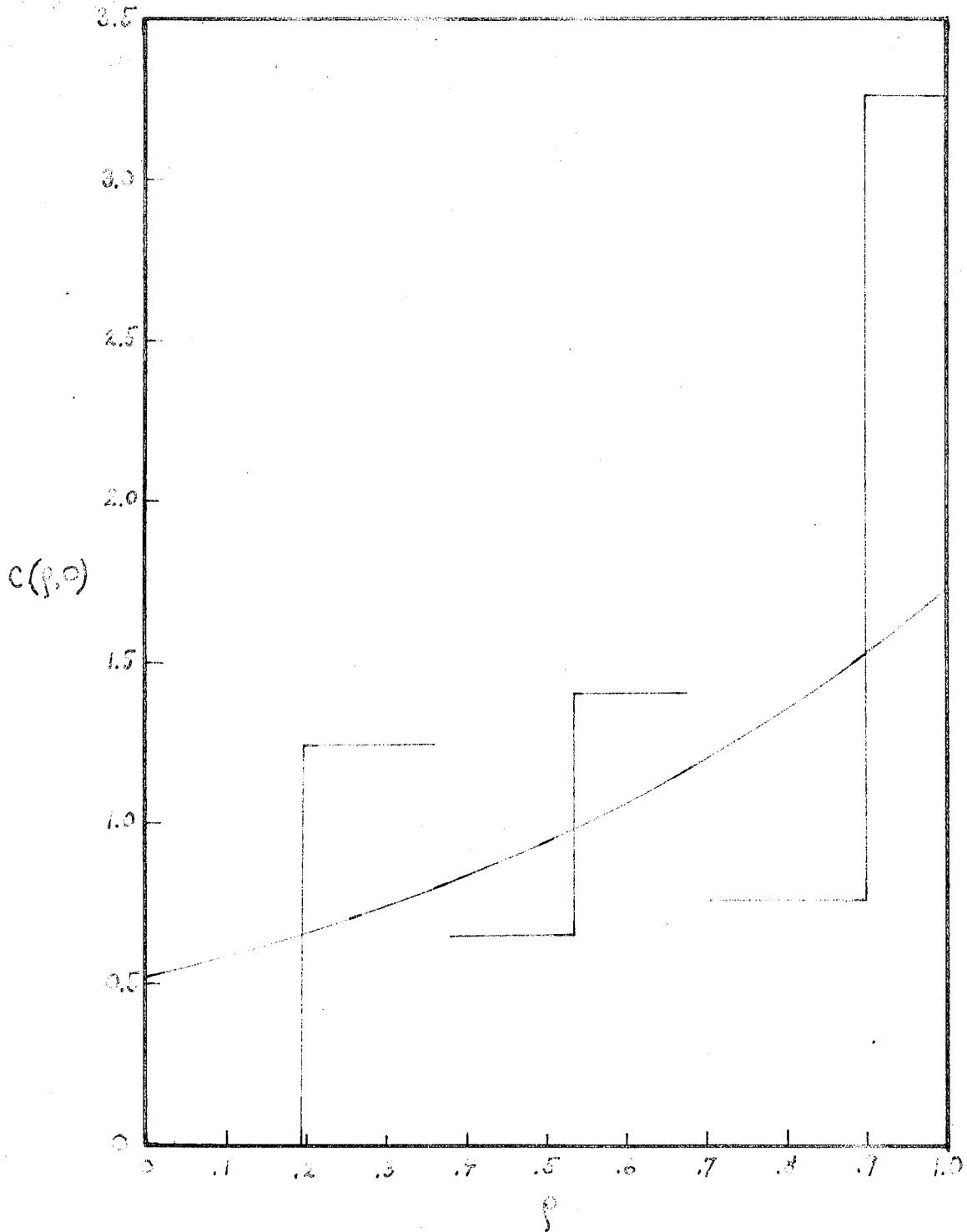


Figure 2. Three of the possible choices for the initial step function causing $A_1^{(0)}$ to vanish if $\alpha = 0.6$, i.e., $(c_2/c_1)_{\text{equil}} = 3.32$. The continuous curve is the final distribution at equilibrium. (The step at $\beta = 0.535$ also causes $A_2^{(0)}$ to vanish and corresponds to the point of intersection of the solid and dashed curves in Figure 1.)

and introducing the step distributions for $f^{(0)}$ and $f^{(1)}$ we solve for $R^{(1)}$ with the result

$$R^{(1)} = - \frac{\int_0^1 d\rho e^{-\alpha\rho} \left\{ (2\rho-1)X_1 + h_1^{(1)} - \frac{\alpha}{4}X_1 \right\} \left\{ [1-A(\rho-\beta)] + R^{(0)}A(\rho-\beta) \right\}}{\int_0^1 d\rho e^{-\alpha\rho} X_1 A(\rho-\beta)}$$

But since $R^{(0)}$ and β are chosen such that $A_1^{(0)}$ vanishes, we have from equation 124

$$R^{(0)} = - \frac{\int_0^1 d\rho e^{-\alpha\rho} X_1 [1-A(\rho-\beta)]}{\int_0^1 d\rho e^{-\alpha\rho} X_1 A(\rho-\beta)}$$

Forming the ratio we find

$$\frac{R^{(1)}}{R^{(0)}} = \frac{\int_0^\beta d\rho e^{-\alpha\rho} [2\rho X_1 + h_1^{(1)}] + R^{(0)} \int_\beta^1 d\rho e^{-\alpha\rho} [2\rho X_1 + h_1^{(1)}]}{\int_0^\beta d\rho e^{-\alpha\rho} X_1}$$

Carrying out the rather tedious integrations we obtain our final expression

$$\frac{R^{(1)}}{R^{(0)}} = \frac{[Q(\beta) - Q(0)] + R^{(0)}[Q(1) - Q(\beta)]}{[1 - \gamma_1 e^{-\beta\alpha}]}$$
(128)

where

$$Q(\rho) = e^{-\alpha\rho} \cos \pi\rho \left\{ \frac{1}{\pi^2 \gamma} \left[-8\alpha + \pi^2 \left(1 - \frac{\alpha^4}{\pi^4} \right) \right] - \left(3 - \frac{\alpha^2}{\pi^2} \right) \rho - \frac{1}{2} \alpha \gamma \rho (1-\rho) \right\}$$

$$+ \pi \gamma e^{-\alpha\rho} \sin \pi\rho \left\{ \frac{1}{\pi^2 \gamma} \left[2\alpha \gamma + 3 - \frac{6\alpha^2}{\pi^2} - \frac{\alpha^4}{\pi^4} \right] + \frac{1}{2\alpha} \left[1 - \frac{8\alpha^2}{\pi^2} - \frac{\alpha^4}{\pi^4} \right] \rho \right.$$

$$\left. + \frac{1}{2} \gamma \rho (1-\rho) \right\}$$

$$\gamma = 1 + \frac{\alpha^2}{\pi^2}$$

$$\gamma_1 = \cos \pi\beta - \left[(\pi^2 - \alpha^2) / 2\pi\alpha \right] \sin \pi\beta$$

We consider now one of the step functions listed in Table V

$$\beta = 0.50, \quad R^{(0)} = 2.17$$

and proceed to calculate $R^{(1)}/R^{(0)}$ from equation 128 remembering that

$\alpha = 0.6$. The result is

$$R^{(1)}/R^{(0)} = 0.077$$

so that

$$\frac{C_{II}}{C_I} = 2.17 [1 + 0.077\lambda] + o(\lambda^2)$$

and since we usually have $\lambda \approx 0.05$, we see that the correction amounts only to about 0.4% of $R^{(0)}$ and is therefore utterly negligible.

In order to examine the influence of first-order terms on the choice of step function in the vicinity of $\beta = 0.194$ which is the pure solvent case, we must proceed in a different manner since we can no longer treat β as fixed and simply account for the first-order correction by varying C_{II}/C_I . For the pure solvent case

$$f(\rho) = \begin{array}{ll} 0 & ; \quad 0 < \rho < \beta \\ C_{II} & ; \quad \beta < \rho < 1 \end{array}$$

and we must now treat β as the quantity which depends on λ .

Writing

$$f(\rho) = C_{II} A(\rho - \beta)$$

and expanding the step function in powers of λ after introducing

$$\beta = \beta^{(0)} + \lambda \beta^{(1)} + \dots$$

we get

$$f(\rho) = C_{II} [A(\rho - \beta^{(0)}) - \lambda \beta^{(1)} \delta(\rho - \beta^{(0)})] + o(\lambda^2)$$

or

$$f^{(0)} = C_{II} A(\rho - \beta^{(0)})$$

$$f^{(1)} = -C_{II} \beta^{(1)} \delta(\rho - \beta^{(0)})$$

where we have introduced the Dirac delta function. Thus from equations 123, on setting

$$A_i^{(0)} = 0$$

$$A_i^{(1)} = 0$$

we obtain the following expressions determining $\beta^{(0)}$ and $\beta^{(1)}$

$$\int_{\beta^{(0)}}^1 d\rho e^{-\alpha\rho} X_i = 0$$

or

$$X_i(\beta^{(0)}) + e^{-(1-\beta^{(0)})\alpha} = 0$$

and

$$\beta^{(1)} = \frac{2\alpha [Q^{(1)} - Q(\beta^{(0)})]}{\pi^2 \gamma e^{-\beta^{(0)\alpha}} X_1(\beta^{(0)})} \quad (130)$$

We have already given the solution of equation 129 for the case $\alpha = 0.6$, namely

$$\beta^{(0)} = 0.194$$

Using this value in equation 130 with $\alpha = 0.6$, we calculate the result

$$\beta^{(1)} = 0.060$$

Thus

$$\begin{aligned} \beta &= 0.194 + 0.060 \lambda + O(\lambda^2) \\ &= 0.194 [1 + 0.31 \lambda] + O(\lambda^2) \end{aligned}$$

For $\lambda = 0.05$ we get

$$\beta = 0.197 + O(\lambda^2)$$

or a correction of about 1.5%. We note that the effect of including the first-order term is to shift the value of β in the direction of larger values.

3. Time Required to Reach Equilibrium

We turn now to a consideration of the saving in time (as compared to the conventional method) brought about by starting with the step distributions derived in the preceding section. For this purpose the zero-order approximation will certainly be adequate since we do not require precise results but merely a fair estimate of the times involved. Thus we take

$$\frac{C(\rho, \tau) - C(\rho, \infty)}{C(\rho, \infty)} = e^{-\alpha \rho} e^{-\frac{\alpha}{2} \tau} \sum_{n=1}^{\infty} \left[\frac{A_n^{(0)} B_n}{A_0^{(0)} B_0} \right] X_n(\rho) e^{-\frac{n^2 \pi^2}{2\alpha} \tau}$$

$$A_n^{(0)} B_n = \frac{2}{(1 + \alpha^2/n^2\pi^2)} \int_0^1 d\rho X_n(\rho) e^{-\alpha \rho} f(\rho)$$

$$A_0^{(0)} B_0 = \frac{2\alpha}{[e^{2\alpha} - 1]} \int_0^1 d\rho f(\rho) \quad (131)$$

$$X_n(\rho) = \cos n\pi\rho + \frac{\alpha}{n\pi} \sin n\pi\rho \quad .$$

Of course, an infinite value of τ is required in order that exact equilibrium be attained. However, for practical purposes, it is sufficient to consider that equilibrium has been effectively arrived at when the concentration distribution deviates nowhere by more than 1% from the distribution at true equilibrium. An asterisk will be used

to denote the equilibrium state and we let τ^* be that value of τ for which

$$\frac{C(o, \tau^*) - C(o, \infty)}{C(o, \infty)} = 0.01 \quad (132)$$

Except when $A_1^{(o)}$ is zero, the $n = 1$ term is sufficient in applying this relationship[†] so that τ^* is computed from

$$0.01 = \frac{A_1^{(o)} B_1}{A_o^{(o)} B_o} e^{-\left[\frac{\alpha}{2} + \frac{\pi^2}{2\alpha}\right] \tau^*} \quad (133)$$

Now in the conventional method

$$f(\rho) = c_o$$

so that we find

$$\frac{A_n^{(o)} B_n}{A_o^{(o)} B_o} = \frac{2 [e^{2\alpha} - 1] [1 - (-1)^n e^{-\alpha}]}{n^2 \pi^2 \left(1 + \frac{\alpha^2}{n^2 \pi^2}\right)^2} \quad (134)$$

which specializes to

$$\frac{A_1^{(o)} B_1}{A_o^{(o)} B_o} = \frac{2 [e^{2\alpha} - 1] [1 + e^{-\alpha}]}{\pi^2 \left(1 + \frac{\alpha^2}{\pi^2}\right)^2} \quad (135)$$

[†] It is easy to show that the $n = 1$ term in equation 131 has a maximum at $\rho = 0$ and this is why we take equation 132 as our criterion for the attainment of equilibrium.

In the "fast method" we take

$$f(\rho) = \begin{cases} C_I & ; \quad 0 < \rho < \beta \\ C_I R^{(0)} & ; \quad \beta < \rho < 1 \end{cases} \quad (136)$$

where $R^{(0)}$ and β are such that $A_1^{(0)}$ vanishes for the assumed value of α . However, ordinarily the true value of α for the system will not agree exactly with the value assumed (also the system may be poly-disperse and therefore possess a range of α -values) since α or the molecular weight is known a priori only approximately. Thus $A_1^{(0)}$ for the system actually differs from zero and the $n=1$ term will control the approach to equilibrium just as in the case of the conventional method. Thus to calculate τ^* for the fast method we again use equation 133 but since $f(\rho)$ is now given by equation 136, we find that equation 134 is to be replaced by

$$\frac{A_n^{(0)} B_n}{A_0^{(0)} B_0} = \frac{2 [e^{2\alpha} - 1] e^{-\beta\alpha} \left\{ e^{\beta\alpha} - \gamma_n - [(-1)^n e^{-(1-\beta)\alpha} - \gamma_n] R^{(0)} \right\}}{n^2 \pi^2 \left(1 + \frac{\alpha^2}{n^2 \pi^2} \right)^2 [\beta + R^{(0)}(1-\beta)]} \quad (137)$$

so that in place of equation 135, we have

$$\frac{A_1^{(0)} B_1}{A_0^{(0)} B_0} = \frac{2 [e^{2\alpha} - 1] e^{-\beta\alpha} \left\{ e^{\beta\alpha} - \gamma_1 + [e^{-(1-\beta)\alpha} + \gamma_1] R^{(0)} \right\}}{\pi^2 \left(1 + \frac{\alpha^2}{\pi^2} \right)^2 [\beta + R^{(0)}(1-\beta)]} \quad (138)$$

with γ_n given by

$$\gamma_n = \cos n\pi\beta - \left[\frac{(n^2\pi^2 - \alpha^2)}{2n\pi\alpha} \right] \sin n\pi\beta$$

so that

$$\gamma_1 = \cos \pi\beta - \frac{[\pi^2 - \alpha^2]}{2\pi\alpha} \sin \pi\beta .$$

We now consider the case where a value of 0.6 has been assumed for α and one of the optimum step functions (derived for this value of α) listed in Table V has been chosen, namely

$$\beta = 0.50 \quad , \quad R^{(0)} = 2.17 .$$

If the actual value of α for the system is 0.6, $A_1^{(0)}$ will vanish and using the $n=2$ term, we find for τ^* a value of 0.06. If the actual value of α differs from 0.6, however, we use the $n=1$ term for the calculation of τ^* . The results are plotted as curve a in Figure 3. The curve indicates the degree of sensitivity of τ^* to the difference occurring between the assumed value of α and the actual value in the system.

For comparison we have also calculated the dependence of τ^* on the value of α in the system when an initially uniform distribution is used (conventional method). These results are plotted as curve b in Figure 3. Curve c in the same figure is obtained by computing the ratio

of the τ^* -values given for the two methods in curves a and b. This ratio attains its maximum, of course, if the value of α in the system is exactly equal to the value assumed in choosing the step function. If the relative error in estimating α is 15%, the use of the step function is expected to lead to a two-fold reduction in time over the conventional method and an eight-fold reduction if there is exact agreement between the assumed and actual α -values.[†]

As we have already pointed out, the α -values of interest for the equilibrium method in the ultracentrifuge lie in the range 0.35-0.70. Therefore from curve b we expect that the values of τ^* for the conventional method should be of the order of 0.5. In the course of his theoretical work on the settling of particles in a uniform gravitational field, Weaver (19) derived the result that regardless of the value of α , the maximum value of τ required for the sensible attainment of

[†] As a line of possible development in order to overcome the limitation on the reduction of time because of one's inadequate a priori knowledge of the molecular weight, Professor Schomaker has suggested that after the cell has been set up with the properly chosen (to the best of one's knowledge) step function distribution, an appropriate pre-run at high speed be interjected in order to obtain an initial distribution of essentially three steps for the main run. Generalizing beyond this, he further suggests that the process be monitored, the speed being readjusted from time to time in accordance with the observed progress of the experiment and a built-in wisdom of the program.

equilibrium[†] (starting with a uniform distribution) should be 2. This value is often applied to the ultracentrifuge (reference 1, equation 108), (20) as a basis for predicting the time required to reach equilibrium. However, it has actual significance only for extremely large values of α which were of interest to Weaver but which are of little concern in ultracentrifuge work. Although still valid in the sense of being the maximum value of τ^* , actually for the small values of α of interest here, it gives much too high an upper bound to be of much use. From the results presented here, we expect that it leads to values of τ^* which are four times larger than actually required.

For calculating absolute values of time, t , we must recall the definition of τ , namely

$$t = \frac{H}{V} \tau$$

where H is the height of the cell

$$H = r_2 - r_1$$

[†] Weaver's criterion for equilibrium is equivalent to demanding that the relative deviation from true equilibrium be very small at $\rho = 1$. If instead, one requires the relative deviation at $\rho = 0$ to be small (as we have done here), one obtains $\tau_{max}^* = 4$ and this is the limiting value which should be approached by curve b. These maximum values are obtained by letting α become very large as this is when the largest τ -values are required for reaching equilibrium. For the much smaller α -values dealt with in Figure 3, the two criteria lead to essentially the same results.

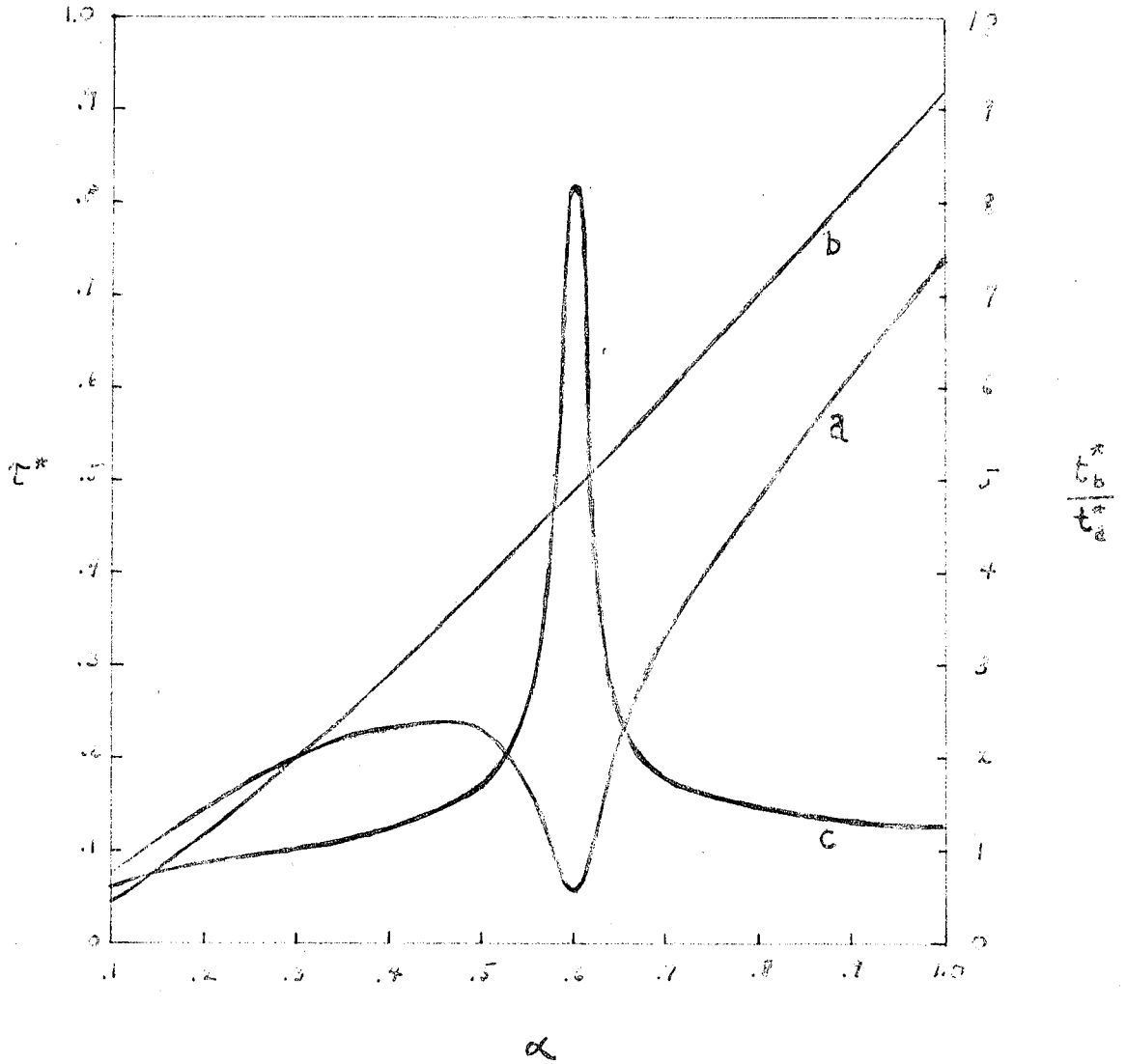


Figure 3. a) The dependence of τ^* on the actual value of α starting with the step distribution, $\beta = 0.5$, $c_{\neq}/c_{\pm} = 2.17$, chosen on the basis of $\alpha = 0.6$. b) The dependence of τ^* on α starting with a uniform solution. c) The ratio of times required to reach equilibrium in systems b and a.

and \bar{V} is the mean velocity of sedimentation

$$\bar{V} = S \omega^2 (r_1 + r_2) / 2$$

so that

$$t^* = \frac{2H}{S \omega^2 (r_1 + r_2)} \tau^*$$

Or alternatively, this can be expressed in terms of the coefficient of diffusion if we remember that

$$\alpha = \frac{\bar{V} H}{2D}$$

so that

$$t = \frac{H^2}{2D\alpha} \tau$$

Thus

$$t^* = \frac{H^2}{2D} \cdot \frac{\tau^*(\alpha)}{\alpha} \quad (139)$$

4. Experimental Results

The theoretical expectations have received preliminary confirmation in experimental runs with ribonuclease (Armour) carried out by Dr. Pasternak. The experiments were done at 13,410 r.p.m. in the Spinco

Model E ultracentrifuge equipped with a temperature control system and phaseplate schlieren optics. A stationary distribution of the protein, which did not appear to be truly homogeneous ($\overline{M}_z = 14,800$), was reached in the case of a uniform initial distribution in about 40 hours compared with the calculated time of 36 hours, and in about 18 hours for an initial step distribution for which c_{II}/c_I was 2.12 and β was 0.53. The speed, ω , chosen from equation 126 was such that the assumed value of M , 13,600, corresponded to an α -value of 0.6 ($(c_2/c_1)_{\text{equil}} = 3.32$) in a 0.61 cm. column of solution.

Unfortunately, Dr. Pasternak left the institute before he had an opportunity to repeat the experiment using the improved knowledge of the molecular weight to adjust the value of α for the system more closely to 0.6 in order to see whether a further reduction in time might be achieved.

Appendix I

From equation 28 we have

$$C(r, \infty) = B \exp \left[\frac{2\alpha}{(r_2^2 - r_1^2)} \cdot r^2 \right]$$

where B can be determined from the requirement that material be conserved

$$\int_{r_1}^{r_2} dr r c(r, 0) = \int_{r_1}^{r_2} dr r c(r, \infty)$$

or

$$C_0 \int_{r_1}^{r_2} dr r = B \int_{r_1}^{r_2} dr r \exp \left[\frac{2\alpha}{(r_2^2 - r_1^2)} r^2 \right]$$

which yields

$$B = 2\alpha C_0 / \left\{ \exp \left[\frac{2\alpha}{(r_2^2 - r_1^2)} r_2^2 \right] - \exp \left[\frac{2\alpha}{(r_2^2 - r_1^2)} r_1^2 \right] \right\}$$

$$= \frac{2\alpha C_0}{(e^{2\alpha} - 1)} \exp \left[- \frac{2\alpha}{(r_2^2 - r_1^2)} r_1^2 \right]$$

Introducing this expression for B into the first equation, we obtain for the equilibrium distribution

$$\begin{aligned} \frac{c(r, \infty)}{c_0} &= \frac{2\alpha}{(e^{2\alpha} - 1)} \exp \left[\frac{2\alpha}{(r_2^2 - r_1^2)} (r^2 - r_1^2) \right] \\ &= \frac{2\alpha}{(e^{2\alpha} - 1)} \exp \left[2\alpha \rho \frac{(r + r_1)}{(r_2 + r_1)} \right] \end{aligned}$$

since

$$\rho = \frac{r - r_1}{r_2 - r_1}$$

The task remaining is to express $(r + r_1)/(r_2 + r_1)$ in terms of ρ and λ . This can be accomplished by the following sequence of equations.

$$\begin{aligned} \frac{r + r_1}{r_2 + r_1} &= \frac{r + r_1 + r_2 - r_2}{r_2 + r_1} \\ &= 1 - \frac{(r_2 - r)}{(r_2 + r_1)} \\ &= 1 - \frac{(r_2 - r)}{2\bar{r}} \end{aligned}$$

$$r = \bar{r} (1 + \lambda \rho) \quad ; \quad \rho = 2\beta - 1$$

$$r_2 = \bar{r} (1 + \lambda)$$

$$\frac{(r_2 - r)}{2\bar{r}} = \frac{\lambda}{2} (1 - \rho)$$

$$= \lambda (1 - \rho)$$

$$\frac{r + r_1}{r_2 + r_1} = 1 - \lambda (1 - \rho)$$

Our final result is therefore

$$\frac{C(r, \infty)}{C_0} = \frac{2\alpha}{(e^{2\alpha} - 1)} e^{2\alpha\rho [1 - \lambda(1 - \rho)]}$$

Appendix II

We are dealing here with the expansion of $u_n^{(1)}$ in terms of the unperturbed eigenfunctions $u_n^{(0)}$ which form a complete orthonormal set

$$u_n^{(1)} = \sum_{m=0}^{\infty} C_{nm} u_m^{(0)}$$

and wish to illustrate a method of obtaining an expression for this infinite series in closed form.

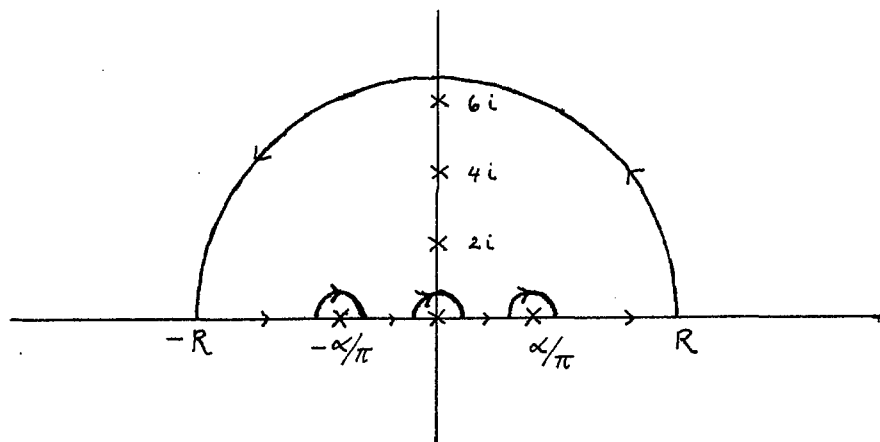
An example of the type of sum one gets when the explicit expressions for C_{nm} and $u_m^{(0)}$ are introduced is for n odd

$$S_n = \sum_{m=2,4,\dots}^{\infty} \frac{\cos m\pi\rho}{\left(m^2 + \frac{\alpha^2}{\pi^2}\right)(m^2 - n^2)^2}$$

To evaluate this sum we construct a contour integral in the complex plane in such a way that the sum of the residues at the poles leads to an expression identical with S_n . Thus we consider the integral

$$I = \int_C dz \frac{\cosh [\pi(\rho - 1/2)z]}{\left(z^2 - \frac{\alpha^2}{\pi^2}\right)(z^2 + n^2)^2 \sinh\left(\frac{\pi}{2}z\right)}$$

where the contour C is



so that it encloses the poles of the integrand at $z = mi$, $m = 2, 4, \dots$ (due to $\sinh(\frac{\pi}{2}z)$) and at $z = ni$ (due to $(z^2 + n^2)^2$) and excludes the poles at $z = \pm \frac{\alpha}{\pi}$ and $z = 0$. From the theory of contour integration we know that (as $R \rightarrow \infty$)

$$I = 2\pi i \sum_{m=2,4,\dots}^{\infty} (\text{Residue at } z = mi) + 2\pi i \times (\text{Residue at } z = ni).$$

The residue at $z = mi$ is found to be

$$(\text{Residue at } z = mi) = \frac{-2 \cos m\pi p}{\pi \left(m^2 + \frac{\alpha^2}{\pi^2}\right) (m^2 - n^2)^2}$$

so that

$$\begin{aligned} I &= -2\pi i \frac{2}{\pi} \sum_{m=2,4,\dots}^{\infty} \frac{\cos 2m\pi\rho}{\left(m^2 + \frac{\alpha^2}{\pi^2}\right) (m^2 - n^2)^2} \\ &\quad + 2\pi i \times (\text{Residue at } z = ni) \end{aligned}$$

or

$$S_n = \frac{1}{4i} \left\{ 2\pi i \times (\text{Residue at } z = ni) - I \right\} .$$

Thus by evaluating the residue at $z = ni$ and the integral I by direct integration over the contour, we can obtain an expression for

S_n . The result is

$$\begin{aligned} S_n &\equiv \sum_{m=2,4,\dots}^{\infty} \frac{\cos 2m\pi\rho}{\left(m^2 + \frac{\alpha^2}{\pi^2}\right) (m^2 - n^2)^2} \quad ; \quad n \text{ odd} \\ &= \frac{1}{2n^4 \alpha^2/\pi^2} \left\{ \frac{\frac{\alpha}{2} \cosh[\alpha(\rho - 1/2)]}{\left(1 + \alpha^2/n^2\pi^2\right)^2 \sinh(\alpha/2)} - 1 \right\} \\ &\quad - \frac{\pi^2(\rho - 1/2)}{8n^4(1 + \alpha^2/n^2\pi^2)} \cos n\pi\rho \\ &\quad + \frac{\pi}{8n^5} \left[1 + 2(1 + \alpha^2/n^2\pi^2)^{-1} \right] \left[1 + \alpha^2/n^2\pi^2 \right]^{-1} \sin n\pi\rho . \end{aligned}$$

By evaluating (in an analogous manner) the other sums similar to \sum_n which arise in the expression for $u_n^{(1)}$ and combining the results, one can obtain (after an extremely tedious algebraic simplification) the result given in equation 99 which was derived more directly by the method presented in the text.

References of Part I

1. Svedberg, T., and Pedersen, K. O., The Ultracentrifuge, Clarendon Press, Oxford, 1940.
2. Perrin, J., *Compt. rend.* 146, 967-970 (1908); 147, 475-476 (1908); *Ann. chim. phys.* (8), 18, 5-114 (1909).
3. Westgren, A., *Arkiv Mat. Astron. Fysik* 9, No. 5, 1-36 (1913); *Z. physik. Chem.* 89, 63-90 (1915).
4. Dumanski, A., Zobotinski, E., und Ewsejew, M., *Kolloid-Z.* 12, 6-11 (1913).
5. Svedberg, T., and Rinde, H., *J. Am. Chem. Soc.* 46, 2677-2693 (1924).
6. Svedberg, T., and Fahraeus, R., *J. Am. Chem. Soc.* 48, 430-438 (1926).
7. Svedberg, T., *Kolloid-Z., Zsigmondy-Festschrift, Erg. Bd. zu* 36, 53-64 (1925); *Z. physik. Chem.* 121, 65-77 (1926).
8. Lamm, O., *Arkiv Mat. Astron. Fysik* 21B, No. 2, 1-4 (1929).
9. Faxen, H., *Arkiv Mat. Astron. Fysik* 21B, No. 3, 1-6 (1929); 25B, No. 13, 1-4 (1936).
10. Oka, S., *Proc. Physico-Math. Soc. Japan* (3) 18, 519-523 (1936).
11. Oka, S., *Proc. Physico-Math. Soc. Japan* (3) 19, 1094-1104 (1937).
12. Archibald, W. J., *Phys. Rev.* 54, 371-374 (1938); *Ann. N. Y. Acad. Sci.* 43, Art. 5, 211-227 (1942).
13. Archibald, W. J., *J. Appl. Phys.* 18, 362-367 (1947).
14. Mason, M., and Weaver, W., *Phys. Rev.* 23, 412-426 (1924).
15. Beams, J. W., *Rev. Mod. Physics* 10, 245-263 (1938).
16. Private Discussion.
17. Courant, R., and Hilbert, D., Methoden der Mathematischen Physik, Vol. 1, J. Springer, Berlin, 1931, page 249.
18. Kegeles, G., *J. Am. Chem. Soc.* 74, 5532-5534 (1952).
Pickels, E. G., Harrington, W. F., and Schachman, H. K., *Proc. Natl. Acad. Sci. U. S.* 38, 943-948 (1952).

19. Weaver, W., Phys. Rev. 27, 499-503 (1926).
20. Beams, J. W., Dixon, III, H. M., Robeson, A., and Snidow, N.,
J. Phys. Chem. 59, 915-922 (1955).

(Reprinted from *Nature*, Vol. 179, pp. 92-94, January 12, 1957)

A Fast Method for reaching Equilibrium in the Ultracentrifuge

THE inherent power of the equilibrium method¹ for study of molecular weight, polydispersion, and activity coefficients in the ultracentrifuge has been limited by the length of time required to reach equilibrium. We have found that this time can be appreciably reduced by using the synthetic boundary cell² and by selecting the starting conditions—speed of the ultracentrifuge, the relative heights and the relative concentrations of the two layers—in accordance with a mathematical analysis of the approach to equilibrium.

The approximate³, as well as the exact⁴, solutions by Archibald of the ultracentrifuge differential equation are not useful in our problem because of the extensive numerical computation needed for each set of experimental conditions. We have obtained a manageable solution by a perturbation treatment of the centrifuge equation, retaining terms of the first order in the parameter $\lambda = (r_b - r_t)/(r_b + r_t) \approx 0.05$, where the r 's are distances of the cylindrical surfaces of the equilibrating solution from the axis of rotation. For the analysis required here, however, the zero order approximation is adequate. This approximation corresponds to the exact solution of Mason and Weaver⁵ for sedimentation in a uniform gravitational field.

The concentration of an equilibrating component having sedimentation and diffusion coefficients S and D is

$$C(\rho, \tau) = C^*(\rho) + \exp \alpha \rho \cdot \exp(-\alpha \tau/2) \sum_{n=1}^{\infty} A_n X_n(\rho) \exp(-n^2 \pi^2 \tau/2\alpha) \quad (1)$$

where

$$\rho = (r - r_t)/H, \quad H = r_b - r_t; \\ \alpha = HV/2D, \quad V = S\omega^2 (r_b + r_t)/2;$$

$$\tau = t/t_0, \quad t_0 = H/V; \quad X_n(\rho) = \cos n\pi\rho + (\alpha/n\pi) \sin n\pi\rho,$$

and where the asterisk denotes equilibrium. Since $C^* = A_0 \exp 2\alpha\rho$, α determines the final distribution in the zero order approximation. It also determines the exact distribution, as is shown by its equivalence with the familiar expression

$$\ln \frac{C_b^*}{C_t^*} = \frac{M(1 - \bar{v}\rho) \omega^2 (r_b^2 - r_t^2)}{2RT} = \frac{S \omega^2 (r_b^2 - r_t^2)}{D \times 2} = \frac{VH}{D} = 2\alpha, \quad (2)$$

For a given value of α the A_n 's are constants which are determined by the initial distribution of concentration.

Because the time exponential in (1) involves n^2 , the deviation from equilibrium after a short time is given by the leading term of the sum, $n = 1$; equilibration will be accelerated if it is possible to choose initial conditions such that A_1 vanishes.

For the initial condition

$$C(\rho,0) = \begin{cases} C_1, & 0 < \rho < \beta \\ C_2, & \beta < \rho < 1 \end{cases}$$

where β is the position of the synthetic boundary, A_1 can be made to vanish if C_2/C_1 and β are chosen so as to satisfy

$$C_2/C_1 = (\gamma_1 - \exp \beta\alpha) / (\gamma_1 + \exp \{-(1-\beta)\alpha\}) \quad (3)$$

with

$$\gamma_1 = \cos \pi\beta - [(\pi^2 - \alpha^2)/2\pi\alpha] \sin \pi\beta$$

In Fig. 1, C_2/C_1 is plotted against β according to equation (3) for the case of $\alpha = 0.6$, that is, $C_2^*/C_1^* = 3.3$. The curve shows that there exists a wide range of choices for the location of the synthetic boundary, all of which are consistent with the vanishing of A_1 . It is interesting to note that pure solvent may be used as the top layer ($C_2/C_1 = \infty$) if the boundary is placed at $\beta = 0.19$. It is also to be noted that in the vicinity of $\beta = 0.55$ the curve has a broad minimum and the system is insensitive to filling errors.

We turn now to a consideration of the saving in time brought about by starting with a step distribu-

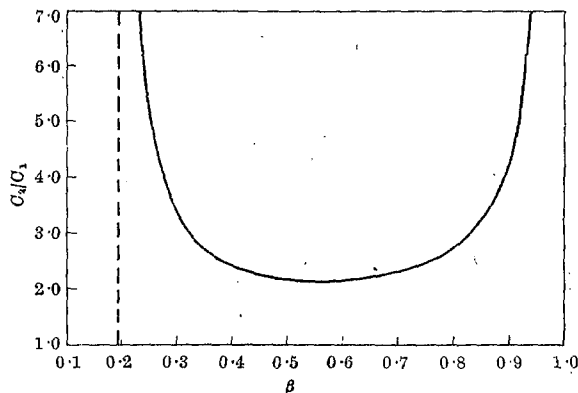


Fig. 1. Position of the step and the corresponding relative concentrations in the layers that cause A_1 to vanish. Calculated from equation (3) for $\alpha = 0.6$, that is, $C_2^*/C_1^* = 3.3$

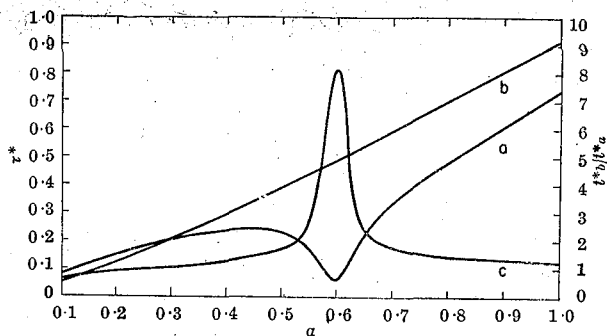


Fig. 2. *a*, The dependence of τ^* on the actual value of α starting with the step distribution, $\beta=0.5$, $C_2/C_1=2.17$, chosen on the basis of $\alpha=0.6$. *b*, The dependence of τ^* on α starting with a uniform solution. *c*, The ratio of times required to reach equilibrium in systems *b* and *a*.

tion chosen in accordance with equation (3). We define equilibrium as the state in which the concentration deviates nowhere by more than 1 per cent from the concentration at true equilibrium, and let τ^* be the value of τ calculated from equation (1) for this equilibrium state. In applying the fast method to an actual system the value of α will be incorrectly estimated (also the system may be polydisperse and therefore possess a range of α values) so that the step distribution will be incorrectly chosen and A_1 will not quite vanish. The effect of an error of this kind on τ^* is shown by curve *a*, Fig. 2. Compared with the conventional method, there is an eight-fold reduction in time when the value of α for the system agrees exactly with the value assumed and about a two-fold reduction when the error in α is approximately 15 per cent, curve *c*. The saving of time results from setting up step distributions to approximate the final distribution and from advantageous combinations of sedimentation and diffusion to transport material.

For the above comparison, we have also evaluated τ^* for an initially uniform distribution from equation (1); the results are plotted as a function of α in curve *b*. The equilibrium distributions of interest in the ultracentrifuge are $C^*_b/C^*_t = 2-4$, and correspondingly, $\alpha = 0.4-0.7$. This leads according to curve *b* to $\tau^* \approx 0.5$, and to values of t^* one-fourth as large as are usually expected⁶ on the basis of $\tau^* = 2$ (ref. 1, equation 108).

The theoretical results have been confirmed with ribonuclease (Armour) in experimental runs at 13,410 r.p.m. in the Spinco Model *E* ultracentrifuge equipped with a temperature-control system and phaseplate schlieren optics. A stationary distribution

of the protein, which did not appear to be truly homogeneous ($\bar{M}_z = 14,800$), was reached in the case of a uniform initial distribution in about 40 hr. compared with the calculated time of 36 hr., and in less than 20 hr. for an initial step distribution for which C_2/C_1 was 2.12 and β was 0.53. The speed, ω , chosen from (2) was such that the assumed value of M , 13,600, corresponded to an α value of 0.6 in a 0.61-cm. column of solution.

This investigation was supported in part by the National Institutes of Health, Bethesda, Maryland, and in part by a grant from the National Science Foundation. A more extensive account will be published later.

R. A. PASTERNAK*
GIRAIR M. NAZARIAN
JEROME R. VINOGRAD

Gates and Crellin Laboratories of Chemistry,
California Institute of Technology,
Pasadena, California.

Sept. 27.

* Present address: Stanford Research Institute, Menlo Park, California.

¹ Svedberg, T., and Pedersen, K. O., "The Ultracentrifuge" (Clarendon Press, Oxford, 1940).

² Kegeles, G., *J. Amer. Chem. Soc.*, **74**, 5532 (1952); Pickels, E. G., Harrington, W. F., and Schachman, H. K., *Proc. U.S. Nat. Acad. Sci.*, **38**, 943 (1952).

³ Archibald, W. J., *J. App. Phys.*, **18**, 362 (1947).

⁴ Archibald, W. J., *Phys. Rev.*, **54**, 371 (1938); *Ann. N.Y. Acad. Sci.*, **43**, Art. 5, 211 (1942).

⁵ Mason, M., and Weaver, W., *Phys. Rev.*, **23**, 412 (1924).

⁶ Beams, J. W., Dixon, III, H. M., Robeson, A., and Snidow, N., *J. Phys. Chem.*, **59**, 915 (1955).

THE DETAILED INTERPRETATION OF THE ANOMALOUS ELECTRON
DIFFRACTION PHOTOGRAPHS OF SOME SYMMETRICAL GAS
MOLECULES WITH THE AID OF COMPLEX SCATTERING
AMPLITUDES

A. INTRODUCTION

The use of the Born approximation for the amplitude of the scattered wave in electron diffraction by gas molecules has led in certain cases to determined structures which are in serious disagreement with the results obtained from other physical measurements. Perhaps the case of uranium hexafluoride has been the most thoroughly explored. As early as 1937, Braune and Pinnow (1) concluded on the basis of their electron diffraction investigation that all of the U-F bond lengths in the molecule are not equal, the different values being 1.78, 1.99, and 2.17 Å. Although their specific assumption of a rhombic bipyramidal model might have been discarded (having been based only on the measurement of the positions of the maxima in the diffraction pattern), nevertheless, the necessity for assuming a lack of octahedral symmetry seemed obvious. A few years later, apparently because of the important role played by uranium hexafluoride in the war effort, several investigations were made pertaining to its structure. These were by means of electron diffraction of the gas (2), x-ray diffraction of single crystals (3), spectroscopic observations (4), and dielectric constant measurements (5). The electron diffraction investigation, conducted by Bauer, was in agreement with the

earlier one in that the regular octahedral structure was ruled out. The model he proposed, however, was that of a distorted octahedron having three short and three long U-F distances with the values 1.86 and 2.16 Å. In striking contrast, the other methods of investigation led to results which are consistent with the regular octahedral structure. In view of this contradictory situation, the suggestion was made to Bauer by Libby in 1944 that perhaps the theory of the diffraction of electrons by very heavy atoms was in need of modification. This possibility was not taken seriously by Bauer (6) (although he did propose that electron diffraction experiments be done on other compounds containing a central uranium atom bonded to light-weight groups) because the electron diffraction investigations of a large number of molecules containing both heavy and light atoms had led to nothing unusual. Unfortunately, his "analysis" of the situation was strongly dependent on taking at face value the "results" obtained by others without due regard to the details and validity of their procurement. Thus, for example, he raised the question "were the departure from a regular octahedron due merely to the atomic weight of the central atom, why would MoF_6 be distorted (as reported by Braune and Pinnow) whereas TeF_6 is regular (7)." A glance at the paper by Braune and Pinnow, however, is sufficient to convince one that because of the meagerness of their data they had not succeeded in showing anything about the structure of MoF_6 (this cannot be said of their work on UF_6). Thus Bauer's arguments, being based in part on false premises, tended to obscure the true cause of the difficulty.

In the meantime, Professor Schomaker and his co-workers, by means of electron diffraction studies extended out to larger scattering

angles, had found apparent splits in distances for molecules other than the hexafluorides. Previous electron diffraction data for these molecules had indicated nothing anomalous and had led to symmetrical structures as expected. Thus it became clear that comparisons between the results found for different molecules (or even the same molecule) should be made with care as to the adequacy of each particular investigation. With the availability of these more extensive results a trend became apparent; namely, that the magnitude of the apparent split found in the distances between a pair of atoms in a molecule is approximately proportional to the difference of their atomic numbers.

<u>Molecule</u>	<u>Distance</u>	<u>ΔZ</u>	<u>Apparent Split (Å)</u> <u>(Obs.)</u>
MoF ₆	Mo-F	33	0.14
Mo(CO) ₆	Mo...O	34	0.13
	Mo-C	36	0.13 (assumed equal)
WCl ₆	W-Cl	57	0.18
WF ₆	W-F	65	0.23
W(CO) ₆	W...O	66	0.23
OsO ₄	Os-O	68	0.23
UF ₆	U-F	83	0.30

Such a systematic variation of the split apparently rules out any purely chemical reason for the effect such as the formation of some sort of peculiar bonds.

Thus Schomaker and Glauber (8) were led to examine the possible interpretation of this simple behaviour in terms of the inaccuracy of the Born approximation for atomic scattering. By noting that the fundamental error resulting from the use of this approximation is that it leads to real instead of complex amplitudes for the scattered waves, they discovered the reason why the conventional analyses of electron diffraction data had led to unsymmetrical structures. Taking the amplitude to be real corresponds to a neglect of the phase shift attendant on scattering. For the scattering from a single atom this change of phase plays no role in determining the intensity of the scattered wave. This is not true, however, for the scattering from a pair of atoms since interference effects arise. This is just the case of interest in electron diffraction by gas molecules where the total intensity of the scattered wave as a function of angle is proportional to

$$\sum_i \sum_j f_i f_j^* \frac{\sin s r_{ij}}{s r_{ij}}$$

the terms with $i \neq j$ resulting from the interference of the waves scattered from atoms i and j separated in the molecule by the distance r_{ij} , where as usual $S = \frac{4\pi}{\lambda} \sin \frac{\theta}{2}$. As implied by the asterisk, the amplitude f_j of the wave scattered by atom j is in general a complex quantity and may therefore be written in the form

$$f_j(\theta) = |f_j(\theta)| e^{i\eta_j(\theta)}$$

where the argument, η_j , corresponds to the phase shift associated with the scattering from atom j . Introducing this more explicit representation of the amplitude, the expression for the intensity takes on the form

$$\sum_i \sum_j |f_i| |f_j| \cos \Delta\eta_{ij} \frac{\sin s r_{ij}}{s r_{ij}} \quad ; \quad \Delta\eta_{ij} = \eta_i - \eta_j$$

which is to be compared with

$$\sum_i \sum_j |f_i^B| |f_j^B| \frac{\sin s r_{ij}}{s r_{ij}}$$

which is the conventional formula and results from the use of the Born approximation

$$f_j(\theta) \sim |f_j^B(\theta)| = f_j^B$$

Thus the correct description of the intensity requires the presence of a factor $\cos \Delta\eta_{ij}$ which is absent from the approximate expression. This factor has an important effect if the atoms i and j differ appreciably in scattering power so that for some critical angle, $(\theta_c)_{ij}$, $\Delta\eta_{ij}$ attains the value $\pi/2$. The cosine then vanishes resulting in a "beat-out" effect on the intensity much as is observed in the diffraction patterns produced by molecules containing both heavy and light atoms. That this behaviour can be simulated in the conventional formula by the introduction of a pair of distances $r_{ij}^{\circ} + \delta_{ij}$, and $r_{ij}^{\circ} - \delta_{ij}$, with

$$\delta_{ij} = \frac{\pi}{2} \frac{1}{(S_c)_{ij}} = \frac{\lambda}{8 \sin(\frac{1}{2}\theta_c)_{ij}}$$

is apparent from the relation

$$\begin{aligned} & \frac{1}{2} \frac{\sin s(r_{ij}^{\circ} + \delta_{ij})}{s(r_{ij}^{\circ} + \delta_{ij})} + \frac{1}{2} \frac{\sin s(r_{ij}^{\circ} - \delta_{ij})}{s(r_{ij}^{\circ} - \delta_{ij})} \\ &= \cos s\delta_{ij} \cdot \frac{\sin sr_{ij}^{\circ}}{sr_{ij}^{\circ}} + O\left(\frac{\delta_{ij}}{r_{ij}^{\circ}}\right) ; \end{aligned}$$

hence the reported asymmetries.

By continuing the Born perturbation procedure to the second stage of approximation and assuming a screened-coulomb potential, Schomaker and Glauber were able to derive a non-vanishing expression for the phase shift, $\eta_{2nd\ Born}$, from which they determined the values of $(S_c)_{ij}$ corresponding to various pairs of heavy-light atoms such that

$$\Delta \eta_{ij}(S_c) = \pi/2$$

The resulting calculated apparent splits

$$2 \delta_{ij} = \pi / (S_c)_{ij}$$

were in excellent agreement with the observed values.

It was found later (9), however, that although the diffraction pattern for UF_6 obtained with 40 kev electrons could be satisfactorily interpreted in terms of a symmetrical structure using $\eta_{2nd\ Born}$ the pattern resulting at 11 kev was in serious disagreement with the predicted one. Thus it appeared that the original agreement had been fortuitous and that further modifications of the theory were necessary. Finally, Hoerni and Ibers (10) using the formalism of partial waves combined with the WKB approximation method and assuming the Thomas-Fermi potential for the uranium atom were able to compute values of $\Delta \eta_{UF}$ which led to excellent agreement between the calculated and observed

intensity patterns both at 40 and 11 kev. Subsequently, they extended their calculations so as to include a large number of the atoms in the periodic table (11).

In the present investigation we apply the theoretical results of Hoerni and Ibers to the detailed reinterpretation of the electron diffraction photographs of the molecules listed in the table on page 107, with the exception of UF_6 . The purpose is two-fold: to provide additional confirmation of the theory and to determine accurately the structures of the molecules in question.

B. OSMIUM TETROXIDE

a.

There is a considerable amount of information in the literature (obtained by methods other than electron diffraction) regarding the structure of the osmium tetroxide molecule.

The reports on the infrared and Raman spectrum indicate that the molecule has a regular tetrahedral structure. Thus the early work (12) on the spectrum of the vapor as well as the recent investigations of the vapor (13) and in addition of the liquid and solid (14) are all in agreement with this structure. The spectrum is particularly simple indicating a highly symmetrical shape for the molecule. In addition the plane square model is ruled out because the observed coincidence of the infrared and Raman frequencies indicates the absence of a center of symmetry.

The polarization of osmium tetroxide has been observed (15) at temperatures of 156° and 288° and found to be constant within the experimental error of 1% leading to the conclusion that the molecule possesses no permanent dipole moment. This result is consistent with the tetrahedral model.

Finally, in the crystal structure investigation (16) the x-ray data imply that the osmium tetroxide molecule is tetrahedral or nearly so, even though the positions of the oxygen atoms cannot be derived from the observed intensities; no other structure yielding reasonable interatomic distances could be found.

In view of the consistency between these observations there would appear to be strong evidence in support of the tetrahedral structure. The previous electron diffraction investigations, however, have not given results in agreement with this simple model. Although Brockway (17) gave the single value of 1.66 ± 0.05 Å for the Os-O distance he made no commitment as to the type of structure or configuration involved. A publication of the details of this work, although reported to have been forthcoming, has never appeared. Next, Braune and Stute (18) fit their electron diffraction observations by assuming two pairs of Os-O distances in the ratio of 1:1.57 the smaller distance being equal to 1.79 \AA . In view of the observed lack of dipole moment (15), they concluded that a distorted tetrahedral structure was improbable and thought a planar configuration to be a more likely possibility. It appears, as pointed out by Sheehan (19), that these authors in actuality determined the mean values of the Os-O and O...O distances which of course bear the ratio

1.63 in a tetrahedral structure. Recently, Sheehan (20) made an electron diffraction investigation in an apparently clear-cut manner arriving at an unsymmetrical structure in complete disagreement with the requirements of the other physical measurements. Although the radial distribution curve did indicate a tetrahedral arrangement of the oxygen atoms, the Os-O distance was "split" there being two sharp peaks corresponding to the distances of 1.59 Å and 1.82 Å thereby destroying any possibility of retaining the regular tetrahedral model.

b.

Because of the availability of the diffraction photographs used by Sheehan we have done no further experimental work in this connection. In his experiments the vapor was at temperatures ranging from 60° to 70°; the electron wave length was 0.06059 Å and the camera distance, 10.94 cm. A new visual curve was not drawn, Sheehan's on the whole proving to be satisfactory. The features especially important for the determination were rechecked by an examination of the photographs in collaboration with Professor Schomaker.

The curves calculated for a regular tetrahedral model are presented in Figure 1. The cut-off point was varied until the most acceptable curve was obtained. The theoretical value $\delta_{\text{Os-O}} = 0.122 \text{ \AA}$ leads to curve 4 which is not considered to be as satisfactory as curves 2 and 3 corresponding to values of 0.110 Å and 0.115 Å, respectively.

Values of 0.10 \AA (curve 1) and 0.13 \AA (curve 5) are clearly not acceptable. The effect of increasing the temperature factor of the $0\dots 0$ term is shown in curve 6.

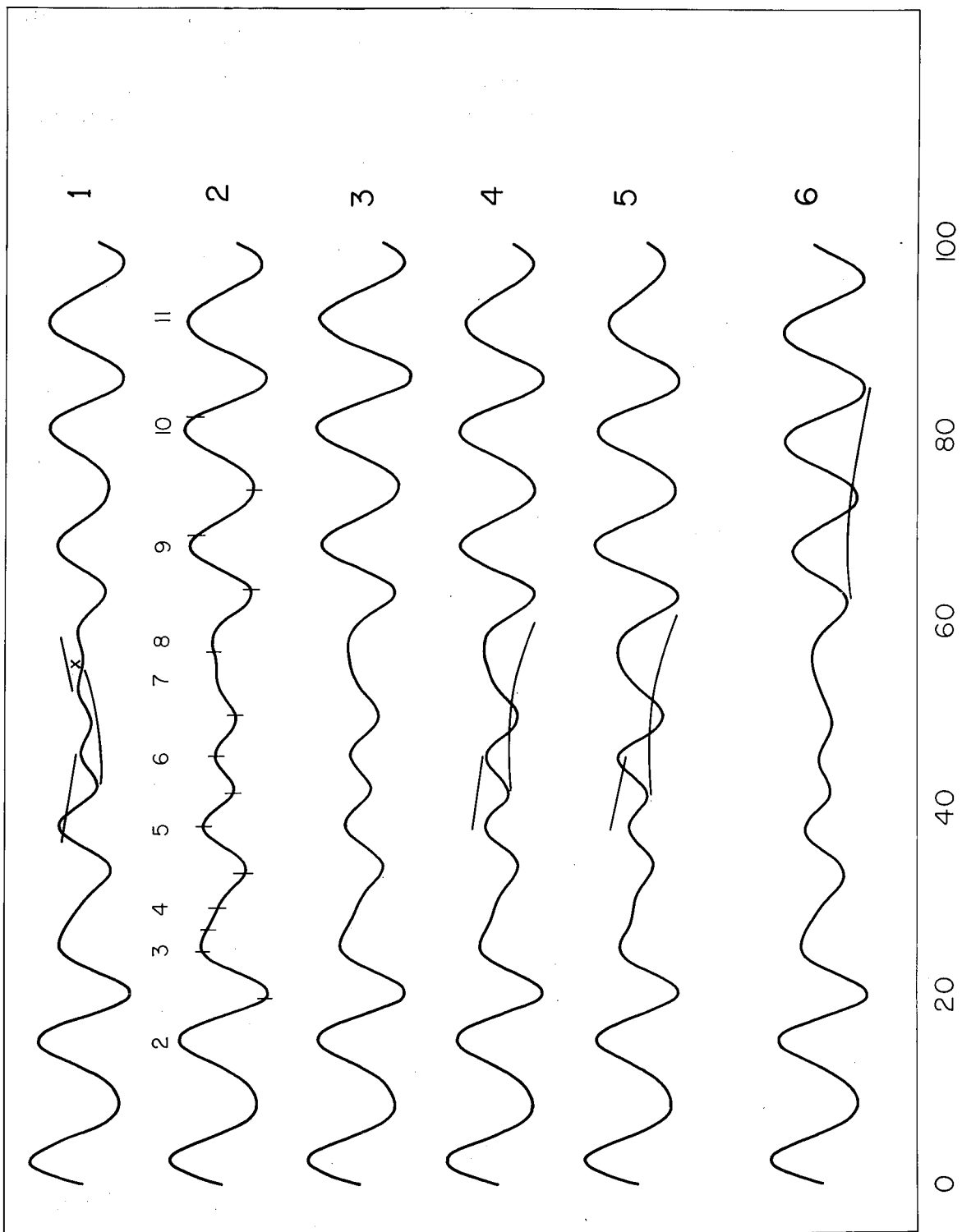


Figure 1. Osmium Tetroxide

Legend of Figure 1. OsO₄

Curve	δ_{Os-O} (Å)	$(a_{0..0} - a_{Os-O}) \times 10^3$ (Å ²)
1	0.100	0.8
2	0.110	0.8
3	0.115	0.8
4	0.120	0.8
5	0.130	0.8
6	0.110	3.3

TABLE I

Scale Factor, Osmium Tetroxide

Min	Max	q_o (V.S.)	q_c/q_o	Wt
3		19.4	1.041	1
	3	24.3	1.049	0
4		26.7	1.049	0
	4	28.8	1.042	0
5		32.5	1.031	1
	5	37.40	1.013	3
6		40.96	1.025	3
	6	44.73	1.017	2
7		49.02	1.010	2
	7	--	--	0
8		55.72	0.996	0
	8	--	--	0
9		62.19	1.008	1
	9	67.77	1.002	2
10		72.59	1.018	1
	10	80.34	0.997	1

Scale Factor 1.016

Ave. Dev. 0.009

$$r_{Os-O} = 1.69 \times 1.016 = 1.717 \text{ \AA}$$

Ave. Dev. 0.015 \AA

TABLE II

Structure of Osmium Tetroxide, T_d

Parameter	Value	Limit of Error
r_{Os-O}	1.717 Å	0.035 Å
$2\delta_{Os-O}$ (apparent split)	0.226 Å	0.02 Å

C. TUNGSTEN HEXAFLUORIDE

a.

Spectroscopic evidence points conclusively to a regular octahedral structure for the tungsten hexafluoride molecule. This conclusion, previously arrived at purely on the basis of the presence of only three lines in the Raman spectrum (21), has been verified by two independent investigations of the infrared spectrum of the vapor (22), (23), in which all but five very weak bands were fit into an identification scheme based on the totally symmetric octahedral structure.

Although the original electron diffraction investigation of Braune and Pinnow (1) on the hexafluorides of uranium, tungsten, and molybdenum leading to unsymmetrical structures was not considered by many to be adequate, the more thorough work of Bauer (2) on uranium hexafluoride clearly indicated that a serious discrepancy did in fact exist with regard to the determination of the structures of these compounds. Tungsten hexafluoride was later investigated by Bastiansen (24) by means of electron diffraction. The radial distribution curve strongly suggested a model containing three short and three long W-F distances and indeed his final model was in accord with this suggestion having for the unequal distances values of 1.73 Å and 1.96 Å. Bauer had obtained the same result in unpublished work (25).

b.

The present investigation is based on Dr. Bastiansen's diffraction photographs (wave length, 0.06048 Å; camera distance, 10.975 cm) although a series of sector-photographs has recently become available and is being studied by Dr. Kimura.

A new visual curve was not drawn, Bastiansen's being used as a guide. Where questionable points arose they were settled by examination of the photographs and the conclusions were based primarily on the observations of Professor Schomaker. The general appearance of the pattern is fairly obvious and serves to determine the location of the cut-off point. The theoretical curves calculated for a regular octahedral model are presented in Figure 2. The first five curves illustrate the manner in which the theoretical pattern depends on the value chosen for δ_{W-F} . Curve 3, which is accepted as being the most satisfactory, corresponds to $\delta_{W-F} = 0.116$ in excellent agreement with the theoretical value 0.115. As shown by curves 6 and 7, two details of the pattern (maximum 5a and minimum 8) are particularly sensitive to the choice made for the temperature factor of the $F \dots F_0$ terms and serve to confine the difference $a_{F \dots F_0} - a_{W-F}$ to a fairly limited range. Visual examination of the photographs indicates that minimum 8 is a fair amount shallower than the average of minima 7 and 9 and also that maximum 5a is very weak. In the theoretical curve the first of these requirements is met the better by a decrease in $a_{F \dots F_0} - a_{W-F}$; the second by an increase. Thus the best choice is determined by a compromise. The final results are presented in Table IV.

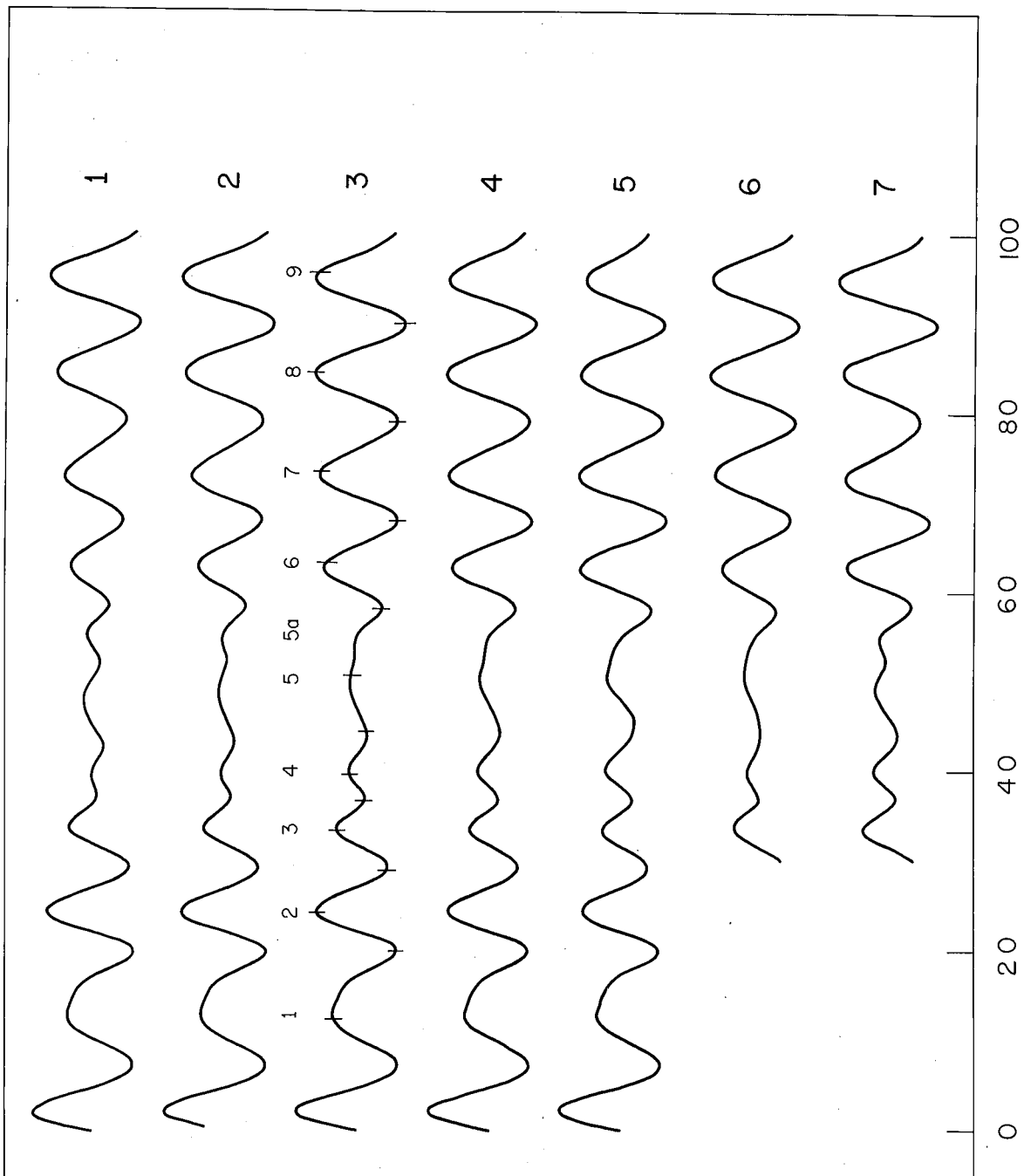


Figure 2. Tungsten Hexafluoride

Legend of Figure 2. WF_6

Curve	$\delta_{W-F} (\text{\AA})$	$(a_{ij} - a_{W-F}) \times 10^3 (\text{\AA}^2)$	
		F..F _O *	F..F _p *
1	0.100	2.2	0.8
2	0.108	2.2	0.8
3	0.116	2.2	0.8
4	0.120	2.2	0.8
5	0.128	2.2	0.8
6	0.116	4.0	1.0
7	0.116	1.0	0.5

* F..F_O means ortho (adjacent) fluorine atoms

F..F_p means para (opposite) fluorine atoms

TABLE III

Scale Factor, Tungsten Hexafluoride

Min	Max	q_o (O.B.)	q_c/q_o	Wt
1		7.9	0.937	0
	1	12.5	1.040	0
2		20.2	0.990	1
	2	24.4	1.004	1
3		29.1	1.010	2
	3	33.50	1.003	3
4		36.89	1.003	3
	4	39.83	1.007	2
5		44.59	0.987	1
	5	50.88	0.975	0
6		58.31	0.998	2
	6	63.52	0.987	3
7		68.14	0.996	3
	7	73.58	0.993	3
8		79.14	0.998	2
	8	84.72	0.995	2
9		90.27	0.995	2
	9	95.92	0.989	1

Scale Factor 0.997

Ave. Dev. 0.006

$$r_{W-F} = 1.84 \times 0.997 = 1.834 \text{ \AA}$$

Ave. Dev. 0.011 \AA

TABLE IV

Structure of Tungsten Hexafluoride, O_h

Parameter	Value	Limit of Error
r_{W-F}	1.834 Å	0.03 Å
$2\delta_{W-F}$ (apparent split)	0.233 Å	0.02 Å

D. TUNGSTEN HEXACARBONYL

a.

The earliest investigation of the structure of tungsten hexacarbonyl was based on a study of the X-ray scattering by the crystal (26). The results were consistent with the assumption of an octahedral structure. However, the tungsten-carbon distance could not be determined (upper limit: 2.3 Å) because of the unfavorably large ratio of the atomic numbers.

Shortly thereafter, an electron diffraction study ($s_{\max} \sim 14$) was made by Brockway, Ewens, and Lister (27), the results of which supported the regular octahedral structure although the evidence was not considered to be conclusive. Also it was not possible to determine whether the tungsten atom is bonded to the carbon atom or oxygen atom of the carbonyl group. Assuming the former to be the case, they obtained for the W-C and C-O distances the values 2.06 ± 0.04 Å and 1.13 ± 0.05 Å, respectively. Later, with electron diffraction photographs extending out to larger angles ($s_{\max} \sim 35$), Sheehan obtained a radial distribution function giving two different values for the W-C distances (1.94 Å and 2.20 Å) as well as for the W..O distances (3.09 Å and 3.31 Å) in the molecule. The resulting need for introducing a large number of parameters into the trial models made the investigation a particularly laborious task to carry through.

In the meantime, the infrared spectrum of solid tungsten hexacarbonyl was obtained in the 2-15 μ region (28) with a view toward determining whether the C-O bond in the compound is similar to the bond in the carbon monoxide molecule or rather more like the one in ketone molecules. A lone band was observed corresponding to the C-O stretching, the frequency being close to that in carbon monoxide. More recently (29), a much more extensive investigation of the infrared spectra of the vapors of chromium hexacarbonyl and molybdenum hexacarbonyl has been carried out. Only preliminary spectra were obtained for the tungsten carbonyl (due to lack of sufficient sample) but these are "very similar to those of the chromium and molybdenum compounds" the spectra of which could be interpreted quite satisfactorily on the basis of an octahedral structure.

b.

In the present investigation we made use of the photographs obtained by Sheehan (temperature, 97° - 109° ; electron wave length, 0.06075 \AA ; camera distance, 10.94 cm).

Theoretical curves were calculated for a regular octahedral model of the molecule in which the tungsten atom is bonded to the carbon atoms of the carbonyl groups. The first five curves presented in Figure 3 show the way in which the theoretical intensity function varies as the shape of the molecule is changed, with the W-C and W..O phase shifts fixed at their theoretical values and the relative temperature factor coefficients assumed to be those of set A. Curve 3 is the most acceptable

in this group thus determining the ratio of the W-C distance to the W..0 distance (207/320). The region beyond q equal 50 as given by curve 3 is in excellent agreement with the appearance of the photographs.

The region between maxima 4 and 9, however, is unsatisfactory so that variations of the relative temperature factor coefficients and of the positions of the cut-offs were considered. The form of maxima 5, 6, and 7 in these curves indicates the need for shifting the cut-off points to larger q-values while the exaggerated appearance of maxima 7a and 8 seems to require the introduction of more severe temperature factors. Therefore pairs of curves were calculated using the relative temperature factor coefficients of sets A and B for each choice of cut-off points. The curves for set B are more like what is wanted than those for set A. Curve 7B, corresponding to $\delta_{w-c} = \delta_{w..o} = 0.115 \text{ \AA}$, is considered to be the best (theoretical prediction: $\delta_{w-c} = 0.127$, $\delta_{w..o} = 0.119$)*.

As for the degree of confirmation obtained for the octahedral model we indicate its virtues by presenting curve 10 which is the calculated intensity using only the W-C, W...O, and bonded C-O terms. The introduction of the non-bonded C...O, O...O, and C...C distances as they occur in the octahedral structure changes the comparison of maxima 1, 2, and 4, introduces minimum 5, sharpens minimum 6, and broadens minimum 7, all as required by the appearance of the photographs. At the same time, these terms do not destroy any general features of the pattern, except in

*

This curve is improved somewhat if the C-O bond distance is increased by a few hundredths of an Ångström while the ratio of the W-C distance to the W...O distance is kept fixed at 207/320.

the region beyond q equal 40 where their influence must be eliminated by the introduction of severe temperature factors*. In addition, the hint of maximum 3 is introduced as indicated by the change in the shape of minimum 4. To achieve a more distinct maximum it is necessary to increase the temperature factor coefficient of the $O...O_o$ terms to a value of about 0.040 \AA^2 in order that the $C...O_p$ and $O...O_p$ contributions which are in phase in this region can exert a sufficient influence. In connection with this maximum there may be the difficulty that the eye is particularly sensitive (especially in this region of small q -values) to the effects of the $C...O_p$ and $O...O_p$ terms because of their extremely high frequency (5.27 \AA and 6.40 \AA , respectively) in a way not sufficiently accounted for in the usual intensity formula. For example, a formula giving greater importance to curvature and therefore to higher frequency terms may be what is required.

With regard to the possibility that another model might also give acceptable results (there is no indication of this, however, in the radial distribution curve of Sheehan) we mention that although no curves were calculated for the trigonal prism model the distances corresponding to such a model are such as to yield a completely unsatisfactory result (especially in the vicinity of maximum 5) when the effects of the non-bonded $C...O$, $O...O$, and $C...C$ terms are introduced into curve 10.

* These large temperature factors appear to be plausible on the basis of the spectroscopic investigation (29) which yielded for the F_{2g} bending vibration the particularly low "frequencies" of 90 cm^{-1} and 80 cm^{-1} for the chromium hexacarbonyl and the molybdenum hexacarbonyl molecules, respectively.

Finally, it has been found that the electron diffraction method appears to be capable of deciding whether the tungsten atom is bonded to the carbon atom or to the oxygen atom of the carbonyl group. Curve 11A, calculated for the model in which the bonding is to the oxygen atom (using the theoretical values for the phase shifts), is definitely inferior in a way which cannot be remedied, it seems, by any variation in the parameter values.

c.

It is necessary here to add a few remarks in connection with what appears at first to be a striking discrepancy between the form of the calculated curves and the "obvious appearance" of the photographs in the region between maxima 4 and 9. The theoretical curves show a strong dominance of maximum 7 whereas the photographs seem to indicate maximum 6 to be the most outstanding feature in this region. This leads to a comparison between maxima 5, 6, and 7, in the visual curve which is the opposite to that obtained in the theoretical curves. The fact, however, that all of the theoretical curves are the same in this respect regardless of the choice made of the available parameters indicates that the visual interpretation of the photographs is in error. The apparent impasse can be resolved if one assumes the theoretical curve, say curve 7B, to be correct and sets about to determine whether such a form might possibly be misinterpreted in the visual examination of the photographs. Noting that what the eye "sees" is strongly affected by the surroundings (background), we expect that the

great strength of maximum 4 will tend to belittle maximum 5, the double minima 6 and 7 will make maximum 6 appear too strong, and the exceptional width of the region of maxima 7 and 8 will result in maximum 7 appearing too weak. (These errors will be diminished if the observation is made at arm's length.) All of these effects will combine to produce the apparent discrepancy existing between the visual and theoretical curves. Such effects did not often play a great role in the visual interpretation since the background usually does not change very much over such small regions and investigators had learned how mentally to draw in the background when making their observations. With the entrance of the beat-out phenomenon resulting from phase shifts, however, sudden changes in background occur as first the influence of one type of term and then that of another dominates the pattern. In such cases apparently even an experienced observer must use extreme care in arriving at a visual interpretation of the photographs. The situation is presumably not much improved when microphotometer tracings of sector pictures are employed since there is the necessity for subtracting out the background which leads again to the same difficulty.

The theoretical intensity formula used in the correlation with visual data was originally derived by taking the ratio of the molecular (oscillating) scattering to the atomic ("background") scattering so that it would yield maxima and minima corresponding to the rings which the eye sees on the photographs. Although the resulting formula succeeds in this and is useful for determining the size of the molecule by a comparison of ring diameters (this was at first the only use made of the formula) it does

not try to take into account the effects involved in the visual estimation of the relative intensities of these rings*. In the past, as mentioned in the preceding paragraph, the observer learned from experience how to change what he actually saw in order that it would correspond more closely to what the formula gives. This no longer appears to be a sufficiently satisfactory method of approach. An intensity function corresponding more closely to the obvious appearance of the photographs to an inexperienced observer would certainly help to improve the situation. Unfortunately, the derivation of such a function (which is at the same time not cumbersome) is no easy task as is evidenced by the fact that no substantial change in the original formula has been made during the more than 25 years that have passed since it was first introduced.

* Unfortunately these effects are even present in the measurement of ring diameters.

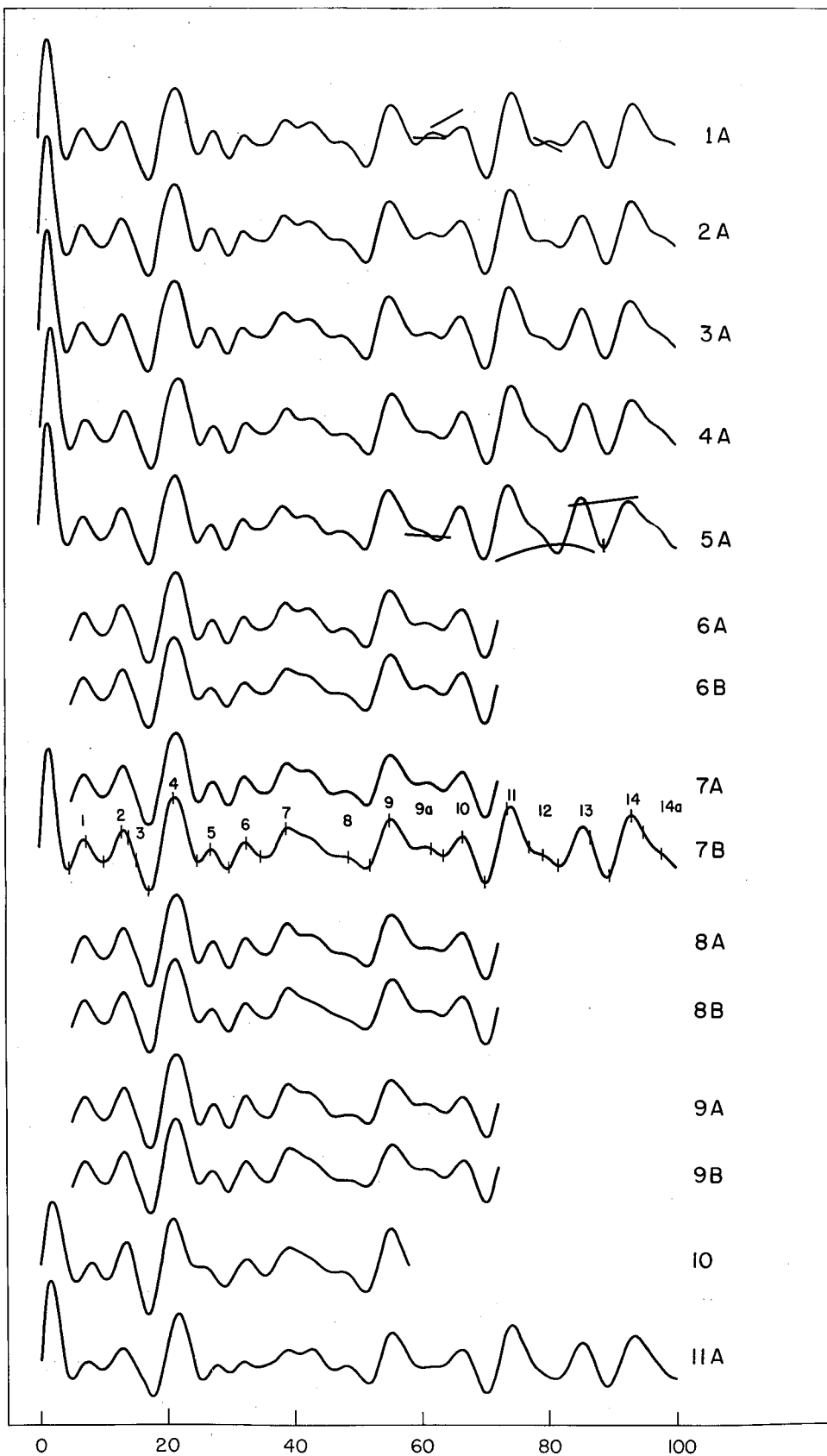


Figure 3. Tungsten Hexacarbonyl

Legend of Figure 3, $W(CO)_6$

Model	$r_{W-C}/r_{W..O}$	δ_{W-C} (Å)	$\delta_{W..O}$ (Å)
1	207/318	0.127 [#]	0.119 [#]
2	207/319	0.127	0.119
3	207/320	0.127	0.119
4	207/321	0.127	0.119
5	207/322	0.127	0.119
6	207/320	0.120	0.120
7	207/320	0.115	0.115
8	207/320	0.120	0.110
9	207/320	0.110	0.110
10*	207/320	0.120	0.120

11 W-O-C bonding with $r_{W..C}/r_{W-O} = 320/207$,
 $\delta_{W..C} = 0.125$, $\delta_{W-O} = 0.120$.

Theor. Value

* W-C, W..O, and C-O terms only.

Legend of Figure 3, $W(CO)_6$ (Cont'd)

Atom Pair	$(a_{ij} - a_{C-O}) \times 10^3 (\text{\AA}^2)$	
	A	B
W-C	0.5	0.5
W..O	0.85	0.85
C..C _p	2.5	4.0
C..O _p	3.5	6.0
O..O _p	4.5	8.0
C..C _o	6.0	10.0
C..O _o	10.0	16.0
O..O _o	20.0	30.0

TABLE V

Scale Factor, Tungsten Hexacarbonyl

Min	Max	q_0 (W.S.)	q_c	q_c/q_0	Wt
1		(4.8)	4.6	0.958	0
	1	(7.5)	7.0	0.933	0
2		(10.2)	10.2	1.000	0
	2	(13.0)	13.25	1.019	1
3		(14.1)	--	--	--
	3	(15.3)	--	--	--
4		(17.2)	17.3	1.006	1
	4	(21.1)	21.3	1.009	1
5		24.8	25.0	1.008	1
	5	26.9	27.0	1.004	2
6		29.8	29.5	0.990	2
	6	32.5	32.25	0.992	3
7		34.8	35.5	1.020	0
	7	38.8	39.0	1.005	1
8		43.7	45.7	1.046	0
	8	48.6	48.2	0.992	0
9		51.8	51.2	0.988	1
	9	54.99	55.2	1.004	3
9a		--	59.1	--	--
	9a	61.50	61.0	0.992	0
10		63.4	63.5	1.002	0
	10	66.39	66.5	1.002	2
11		69.94	70.0	1.001	3
	11	73.46	74.0	1.007	3
12		76.9	78.0	1.014	0
	12	79.1	79.2	1.001	0
13		81.4	81.25	0.998	0
	13	86.4	85.5	0.990	2
14		89.46	89.0	0.995	1
	14	92.8	93.1	1.003	1
14a		94.7	96.5	1.019	0
	14a	97.5	98.0	1.005	0

() denotes obs. of V.S.

Scale Factor 1.001
Ave. Dev. 0.006

$r_{W-C} = 2.071 \times 1.001 = 2.073 \text{ \AA}$
Ave. Dev. 0.012 \AA

$r_{W..O} = 3.201 \times 1.001 = 3.204 \text{ \AA}$
Ave. Dev. 0.019 \AA

TABLE VI

Structure of Tungsten Hexacarbonyl, O_h

Parameter	Value	Limit of Error
r_{W-C}	2.073 Å	0.04 Å
$r_{W...O}$	3.204 Å	0.065 Å
$2\delta_{W-C}$	0.230 Å	0.03 Å
(apparent splits)		
$2\delta_{W...O}$	0.230 Å	0.03 Å

E. MOLYBDENUM HEXACARBONYL

a.

The X-ray scattering by the crystal of molybdenum hexacarbonyl was interpreted on the basis of an octahedral structure (26) with the values 2.13 \AA and 1.15 \AA assigned to the Mo-C and C-O distances, respectively.

This was followed by the electron diffraction study made by Brockway and co-workers (27) which led to results very similar to those which they obtained for the tungsten compound. They reported the value $2.08 \pm 0.04 \text{ \AA}$ for the Mo-C distance and $1.15 \pm 0.05 \text{ \AA}$ for the C-O distance in the regular octahedral structure. As in the case of tungsten hexacarbonyl, however, Sheehan (20) was forced to interpret his electron diffraction data (which included larger angles of scattering than those of Brockway) in terms of a model having a short Mo-C distance (1.99 \AA) and a long Mo-C distance (2.12 \AA), assuming all of the C-O distances to be equal.

Very recently the infrared investigation (29) has, however, confirmed the regular octahedral structure for the molecule.

b.

The electron diffraction data used in this investigation are those of Sheehan (temperature, $90^{\circ} - 112^{\circ}$; electron wave length, 0.06042 \AA ; camera distance, 10.92 cm).

Theoretical curves were calculated for a regular octahedral model of the molecule in which the molybdenum atom is bonded to the carbon atoms of the carbonyl groups. The first five curves in Figure 4 show the way in which the theoretical intensity function varies as the shape of the molecule is changed, with the Mo-C and Mo..O phase shifts fixed at their theoretical values and the relative temperature factor coefficients assumed are those of set A. Curve 3 is the most acceptable in this group thus determining the ratio of the Mo-C distance to the Mo..O distance at 207/320. This curve would be improved if minimum 7 could be made deeper and maximum 9 could be made stronger. A shift in the cut-off point (theoretical $(q_c)_{\text{Mo-C}} = 68.5$) of the Mo-C term to a larger q-value should help to bring about both of these changes. However, if the cut-off point of the Mo..O term is to be shifted at all from the theoretical value ($(q_c)_{\text{Mo..O}} = 78$), it should not be shifted toward larger q-values because this has the effect of making minimum 11 deeper and of weakening maximum 12, both of which changes are not desired. Thus the amount by which the cut-off point of Mo-C can be shifted is limited if $\delta_{\text{Mo-C}}$ is to remain greater than $\delta_{\text{Mo..O}}$.

Curves 6, 7, 8, and 9, serve to illustrate the form of the intensity function for various choices of the cut-off points and relative temperature factor coefficients. Curve 6A is quite satisfactory in the region q greater than 60 but not as good for q less than 60. In particular, minimum 7 should be deeper and maximum 9 stronger. Curve 8A is better in these latter respects but not as good for q greater than 60, minimum 11 being too deep and maximum 12 too weak. A choice lying somewhere between

the two curves is best so that we take $2\delta_{\text{Mo-C}} = 2\delta_{\text{Mo..O}} = 0.135$
(theoretical prediction: $2\delta_{\text{Mo-C}} = 0.146$, $2\delta_{\text{Mo..O}} = 0.128$). The need for more severe temperature factors such as those of set B is not as clearly indicated here as it is in the case of the tungsten carbonyl. Maximum 3 is already quite distinct and there is no exaggerated feature to be eliminated from the curves. The only apparent improvement obtained by using set B is that maximum 9 is strengthened. In connection with this feature and the one immediately succeeding it (maximum 10), we remark that a situation arises similar to the one experienced in the case of tungsten hexacarbonyl (maxima 6 and 7) in that the obvious appearance of the photographs suggests that maximum 9 is stronger than maximum 10 by a considerable amount. However, in none of the theoretical curves (which are reasonably acceptable otherwise) is this found to be the case. The answer to the apparent difficulty again lies in the need for giving due consideration to background effects. Maximum 9 is preceded by a deep minimum with the curve rising sharply, whereas maximum 10 is preceded by a shallow minimum with the curve falling off very gradually resulting in a broad maximum. Under such conditions and particularly at close examination of the photographs we should expect an appearance similar to the one actually found. This kind of situation arises in these carbonyl compounds as the cut-off region is approached where the C-O term is becoming dominant producing broad maxima which appear weak. We note also that in the case of the molybdenum compound, maximum 7 compares quite favorably with maximum 6 in the appearance of the photographs (unlike the tungsten case) since the cut-off points are quite distant and maximum 7 is now preceded by a deep minimum.

The trigonal prism model as well as the possibility of Mo-O-C bonding are both ruled out in exact analogy to the case of tungsten hexacarbonyl.

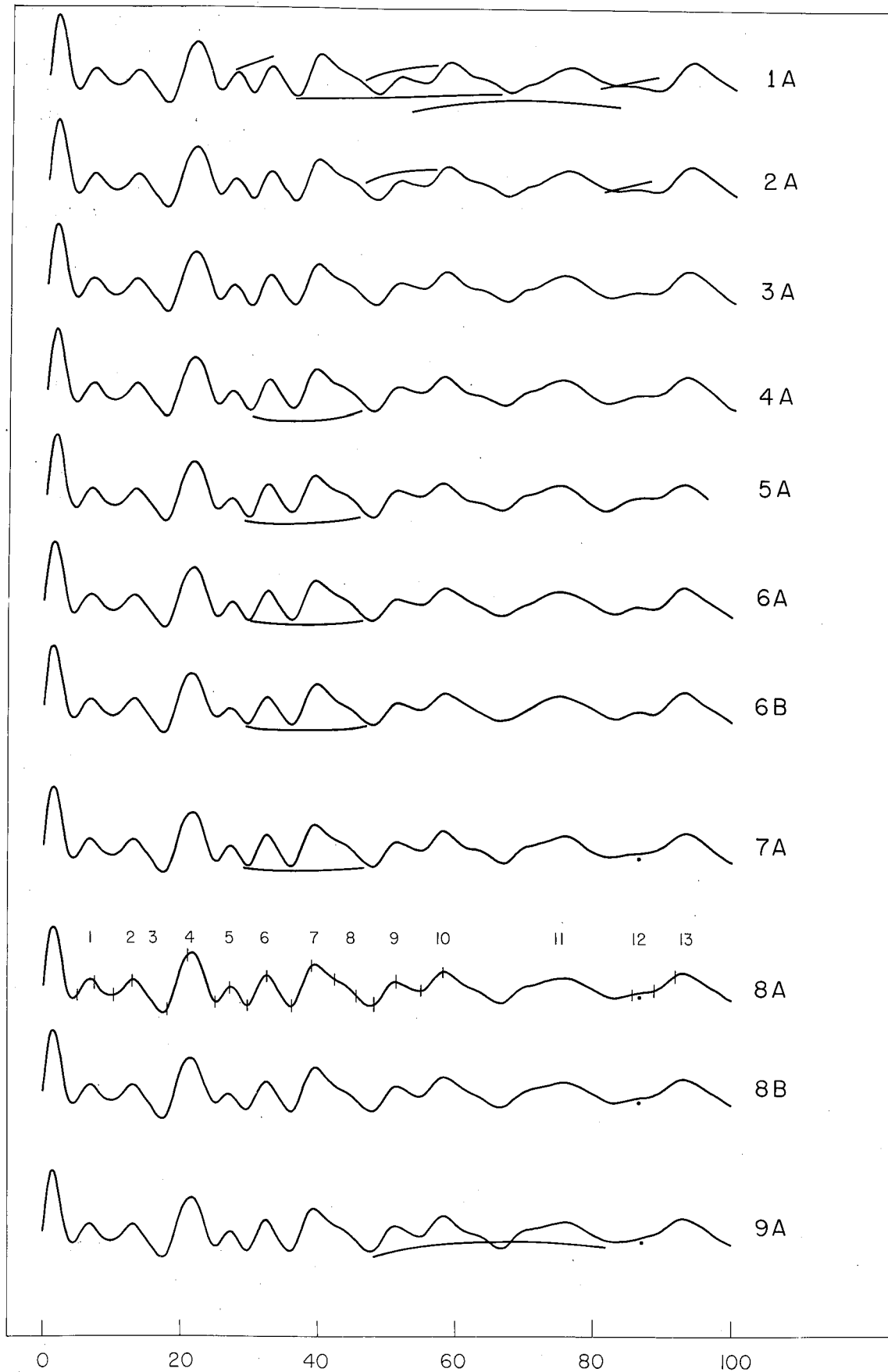


Figure 4. Molybdenum Hexacarbonyl

Legend of Figure 4, Mo(CO)₆

Model	$r_{\text{Mo-C}}/r_{\text{Mo..O}}$	$\delta_{\text{Mo-C}} (\text{\AA})$	$\delta_{\text{Mo..O}} (\text{\AA})$
1	207/318	0.073*	0.064*
2	207/319	0.073	0.064
3	207/320	0.073	0.064
4	207/321	0.073	0.064
5	207/322	0.073	0.064
6	207/320	0.070	0.070
7	207/320	0.070	0.060
8	207/320	0.065	0.065
9	207/320	0.065	0.060

* Theor. Value

Legend of Figure 4, Mo(CO)₆ (Cont'd)

$(a_{ij} - a_{C-O}) \times 10^3 (\text{\AA}^2)$

Atom Pair	A	B
Mo-C	0.5	0.5
Mo..O	0.85	0.85
C..C _p	2.5	4.0
C..O _p	3.5	6.0
O..O _p	4.5	8.0
C..C _o	6.0	10.0
C..O _o	10.0	16.0
O..O _o	20.0	30.0

TABLE VII

Scale Factor, Molybdenum Hexacarbonyl

Min	Max	q_o (W.S.)	q_c/q_o	Wt
1		5.0	0.880	0
	1	7.5	0.907	0
2		10.4	0.962	0
	2	13.0	1.015	0
3		--	--	0
	3	--	--	0
4		18.2	0.951	0
	4	20.97	1.030*	1
5		25.06	1.002	1
	5	27.28	0.999	1
6		29.86	0.991	2
	6	32.59	0.994	3
7		36.24	0.986	2
	7	39.1	1.004	1
8		42.5	0.981	0
	8	45.6	0.965	0
9		48.2	0.983	1
	9	51.43	0.992	3
10		55.08	0.995	1
	10	58.39	0.998	1
11		--	--	0
	11	--	--	0
12		--	--	0
	12	86.0	1.003	1
13		89.1	0.999	1
	13	92.3	1.008	1

Scale Factor 0.995

Ave. Dev. 0.005

$$r_{\text{Mo-C}} = 2.071 \times 0.995 = 2.061 \text{ \AA}$$

$$\text{Ave. Dev.} \quad \quad \quad 0.010 \text{ \AA}$$

$$r_{\text{Mo..O}} = 3.201 \times 0.995 = 3.185 \text{ \AA}$$

$$\text{Ave. Dev.} \quad \quad \quad 0.016 \text{ \AA}$$

* Rejected

TABLE VIII

Structure of Molybdenum Hexacarbonyl, O_h

Parameter	Value	Limit of Error
$r_{\text{Mo-C}}$	2.061 Å	0.04 Å
$r_{\text{Mo..O}}$	3.185 Å	0.065 Å
$2\delta_{\text{Mo-C}}$	0.135 Å	0.02 Å
$2\delta_{\text{Mo..O}}$ (apparent splits)	0.135 Å	0.02 Å

F. TUNGSTEN HEXACHLORIDE

a.

On the basis of their electron diffraction investigation ($s_{\max} \sim 15$) Ewens and Lister (30) reported a regular octahedral structure for the tungsten hexachloride molecule with the W-Cl distance equal to $2.26 \pm 0.02 \text{ \AA}$. Their radial distribution function had single peaks at 2.28 \AA and 3.15 \AA . The general appearances of the five maxima which were visible on their pictures were in agreement with those of the calculated curves.

The X-ray study (31) indicated that the molecule is present in the crystal with the structure of a slightly deformed octahedron which result was considered to be in agreement with that of the electron diffraction investigation. The W-Cl distance was assigned the value 2.24 \AA .

The electron diffraction photographs obtained by Rundle were described by Spurr (32) as being in full agreement with the observations of Ewens and Lister. Later, however, Professor Schomaker re-examined the photographs giving particular attention to the region of large scattering angles with a view toward determining the presence of a beat-out and resulting apparent split which was expected because of the phase shift phenomenon. Indeed the effect was observed to be present and a rough estimate was made of the apparent split (0.18 \AA).

b.

For the purpose of the present investigation Professor Schomaker drew a visual curve based on his study of the photographs. The theoretical

curves were next calculated (curves 1-5) and were all found to be in serious disagreement with the visual curve in the region immediately following maximum 4. Maximum 5, which is present in the theoretical curves, is absent in the visual curve*. A careful re-examination of the photographs in this region failed to change the situation. Since it appeared that a shortening of the Cl..Cl_o distance relative to that given by the octahedral model would tend to send this region of the theoretical curves into general agreement with the visual observation, Professor Schomaker suggested that the vapor actually present at the time the photographs were taken may have been that of tungsten oxychloride which is easily formed from the hexachloride in the presence of oxygen or moisture and has a considerably higher vapor pressure.

To test the possible validity of this hypothesis, a theoretical intensity pattern (curve 6) was calculated for a model of the tungsten oxychloride molecule in which the Cl..Cl_o distance in the octahedral model was decreased slightly to a value which it was guessed would lead to the desired effect. The form of curve 6 in the region in question is in excellent agreement with the visual curve although for some of the other features in the portion of the curve corresponding to q less than 50 the visual curve seems to lie somewhere between the curves for WCl_6 and $WOCl_4$, possibly indicating that a mixture of these substances had been present. Unfortunately, the photographs are only five in number and the features

* Ewens and Lister state that maximum 4 is unsymmetrical, falling more slowly to the outside. This is more in agreement with our theoretical curves than with the photographs.

which are present in the region beyond q equal 50 are very difficult to observe. On the basis of his study of the first four pictures (which are poor in this region) taken in the course of the experiment, Professor Schomaker had drawn a visual curve which somewhat resembles curve 5 (WCl_6) at these large q -values. On examining the fifth picture taken (which is much clearer), however, he had made a sketch of the appearance of this region which bears a striking resemblance to the $WOCl_4$ curve. Had this sketch instead been more like the curves for WCl_6 at these q -values, the possibility that $WOCl_4$ had been present originally but had been gradually depleted would appear plausible. However, maximum 5, which is associated with WCl_6 , is not observed on this photograph either so that it seems likely that even during the taking of the last picture the vapor of the oxychloride was the predominant one present. The rough agreement (in the region q greater than 50) of the visual curve based on the first pictures with the theoretical curves of WCl_6 must either be accidental or else due to the difficulty of obtaining a reliable visual curve from such poor pictures. In any case all that one can conclude is that there is sufficient evidence for suspecting contamination to have occurred. Pictures of pure WCl_6 must be obtained in order for the investigation of its structure to proceed.

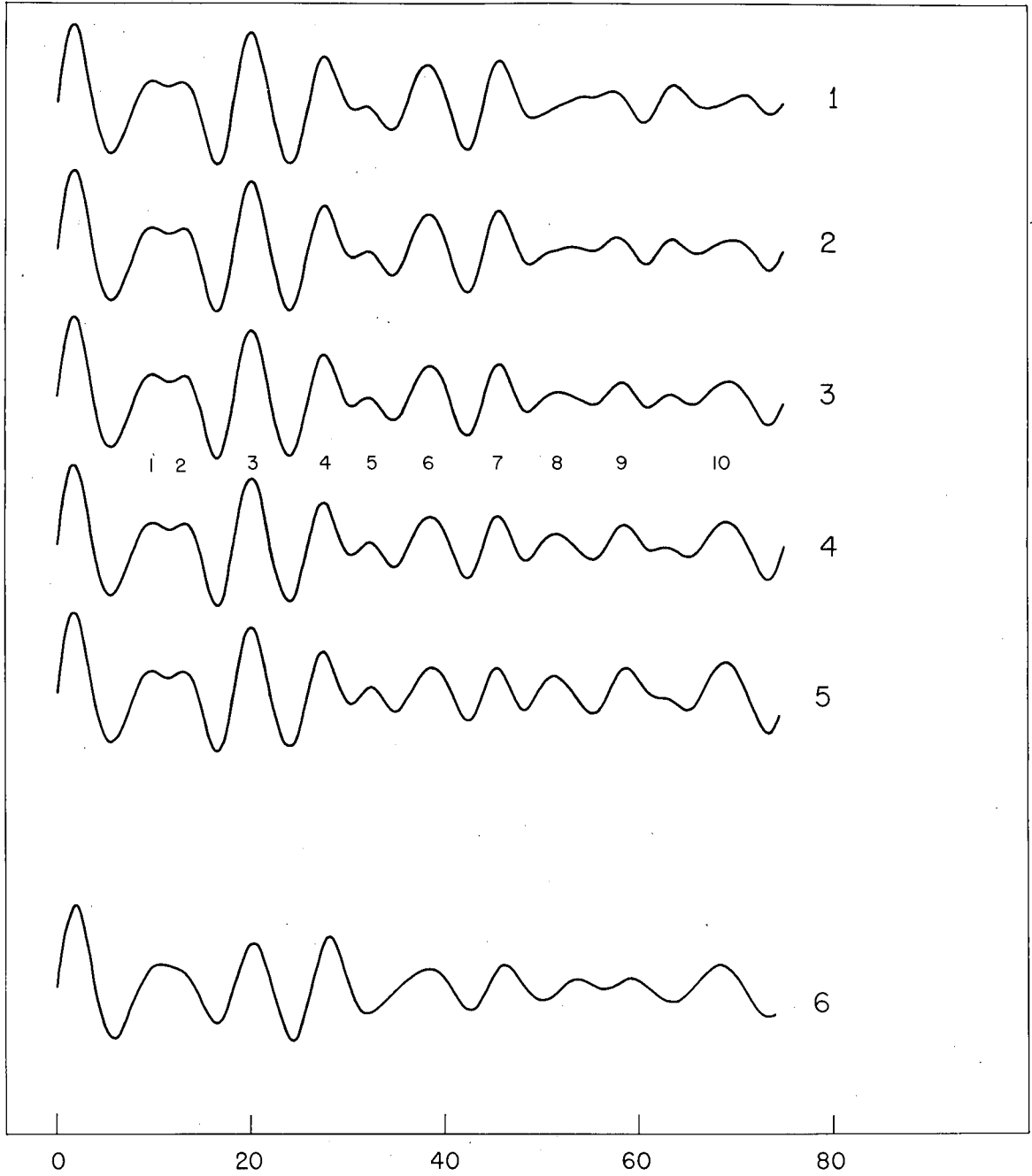


Figure 5. Tungsten Hexachloride

Legend of Figure 5, WCl_6

Curve	δ_{W-Cl} (Å)	$(a_{ij} - a_{W-Cl}) \times 10^3$ (Å ²)	
		$Cl_1..Cl_1$	$Cl_1..Cl_1$ _p
1	0.072	3.0	1.0
2	0.080	3.0	1.0
3	0.088	3.0	1.0
4	0.096	3.0	1.0
5	0.104	3.0	1.0

6

WCl_4

Model

$$r_{W-Cl_1} = r_{W-Cl_2}$$

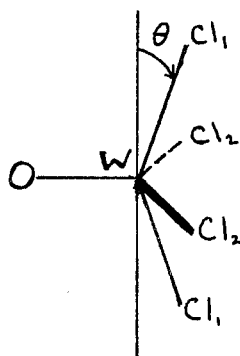
$$\langle Cl_1 W Cl_2 \rangle = \psi$$

$$\langle Cl_1 W Cl_1 \rangle = \pi - 2\theta$$

$$\langle Cl_2 W O \rangle = 3\pi/4$$

$$\langle Cl_2 W Cl_2 \rangle = \pi/2$$

$$\langle Cl_1 W O \rangle = \pi/2 + \theta$$



Parameter Values

$$\sin \theta = \sqrt{2} \cos \psi$$

$$r_{W-Cl} = 2.26 \text{ Å}; r_{W-O} = 1.70 \text{ Å}$$

$$\delta_{W-O} = 0.120 \text{ Å}; \delta_{W-Cl} = 0.090 \text{ Å}$$

$$\theta = 4^{\circ}50'*$$

(cont'd)

* Chosen so that $\frac{r_{Cl_1..Cl_2}}{r_{W-Cl}} = \frac{310}{226}$

Legend of Figure 5, WCl_6 (Cont'd)

Atom Pair	$(a_{ij} - a_{\text{W-Cl}}) \times 10^3 (\text{\AA}^2)$
W-O	0.0
$\text{Cl}_1 \dots \text{Cl}_2$	3.0
$\text{Cl}_2 \dots \text{Cl}_2$	3.0
$\text{Cl}_1 \dots \text{Cl}_1$	4.0
$\text{Cl}_1 \dots \text{O}$	4.0
$\text{Cl}_2 \dots \text{O}$	6.0

G. MOLYBDENUM HEXAFLUORIDE

a.

As in the case of the tungsten compound, the spectroscopic evidence is strongly in favor of a regular octahedral structure for the molybdenum hexafluoride molecule (21), (22), (23).

In the electron diffraction investigation by Braune and Pinnow (1), only three measurable maxima were obtained ($s_{\max} \sim 11$). The first was discarded and the remaining two were consistent within the experimental error with a regular octahedral structure. However, having found that the assumption of an unsymmetrical model was necessary for the uranium compound, and likely for the tungsten compound, they postulated a similar structure for molybdenum hexacarbonyl. Later, Bastiansen using considerably more extensive data observed a split of 0.14 \AA in the Mo-F distance, the two unequal values being 1.77 \AA and 1.91 \AA . Bauer had also obtained this result (25).

b.

The present investigation is based on Bastiansen's diffraction photographs (wave length, 0.06045 \AA ; camera distance, 10.985 cm).

No features could be observed in the cut-off region on these photographs so that his visual curve (which he had drawn as a dashed line in this region to indicate uncertainty) had to be used with the hope that

it might prove sufficient for the purpose of roughly placing the location of the cut-off point.

Five theoretical intensity curves were calculated for a regular octahedral model for different values of $\delta_{\text{Mo-F}}$. Curve 4, corresponding to $\delta_{\text{Mo-F}} = 0.072 \text{ \AA}$ (theoretical: $\delta_{\text{Mo-F}} = 0.060 \text{ \AA}$), is judged to be the best in agreement with Bastiansen's conclusion. The details of the features in the cut-off region are, however, not in very satisfactory agreement with the visual curve*. An increase in the temperature factors of the F_{O} and F_{p} terms would probably help to improve the situation to some extent. Plans had been made to calculate additional curves with such revised temperature factors but this was made impossible to execute because of the mechanical breakdown of the Datatron computer during the last days in which this thesis was written.

* This may in large part be due to the extreme uncertainty involved in the visual observation.

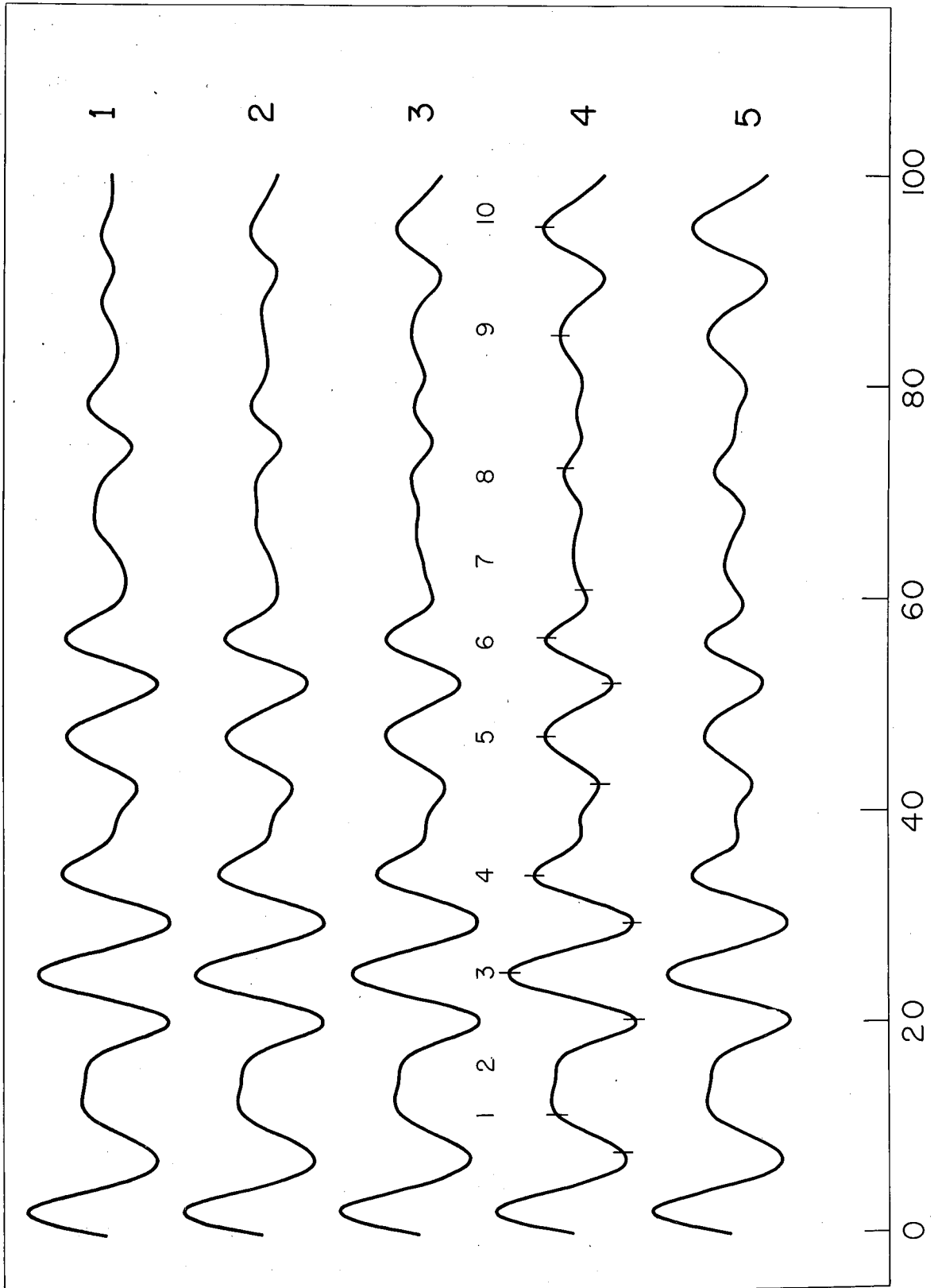


Figure 6. Molybdenum Hexafluoride

Legend of Figure 6, MoF₆

Curve	$\delta_{\text{Mo-F}} (\text{\AA})$	$(a_{ij} - a_{\text{Mo-F}}) \times 10^3 (\text{\AA}^2)$	
		F..F _o	F..F _p
1	0.054	2.2	0.75
2	0.060*	2.2	0.75
3	0.066	2.2	0.75
4	0.072	2.2	0.75
5	0.078	2.2	0.75

* Theor. Value

TABLE IX

Scale Factor, Molybdenum Hexafluoride

Min	Max	q_o (O.B.)	q_c/q_o	Wt
1		7.76	0.928	0
	1	11.35	1.101	0
2		--	--	0
	2	--	--	0
3		20.30	0.990	1
	3	24.70	0.996	1
4		29.40	1.003	2
	4	33.85	1.004	2
5		42.46	0.994	0
	5	46.91	1.002	1
6		51.97	1.001	2
	6	56.23	0.998	1
7		60.80	0.985*	1
	7	--	--	0
8		--	--	0
	8	72.29	0.993	0
9		--	--	0
	9	84.76	1.002	1
10		--	--	0
	10	95.10	0.998	2

Scale Factor 1.000

Ave. Dev. 0.003

$$r_{Mo-F} = 1.84 \times 1.000 = 1.840 \text{ \AA}$$

$$\text{Ave. Dev. } 0.006 \text{ \AA}$$

* Rejected.

TABLE X

Structure of Molybdenum Hexafluoride, O_h

Parameter	Value	Limit of Error
$r_{\text{Mo-F}}$	1.840 Å	0.02 Å
$2\delta_{\text{Mo-F}}$	0.14 Å	0.03 Å

References of Part II

1. Braune, H., and Pinnow, P., Z. physik. Chem. B35, 239-255 (1937).
2. Bauer, S. H., Columbia Report A-1209. Declassified October 14, 1946.
J. Chem. Phys. 18, 27-41 (1950); 18, 994 (1950).
3. Hoard, J. L., and Stroupe, J. D., Columbia Report A-1242, (March 1944).
Declassified October 7, 1946.
4. Bigeleisen, J., Mayer, M. G., Stevenson, P. C., and Turkevich, J.,
J. Chem. Phys. 16, 442-445 (1948).
5. Magnuson, D. W., J. Chem. Phys. 19, 1614 (1951).
6. Bauer, S. H., J. Phys. Chem. 56, 343-351 (1952).
7. Brockway, L. O., and Pauling, L., Proc. Natl. Acad. Sci. 19, 68-73
(1933).
8. Schomaker, V., and Glauber, R., Nature 170, 290-291 (1952); Phys.
Rev. 89, 667-671 (1953).
9. Ibers, J. A., Thesis, California Institute of Technology, 1954.
10. Hoerni, J. A., and Ibers, J. A., Phys. Rev. 91, 1182-1185 (1953).
11. Ibers, J. A., and Hoerni, J. A., Acta Cryst. 7, 405-408 (1954).
12. Langseth, A., and Qviller, B., Z. physik. Chem. B27, 79-99 (1934).
13. Hawkins, N. J., and Sabol, W. W., J. Chem. Phys. 25, 775-776 (1956).
14. Woodward, L. A., and Roberts, H. L., Trans. Faraday Soc. 52, 615-619
(1956).
15. Linke, R., Z. physik. Chem. B48, 193-196 (1941).
16. Zalkin, A., and Templeton, D. H., Acta Cryst. 6, 106 (1953).
17. Brockway, L. O., Rev. Mod. Phys. 8, 231-266 (1936).
18. Braune, H., and Stute, K. W., Angew. Chem. 51, 528 (1938).
19. Sheehan, Jr., W. F., Thesis, California Institute of Technology, 1952,
Proposition 6.
20. Sheehan, Jr., W. F., Thesis, California Institute of Technology, 1952.

21. Tanner, K. N., and Duncan, A. B. F., J. Am. Chem. Soc. 73, 1164-1167 (1951).
22. Burke, T. G., Smith, D. F., and Nielsen, A. H., J. Chem. Phys. 20, 447-454 (1952).
23. Gaunt, J., Trans. Faraday Soc. 49, 1122-1131 (1953).
24. Bastiansen, O., "Electron Diffraction Investigations of Molybdenum, Wolfram, and Uranium Hexafluoride." (A Report Submitted to Professor V. Schomaker, 1950)
25. Bauer, S. H., J. Phys. Chem. 56, 343-351 (1952).
26. Rüdorff, W., and Hofmann, U., Z. physik. Chem. B28, 351-370 (1935).
27. Brockway, L. O., Ewens, R. V. G., and Lister, M. W., Trans. Faraday Soc. 34, 1350-1357 (1938).
28. Sheline, R. K., J. Am. Chem. Soc. 72, 5761-5762 (1950).
29. Hawkins, N. J., Mattraw, H. C., Sabol, W. W., and Carpenter, D. R., J. Chem. Phys. 23, 2422-2427 (1955).
30. Ewens, R. V. G., and Lister, M. W., Trans. Faraday Soc. 34, 1358-1362 (1938).
31. Ketelaar, J. A. A., and van Oosterhout, G. W., Rec. trav. chim. 62, 197-200 (1943).
32. Spurr, R. A., Thesis, California Institute of Technology, 1942.

Propositions

1. The time derivative of the concentration at any point in the cell decays exponentially (after a short initial period) during the approach to equilibrium in the ultracentrifuge. The perturbation theory gives an accurate explicit formula for the decay constant so that both the molecular weight and sedimentation constant can be determined from a single experiment.
2. It is shown that the second virial coefficient of a two-dimensional gas can be positive at a given temperature even if that of a three-dimensional gas is negative at the same temperature. This may explain the experiments of Wilkins (1) in which he found the type of adsorption corresponding to repulsive forces at a temperature at which the virial coefficient of the three-dimensional gas is negative.
3. The integral equation for the radial distribution function in a two-dimensional fluid has been obtained using the superposition approximation. The kernel is more complicated than in the three-dimensional case. Analytical solutions are obtained for the case of hard sphere interactions by approximating the kernel by its asymptotic form.
4. A theory of multilayer adsorption based on the use of molecular distribution functions is presented. The non-linear integral equation satisfied by the density can only be solved by approximation methods. The amount adsorbed is obtained by integrating the density function over the entire adsorption region.

5. The statement of Wilkins (1) that the Langmuir adsorption isotherm is equivalent to the assumption of hard sphere interactions between the adsorbed atoms in the monolayer is shown to be incorrect.
6. A consideration of the problem of sedimentation in a medium with constant density gradient is shown to lead to the Hermite differential equation resulting in a close analogy with the problem of a harmonic oscillator in quantum mechanics.
7. The unusually low values found for the frequency factor in the expression for the thermal rate of escape of trapped electrons and holes in semiconductors and luminescent materials may be explained by applying Chandrasekhar's expression (2) for the rate of escape of particles over potential barriers. In this way the frequency factor can be related to the friction constant (inverse mobility) of the electrons and holes.
8. The expression obtained for the phosphorescence intensity assuming first order kinetics for the rate of escape from traps is shown to be the Laplace Transform of the distribution of trapping levels. The often observed inverse power decay may then be interpreted as due to a peaked distribution with a slight spread rather than to the usually assumed exponential distribution.
9. The attempt has been made to calculate the molecular friction constant in a fluid by replacing the remaining $N-1$ molecules by an elastic continuum. The use of the Kirkwood expression (3) for the friction constant in terms of the force correlation yields, however, a vanishing result not only in the harmonic approximation for the vibrations

in the medium but also in the anharmonic approximation. The consistency of this result with that of Peierls (4) in connection with the thermal conductivity of solids is pointed out.

10. Some interesting results are obtained in a theoretical investigation on the manner of the variation of the density from that of bulk liquid to that of bulk vapor in passing through the surface zone separating the two phases.

References for Propositions

1. Wilkins, M. H. F., Proc. Roy. Soc. A164, 496, 510 (1938).
2. Chandrasekhar, S., Rev. Mod. Phys. 15, 1-89 (1943).
3. Kirkwood, J. G., J. Chem. Phys. 14, 180-201 (1946).
4. Peierls, R., Ann. Physik 3, 1055 (1929).